

# **The proteasome activator Blm10 facilitates nuclear import of mature proteasome core particles in yeast**

Von der Fakultät Energie-, Verfahrens- und Biotechnik der  
Universität Stuttgart zur Erlangung der Würde eines  
Doktors der Naturwissenschaften (Dr. rer. nat.)  
genehmigte Abhandlung

Vorgelegt von  
Dipl.-Biol. (t.o.)  
Marion Weberruß  
aus Mühlacker

Hauptberichter: Prof. Dr. Dieter H. Wolf  
Mitberichter: Priv. Doz. Dr. Hans Rudolph  
Tag der mündlichen Prüfung: 8. April 2014

Institut für Biochemie der Universität Stuttgart  
2014



## **Eidesstattliche Erklärung**

Hiermit erkläre ich, dass ich diese Arbeit selbst verfasst habe und keine anderen als die angegebenen Quellen und Hilfsmittel verwendet habe.

Vaihingen/Enz, den 08.12.2013

(Marion Weberruß)



## Table of Contents

I. List of Abbreviations .....	IX
II. List of Figures.....	XIII
III. List of Tables.....	XV
IV. Abstract .....	XVII
V. Zusammenfassung.....	XIX
1. Introduction .....	1
1.1. The yeast <i>Saccharomyces cerevisiae</i> .....	1
1.2. The intracellular proteolytic system in yeast .....	1
1.3. The ubiquitin system.....	2
1.4. The proteasome .....	4
1.5. Structure of the 20S core particle .....	5
1.6. Proteasome activators.....	7
1.7. The 19S regulatory particle .....	8
1.8. The proteasome activator Blm10.....	11
1.9. Biogenesis of the 20S core particle in yeast.....	13
1.10. Proteasome localization in yeast .....	15
1.11. Nuclear transport.....	17
1.12. Nuclear transport of proteasomes .....	21
1.13. Thesis Rationale.....	22
2. Material and methods.....	25
2.1. Material.....	25
2.1.1. Antibodies .....	25
2.1.2. Enzymes .....	25
2.1.3. Ladders and standards .....	26
2.1.4. Kits.....	26
2.1.5. Chemicals and consumables .....	27
2.1.6. Instruments and software.....	28
2.2. Media and strains .....	29
2.2.1. Media for cultivation of <i>E. coli</i> .....	29
2.2.2. Growth media for <i>S. cerevisiae</i> .....	30
2.2.3. <i>S.cerevisiae</i> strains.....	31
2.2.4. <i>E. coli</i> strains .....	32
2.3. Oligonucleotides .....	33

## Table of Contents

2.4. Plasmids.....	33
2.5. Cell culture and cell-biological methods .....	34
2.5.1. Growth conditions for <i>E. coli</i> cultures.....	34
2.5.2. Growth conditions for <i>S. cerevisiae</i> cultures.....	34
2.5.3. Measurement of cell growth.....	34
2.5.4. Glycerol stocks of <i>E.coli</i> and <i>S. cerevisiae</i> strains.....	35
2.5.5. Direct fluorescence microscopy .....	35
2.6. Molecular biological Methods .....	35
2.6.1. Isolation of plasmid DNA from <i>E. coli</i> .....	35
2.6.2. Easy Plasmid Miniprep .....	35
2.6.3. Isolation of genomic DNA from <i>S. cerevisiae</i> .....	36
2.6.4. Polymerase chain reaction (PCR).....	36
2.6.5. Restriction digestion of plasmid DNA.....	37
2.6.6. Agarose gel electrophoresis .....	37
2.6.7. Extraction of DNA fragments out of agarose gels .....	38
2.6.8. Ligation of DNA fragments.....	38
2.6.9. Construction of pMW1 and pMW2 .....	39
2.6.10. Transformation of <i>E. coli</i> .....	39
2.6.11. Transformation of <i>S. cerevisiae</i> with lithium acetate.....	39
2.6.12. Plasmid transformation in <i>S. cerevisiae</i> .....	40
2.6.13. Transformation of <i>S. cerevisiae</i> by electroporation.....	41
2.7. Methods in protein biochemistry .....	41
2.7.1. Cycloheximide chase analysis .....	41
2.7.2. Protein purifications .....	41
2.7.3. Solution binding assays .....	45
2.7.4. Thrombin cleavage .....	47
2.7.5. Reconstitution of CP import into reconstituted <i>Xenopus</i> egg nuclei.....	47
2.7.6. Cell disintegration and protein precipitation by Yaffe and Schatz .....	48
2.7.7. Protein precipitation .....	48
2.7.8. Native glass bead cell disintegration.....	48
2.7.9. Cell disintegration by French Pressure Cell press .....	49
2.7.10. Native polyacrylamide gel electrophoresis.....	49
2.7.11. Analysis of native gels by phosphofluoroimaging.....	50
2.7.12. SDS polyacrylamide gel electrophoresis (SDS PAGE) .....	50
2.7.13. Western blot.....	51
2.7.14. Immuno detection .....	53
2.7.15. Inhibition of the proteasomal activity with MG-132.....	53

## Table of Contents

2.7.16. Centrifugation in a glycerol density gradient .....	54
2.7.17. Measurement of proteasomal activity with fluorogenic substrates (peptide cleavage assay) .....	54
2.7.18. Test for phleomycin sensitivity .....	54
3. Results .....	57
3.1. Blm10 is involved in the sequestration of proteasomes into PSGs.....	57
3.1.1. Blm10 is required for the sequestration of the CP into PSGs .....	57
3.1.2. The sequestration of the RP into PSGs is independent of Blm10.....	59
3.1.3. Blm10 localizes to PSGs in stationary phase.....	60
3.2. PSGs function as stocks for mature proteasomal particles .....	61
3.2.1. Analysis of proteasome configuration in non-dividing cells .....	61
3.2.2. Analysis of the degradation of the model substrate $\Delta$ ss-CPY* in non- dividing <i>blm10</i> $\Delta$ cells.....	64
3.3. The re-import of mature CPs into the nucleus is dependent on Blm10.....	66
3.3.1. Nuclear uptake of mature CPs is dependent on Blm10 .....	66
3.3.2. The nuclear uptake of the RP base and lid is independent of Blm10.....	68
3.3.3. The recovery of nuclear RP-CP complexes is delayed in <i>blm10</i> $\Delta$ cells .	69
3.3.4. Non-dividing <i>blm10</i> $\Delta$ cells are sensitive to phleomycin.....	72
3.4. Blm10 acts as importin for mature CPs .....	73
3.4.1. Blm10 facilitates the uptake of yeast CP into reconstituted <i>Xenopus</i> egg nuclei	74
3.4.2. Re-import of mature CPs and Blm10 is independent of Srp1/importin $\alpha$	78
3.4.3. Blm10 interacts with Nup53 and enhances binding of CPs to Nup53 ....	79
3.4.4. The import of Blm10 is dependent on the Ran cycle.....	82
3.4.5. Analysis of the interaction of Blm10 and Gsp1-GTP .....	84
3.4.6. Association of Gsp1-GTP dissociates a CP-Blm10 complex .....	91
4. Discussion.....	95
4.1. The sequestration of the CP into PSGs is dependent on Blm10 .....	95
4.2. PSGs function as proteasome stocks.....	97
4.3. The import of mature CPs is dependent on Blm10 .....	99
4.4. Blm10 represents the importin for mature CPs.....	101
4.5. Future directions.....	108
4.5.1. The sequestration of the CP into PSGs .....	108
4.5.2. The function of PSGs.....	109
4.5.3. The function of Blm10 as importin for mature CPs.....	110
4.5.4. Nuclear import of Blm10 .....	112
5. References.....	115

## Table of Contents

6. Acknowledgements .....	133
7. Lebenslauf .....	135



## I. List of Abbreviations

ADP	Adenosine diphosphate
AMC	Aminomethylcoumarin
Amp	Ampicillin
AMP	Adenosine monophosphate
APS	Ammoniumpersulfate
ATP	Adenosine triphosphate
BAPTA	1,2-bis(o-aminophenoxy)ethane-N,N,N',N'-tetraacetic acid
Bp	Base pair
BP	Binding protein
BSA	Bovine serum albumin
CHX	Cycloheximide
CM	Complete media
cNLS	Classical nuclear localization sequence
CP	Core particle
CPY	Carboxy peptidase Y
ddH <sub>2</sub> O	Ultrapure water
DMSO	Dimethyl sulphoxide
DNA	Deoxyribonucleic acid
dNTP	Deoxyribonucleotide
DUB	Deubiquitinating enzyme
ECL	Enhanced chemoluminescence
<i>E. coli</i>	<i>Escherichia coli</i>
EDTA	Ethylendiaminetetraacetic acid
ER	Endoplasmic reticulum
ERAD	ER associated degradation
FG	Phenylalanine, glycine
Fig.	Figure
FRAP	Fluorescence recovery after photobleaching
fwd	Forward
GAP	GTPase activating protein
GDP	Guanosine diphosphate
GEF	Guanine nucleotide exchange factor

## List of Abbreviations

GFP	Green fluorescencet protein
GST	Glutathione S-transferase
GTP	Guanosine triphosphate
HA	Hemagglutinin
HABA	2-(4-Hydroxyphenylazo)benzoic acid
HbYX	Hydrophobic-tyrosine-X
HEAT	Huntingtin, elongationsfactor 3, protein phosphatase 2A, TOR1
HECT	Homologous to E6AP Carboxy Terminus
HRPO	Horseradish peroxidase
Hsp	Heat shock protein
IgG	Immunglobulin G
IPOD	Insoluble protein deposit
IPTG	Isopropyl $\beta$ -D-1-thiogalactopyranoside
JUNQ	Juxtannuclear quality control compartment
kb	Kilobase
kDa	Kilodalton
LB	Lysogeny broth medium
LiOAc	Lithium acetate
M	Molar
MHC	Major histocompatibility complex
mM	Millimolar
MPN	Mpr1 and Pad1
NC	Nitrocellulose
NE	Nuclear envelope
NES	Nuclear export signal
NLS	Nuclear localization sequence
NPC	Nuclear pore complex
Nup	Nuclear pore protein
OD <sub>600</sub>	Optical density measured at 600 nm
OG	Oregon Green 488 succinimidyl ester
ON	Over night
PA	Proteasome activator/activating

## List of Abbreviations

PAGE	Polyacrylamide gel electrophoresis
PBS	Phosphate buffered saline
PC	Proteasome/cyclosome
PCI	Proteasome, COP9, initiation factor3
PCR	Polymerase chain reaction
PDB	Protein data bank
PEG	Polyethylene glycol
PGK	Phosphoglycerate kinase
PGPH	Peptidylglutamyl-peptide hydrolytic
ProA	Protein A
PSG	Proteasome storage granule
PVDF	Polyvinylidene difluoride
Ran	Ras-related nuclear protein
rev	Reverse
RFP	Red fluorescent protein
RING	Really interesting new gene
RNA	Ribonucleic acid
RP	Regulatory particle
rpm	Rotations per minute
RT	Room temperature
S	Svedberg unit
<i>S. cerevisiae</i>	<i>Saccharomyces cerevisiae</i>
SDS	Sodium dodecyl sulfate
SOC	Super optimal broth with catabolite repression
ssDNA	Single stranded DNA
Tab.	Table
<i>T. Acidophilum</i>	<i>Thermoplasma acidophilum</i>
TAE	Tris acetate EDTA
TCA	Trichloroacetic acid
TE	Tris EDTA
TEMED	N,N,N',N'-Tetramethylethylenediamine
Tev	Tobacco etch virus
U	Unit
U-box	UFD2 homology

## List of Abbreviations

UV	Ultraviolet
v/v	Volume per volume
wt	Wildtype
w/o	Without
w/v	Weight per volume
YPD	Yeast peptone dextrose medium

## II. List of Figures

Figure 1: Mechanism of polyubiquitylation.....	3
Figure 2: Schematic representation of a 30S proteasome.....	4
Figure 3: Crystal structure of the yeast CP.....	6
Figure 4: Composition of the 30S proteasome. ....	9
Figure 5: Crystal structure of the Blm10-CP-Blm10 complex.....	12
Figure 6: The nuclear import (left) and export (right) cycle..	20
Figure 7: CP localization in logarithmic and stationary phase.....	57
Figure 8: <i>BLM10</i> deletion prevents the sequestration of the CP into PSGs in stationary phase. ....	58
Figure 9: Sequestration of RP base and lid is not dependent on Blm10.....	60
Figure 10: Blm10 localization in logarithmic and stationary phase. ....	61
Figure 11: Analysis of proteasome configurations. ....	62
Figure 12: The degradation of $\Delta$ ssCPY*-Leu2Myc is not delayed in <i>blm10</i> $\Delta$ cells. ..	65
Figure 13: The re-import of the CP into the nucleus is dependent on Blm10.....	67
Figure 14: The re-import of RP base and lid is not dependent on Blm10..	69
Figure 15: Recovery of associated RP-CP complexes is delayed by <i>BLM10</i> deletion .....	71
Figure 16: Quiescent <i>blm10</i> $\Delta$ cells are sensitive against phleomycin.....	73
Figure 17: Blm10 binds to OG labeled yeast CP. ....	76
Figure 18: Blm10 facilitates the uptake of yeast CP into reconstituted <i>Xenopus</i> egg nuclei. ....	77
Figure 19: The import of mature CP and Blm10 is not dependent on importin $\alpha$ .....	79
Figure 20: Blm10 interacts with GST-Nup53. ....	80
Figure 21: Blm10 enhances the affinity of the CP to GST-Nup53.....	82
Figure 22: The import of Blm10 is dependent on a functional Gsp1 gradient..	83
Figure 23: Blm10 interacts with Gsp1-GTP with its C-terminal region..	85
Figure 24: Blm10 contains an acidic patch .....	88
Figure 25: Mutation of Blm10's W2021 affects the binding of Blm10 1749-2143 to Gsp1-GTP..	90
Figure 26: Expression of Gsp1G21V dissociates Blm10-CP complexes <i>in vivo</i> .....	92
Figure 27: Gsp1-GTP dissociates Blm10-CP complexes <i>in vitro</i> .....	93
Figure 28: Model of CP import in logarithmic phase .....	102

List of Figures

Figure 29: Model of the CP import in stationary phase..... 107

### III. List of Tables

Table 1: List of antibodies used in this work .....	25
Table 2: List of chemicals and consumables used in this work.....	27
Table 3: List of instruments used in this work .....	28
Table 4: List of <i>S. cerevisiae</i> strains used in this work .....	31
Table 5: List of <i>E. coli</i> strains used in this work .....	32
Table 6: List of oligonucleotides used in this work .....	33
Table 7: List of plasmids used in this work .....	33
Table 8: Composition of a 1.5 mm 3.5%-6% native gel .....	50
Table 9: Composition of 5 ml separating gel.....	51
Table 10: Composition of 4 ml stacking gel (5%).....	51





## IV. Abstract

The proteasome is a multi-subunit protease complex which is responsible for the degradation of misfolded and short-lived proteins. It exists in different configurations that all contain the proteolytically active core particle (CP) but differ in the number of associated regulatory particles (RP) and accessory proteins. The localization and configuration of proteasomes are highly dynamic. The regulation of both these factors is not only relevant for the function and activity of proteasomes but also represents a cellular adjustment mechanism to changing environmental conditions. In proliferating yeast cells, proteasomes are primarily localized to the nucleus (Russell et al., 1999; Laporte et al., 2008). When cells reach stationary phase, RP-CP assemblies dissociate and RP and CP are sequestered separately into cytosolic proteasome storage granules (PSGs) (Bajorek et al., 2003; Laporte et al., 2008). These motile cytosolic structures were found to resolve rapidly when cells resume proliferation and the proteasome is re-imported into the nucleus (Laporte et al., 2008). This work shows that the sequestration of the proteasome CP is dependent on the conserved proteasome activator Blm10. Blm10 consists of 32 HEAT-like repeats and is structurally related to transport factors, such as importin  $\beta$  (Sadre-Bazzaz et al., 2010; Huber & Groll, 2012). In addition to CP sequestration, Blm10 was identified in this study to be essential for the fast nuclear re-import of CPs upon PSG dissolution. Reconstitution of nuclear import of yeast CP into *Xenopus* egg nuclei and solution binding assays suggest that Blm10 facilitates nuclear import of mature CPs by mediating the contact of the CP-Blm10 complex to proteins of the NPC. Furthermore, Blm10 interacts *in vitro* with Gsp1-GTP, the yeast homologue of Ran-GTP, through its C-terminal region. This association of Gsp1-GTP to the Blm10-CP complex results in the dissociation of the complex and in the release of the CP. Taken together these results suggest that in yeast, Blm10 represents the importin for mature CPs.

Parts of this thesis were published in:

**Weberruss, M.H., Savulescu, A.F., Jando, J., Bissinger, T., Harel, A., Glickman, M.H., and Enenkel, C.** (2013). Blm10 facilitates nuclear import of proteasome core particles. *EMBO J* **32**, 2697-2707.



## V. Zusammenfassung

Das Proteasom ist ein Proteasekomplex, welcher für die Degradation fehlgefalteter und kurzlebiger Proteine essentiell ist. Proteasomen existieren in verschiedenen Konfigurationen. Der Kern jeder Konfiguration wird vom 20S Kernkomplex (CP) gebildet, an welchen der 19S regulatorische Partikel (RP), andere Proteasomaktivatoren oder auch Proteasom-assoziierte Proteine binden können. Die intrazelluläre Lokalisation und die Konfiguration von Proteasomen sind dynamisch. Die Regulation beider Faktoren ist nicht nur für die Proteasomfunktion von Relevanz sondern stellt auch einen Anpassungsmechanismus der Zelle an verschiedene Umweltbedingungen dar. In teilenden Hefezellen liegen 80% der Proteasomen im Zellkern vor (Russell et al., 1999; Laporte et al., 2008) und die vorherrschende Proteasomkonfiguration stellen RP-CP oder RP-CP-RP Komplexe dar, welche essentiell für die Degradation polyubiquitinerter Proteine sind (Bajorek et al., 2003). Wenn Hefezellen jedoch die stationäre Wachstumsphase erreichen, verändern sich sowohl Konfiguration als auch Lokalisierung der Proteasomen. RP-CP Komplexe dissoziieren in freie RPs und CPs und liegen in cytosolischen Granuli (PSG) vor (Bajorek et al., 2003; Laporte et al., 2008). Diese Granuli stellen motile Strukturen dar, welche rasch aufgelöst werden, wenn die Zellproliferation wiederaufgenommen wird (Laporte et al., 2008). In PSG gespeicherte Proteasomen werden dabei innerhalb weniger Minuten in den Kern importiert (Laporte et al., 2008). Diese Arbeit zeigt, dass die Sequestrierung von Proteasom Kernkomplexen in die PSGs abhängig von Blm10 ist. Blm10 ist ein konservierter Proteasomaktivator, welcher an die  $\alpha$ -Ringe des CPs assoziieren kann. Blm10 besteht aus 32 HEAT-repeats und ist somit strukturell mit Transportfaktoren wie Importin  $\beta$  verwandt (Sadre-Bazzaz et al., 2010; Huber & Groll, 2012). Der schnelle Import von maturierten CPs in den Zellkern, der nach dem Auflösen der PSGs statt findet, ist ebenso abhängig von Blm10. Während des Transports des Blm10-CP Komplexes in den Zellkern vermittelt Blm10 den Kontakt zu Proteinen der Kernpore und interagiert im Kern mit Gsp1-GTP, dem Hefehomolog von Ran-GTP. Die Bindung von Blm10 an Gsp1-GTP erfolgt über den C-Terminus von Blm10 und hat die Dissoziation des Blm10-CP Komplexes zur Folge. Blm10 stellt somit das erste identifizierte Importin für den maturierten Kernkomplex dar.

## Zusammenfassung

Teile dieser Arbeit wurden publiziert in:

**Weberruss, M.H., Savulescu, A.F., Jando, J., Bissinger, T., Harel, A., Glickman, M.H., and Enekel, C.** (2013). Blm10 facilitates nuclear import of proteasome core particles. *EMBO J* **32**, 2697-2707.

# 1. Introduction

## 1.1. The yeast *Saccharomyces cerevisiae*

The baker's yeast *Saccharomyces cerevisiae* (*S. cerevisiae*) is widely used as a eukaryotic model organism. It combines the feature of modest and easy cultivation that is typical for unicellular organisms with the feature of being structurally related to higher eukaryotic cells, such as mammalian cells. *S. cerevisiae* belongs to the domain of Eukarya, and as such shows the typical compartmentalization of cells. This makes yeast metabolism more comparable to the metabolism of higher eukaryotic cells than to prokaryotes (Guthrie & Fink, 1991). Furthermore, cultivation of yeast is easy and fast with only modest requirements for equipment and media. Yeast can stably exist in a haploid or a diploid form. The haploid genome of *S. cerevisiae* consists of  $1.2 \times 10^7$  bps on 16 chromosomes, on which approximately 6000 genes are encoded (Goffeau et al., 1996; Hieter et al., 1996). In comparison to higher eukaryotic cells, the yeast genome is small and easy to manipulate (Orr-Weaver et al., 1981; Sikorski & Hieter, 1989) and since there is just one allele of each gene in haploid cells, phenotypes of deletions or mutations can be easily examined (Guthrie & Fink, 1991).

Due to the relatively close phylogenetic relation between yeast and mammalian cells, yeast cells are a suitable model organism to study certain cellular processes. Knowledge gained can either be transferred directly to higher eukaryotes or can provide a lead for research in higher eukaryotes (Guthrie & Fink, 1991; Botstein et al., 1997).

## 1.2. The intracellular proteolytic system in yeast

Proteins are basic components of all cells and their expression and activity in the cell has to be regulated strictly to prevent them from malfunctioning. The cell can regulate the activity of proteins by covalent modifications such as phosphorylation, by stimulation of protein synthesis, or by degradation of the protein. In addition to regulation, proteolysis is an important process in the cell to dispose of misfolded proteins, which can potentially form protein aggregates. In yeast, two important degradation pathways can be distinguished: Selective proteolysis is mainly achieved by a large

## Introduction

multisubunit complex, called the proteasome (reviewed in Wolf & Hilt, 2004). The second degradation pathway occurs via the vacuole, the yeast analogue of the lysosome. In the vacuole, proteins and also complete organelles such as mitochondria, are degraded (reviewed in Achstetter & Wolf, 1985; Rendueles & Wolf, 1988). In contrast to the highly selective degradation by the proteasome, vacuolar degradation is rather unspecific (Rendueles & Wolf, 1988).

### 1.3. The ubiquitin system

The degradation of a protein is one possible mechanism to remove its activity from the cell. In order to prevent the cell from degrading proteins that are still useful, it is essential that a mechanism exists to differentiate between proteins targeted for degradation and proteins that are not. In eukaryotes one possible way for this differentiation is the covalent attachment of molecules, which function as a degradation signal. The most important molecule for this targeting is a small protein called ubiquitin ( Ciehanover et al., 1978; Wilkinson et al., 1980). Ubiquitin is a polypeptide consisting of 76 amino acids, with a molecular mass of 8.5 kDa. Early studies showed that ubiquitylation of a protein is an ATP-dependent process (Hershko & Tomkins, 1971; Hershko et al., 1983), which requires three different types of enzymes: the ubiquitin activating enzyme (E1), the ubiquitin conjugating enzyme (E2) and the ubiquitin protein ligase (E3) (Hershko et al., 1979; Hershko et al., 1983).

The process of ubiquitylation starts with the activation of the ubiquitin molecule by the E1. After ATP hydrolysis, the carboxyl group of the C-terminal amino acid of ubiquitin, a glycine, is linked to the AMP and then transferred to a cysteine side chain of the E1. The formed bond is a thioester bond, which is rich in energy. In a second step, the ubiquitin is passed on to a cysteine side chain of the E2. Finally, the E3 is required for the transfer of the ubiquitin onto the substrate. Generally, several classes of E3 can be distinguished with the most important of these classes containing the RING (Really Interesting New Gene), HECT (Homologous to E6AP Carboxy Terminus) and U-box (UFD2 homology) ligases. E3 classes differ in the way that the ubiquitin is transferred onto the substrate. In the case of HECT domain containing E3s, the ubiquitin is transferred from the E2 onto the E3, and finally from the E3 to the substrate (Scheffner et al., 1995). In contrast, E3 RING ligases act as a bridge by binding to the E2 and bringing E2 and substrate in close proximity to allow the transfer of the ubiquitin from the E2 to the substrate (for an overview see Pickart & Eddins,

## Introduction

2004). Ubox E3 ligases represent the smallest class of E3. They contain an E2 binding domain and function similarly to RING ligases (Aravind & Koonin, 2000; Hatakeyama & Nakayama, 2003).

When ubiquitin is transferred onto the substrate, the carboxyl group of ubiquitin's C-terminal glycine forms an isopeptide bond with an  $\epsilon$ -amino group of a lysine in the substrate. For elongation of the ubiquitin chain, the proceeding ubiquitin forms with its C-terminal carboxyl group an isopeptide bond with the side chain of lysine 48 (K48) in the previous ubiquitin (Chau et al., 1989). For proteasomal degradation, this K48 linkage is the most important linkage and an efficient degradation signal requires a polyubiquitin chain of at least four ubiquitin molecules (Thrower et al., 2000; Chau et al., 1989). The polyubiquitylated substrate is subsequently recognized either directly by the proteasome or by proteasome associated proteins. Prior to proteolysis, deubiquitinating enzymes (DUBs) cleave off the ubiquitin molecules to recycle the ubiquitin (Papa & Hochstrasser, 1993; Park et al., 1997; Amerik et al., 1997; Amerik et al., 2000).

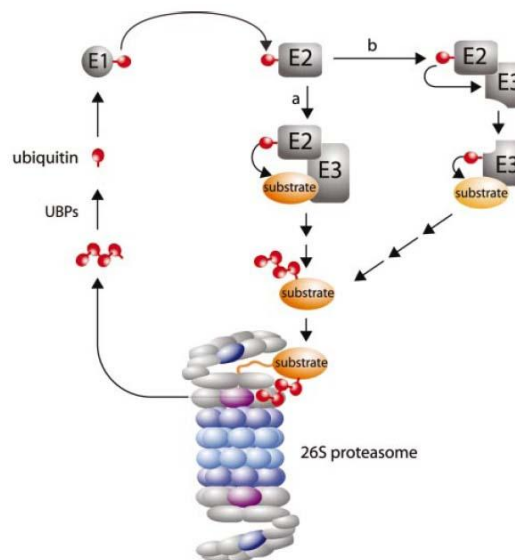


Figure 1: Mechanism of polyubiquitylation. The ubiquitin system targets proteins for degradation by attachment of a polyubiquitin chain. The E1 enzyme activates the ubiquitin in an ATP-dependent manner. Ubiquitin is subsequently transferred onto the E2, before it is finally transferred onto the substrate with the help of the E3. The latter transfer occurs in two different ways: Either the E3 forms a scaffold for the transfer of the ubiquitin from the E2 onto the substrate (a) or the ubiquitin is passed from the E2 to the E3, and then from the E3 to the substrate (b). The 26S proteasome degrades the polyubiquitylated substrates. Figure: Kostova & Wolf, 2003.

## 1.4. The proteasome

The proteasome is responsible for the selective degradation of most cellular proteins, e.g. ubiquitylated proteins (Rock et al., 1994). Prior to its identification, it was known that large protease complexes of unknown cellular function exist in a variety of different organisms such as archaeobacteria, yeasts, the fruit fly *Drosophila* and mammals (Arrigo et al., 1987; Dahlmann et al., 1989). All these protease complexes were found to have a comparable shape and a sedimentation coefficient of approximately 20S (Arrigo et al., 1987). Subsequently, these complexes were found to be homologues that were named proteasomes (Arrigo et al., 1988). In the yeast *S. cerevisiae*, the yscE protease complex was found to be the homologue of mammalian and *Xenopus* proteasomes (Kleinschmidt et al., 1988). Since then, proteasomes were identified in all eukaryotes, most archaeobacteria and also some bacteria (Gille et al., 2003).

Proteasomes exist in different configurations. The centre of each configuration is the 20S core particle (CP), which contains the catalytically active sites (Löwe et al., 1995; Groll et al., 1997). The CP can exist as free particle or associate with proteasome activating (PA) complexes or proteins. The association of the CP with the so-called regulatory particle (RP) occurs in an ATP dependent manner (Chu-Ping et al., 1994; Eytan et al., 1989). The CP in association with one RP forms the 26S proteasome, while association of the CP with two RPs results in the formation of the 30S complex (Eytan et al., 1989, Hoffman et al., 1992).

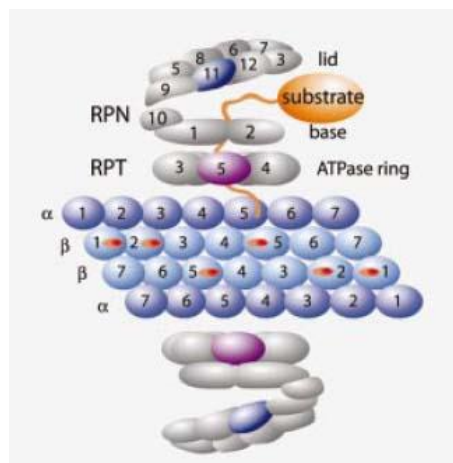


Figure 2: Schematic representation of a 30S proteasome. 30S proteasomes consist of two RPs (grey) and the CP (blue). The catalytically active subunits are indicated by red markers. Figure: Kostova & Wolf, 2003.

Proteins targeted for degradation have to be delivered to the proteasome or have to be recognized by the proteasome itself. Neither substrate recognition nor processing



## Introduction

is achieved by the CP, but additionally requires the presence of the RP (Waxman et al., 1987; Rock et al., 1994). In yeast, substrate delivery and recognition is achieved by special shuttle proteins, such as Dsk2, Rad23 and Ddi1, which bind the polyubiquitin chain and also associate with the RP (Schauber et al., 1998; Wilkinson et al., 2001; Rao & Sastry, 2002; Elsasser et al., 2002; Medicherla et al., 2004; Rosenzweig et al., 2012). Alternatively, a direct recognition and binding of polyubiquitin chains by the proteasome can occur via the RP subunits Rpn10 and Rpn13 (Deveraux et al., 1994; Elsasser et al., 2004; Seong et al., 2007; Husnjak et al., 2008; Schreiner et al., 2008; Isasa et al., 2010).

The purpose of proteasomal degradation can briefly be summarized in two functions: first, degradation of proteins that are potentially harmful or no longer useful for the cell, and second, regulation of protein levels. The first function is important, since misfolded or damaged proteins can compete with native proteins for binding partners and substrates, or form toxic protein aggregates within the cell (Goldberg, 2003). An example of the second function is found in the role of the proteasome in the cell cycle as the levels of different cyclins need to be regulated strictly to ensure proper cell division (Koepp et al., 1999; reviewed in Rastogi & Mishra, 2012).

The conjugation of ubiquitin to proteasomal substrates is the most common degradation signal. Nevertheless, proteasomes seem to be able to degrade oxidized and unfolded proteins without any further targeting signal (Liu et al., 2003; Goldberg, 2003; Jung et al., 2009). In addition to that, a few examples of proteins are known that are degraded independently from ubiquitylation. One well studied example is the degradation of ornithine decarboxylase (Zhang et al., 2003; Hoyt & Coffino, 2004).

### **1.5. Structure of the 20S core particle**

Before crystal structures of proteasomes were published, it was known that they were large multisubunit and multicatalytic protease complexes with a molecular weight of approximately 700 kDa and a sedimentation coefficient of approximately 20S (Arrigo et al., 1988). The first detailed view into the structure of the CP came from the crystal structure of the CP from the archaeobacterium *Thermoplasma acidophilum* (Löwe et al., 1995). The archaeobacteria CP consists of four rings of seven subunits each, forming a barrel-like shape. Each outer ring consists of seven identical  $\alpha$  subunits

## Introduction

and each inner ring of seven identical  $\beta$  subunits (Dahlmann et al., 1989; Löwe et al., 1995).

The CP from the yeast *S. cerevisiae* was the first eukaryotic CP whose crystal structure was solved (Groll et al., 1997). In contrast to the archaeobacteria CP, the yeast CP consists of seven different  $\alpha$  subunits ( $\alpha 1$ - $\alpha 7$ ) and seven different  $\beta$  subunits ( $\beta 1$ - $\beta 7$ ). The topology of the different subunits is similar to the one found in *T. acidophilum*. Likewise, eukaryotic CPs consist of a stack formed by four rings with seven subunits per ring. The outer rings are formed by the subunits  $\alpha 1$ - $\alpha 7$  and the inner rings by the subunits  $\beta 1$ - $\beta 7$ , which all have unique positions in their respective ring (Groll et al., 1997). The whole complex is 15 nm in length and 11 nm in diameter and shows a C2 symmetry axis (Groll et al., 1997; Baumeister et al., 1998).

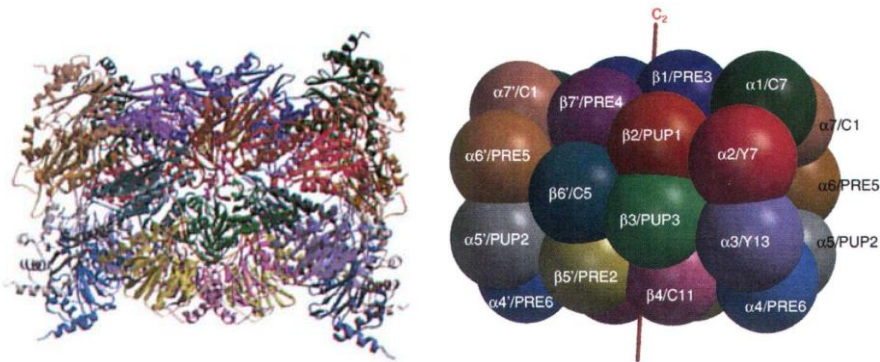


Figure 3: Crystal structure of the yeast CP. Left: Ribbon representation, right: sphere representation. Like archaeobacteria proteasomes, yeast CP forms a stack consisting of four rings of seven subunits each. Figure: Groll et al., 1997.

The general architecture of the mammalian proteasome, including the arrangement of the  $\alpha$  and  $\beta$  subunits in the complex, is identical to its yeast homologue and differs only in the N-terminal regions of the  $\beta$  subunits (Unno et al., 2002). Four additional proteasome subunits were identified in mammals. Three of them,  $\beta 1i/LMP2$ ,  $\beta 2i/MECL$  and  $\beta 5i/LMP7$ , are interferon- $\gamma$  inducible (Martinez & Monaco, 1991; Kelly et al., 1991; Hisamatsu et al., 1996). In newly assembled proteasomes, they can replace their constitutively expressed counterparts, resulting in a complex called the immunoproteasome (Eleuteri et al., 1997). Peptides generated by immunoproteasomes are presented on MHC class I molecules and are an important part of the immune response (Kloetzel, 2001). The fourth additional mammalian subunit is  $\beta 5t$ , whose incorporation results in the formation of thymoproteasomes, which are involved in selection of T cells (Murata et al., 2007).

## Introduction

Unlike the archaeobacterial proteasome, the eukaryotic proteasome contains three different catalytically active  $\beta$  subunits (Löwe et al., 1995; Groll et al., 1997), which show different cleavage efficiencies against different peptide substrates labeled with chromogenic reporter groups. Based on that finding,  $\beta$ 1 was classified as having caspase-like activity (originally also referred to as peptidylglutamyl-peptide hydrolytic (PGPH) activity),  $\beta$ 2 trypsin-like activity and  $\beta$ 5 chymotrypsin-like activity (Heinemeyer et al., 1997; Jäger et al., 1999). Studies showed that the chymotrypsin-like activity and the caspase-like activity allosterically activate and inhibit each other (Kisselev et al., 1999).

Early studies using electron microscopy indicated the presence of three cavities in the CP (Baumeister et al., 1988), which was further confirmed by the crystal structures of the archaeobacteria, the yeast and the bovine proteasomes (Löwe et al., 1995; Groll et al., 1997; Unno et al., 2002). The two outer cavities, the antechambers, are formed between one  $\alpha$  and one  $\beta$  ring and serve mainly the accommodation of proteins. The third cavity is formed in between the two  $\beta$  rings and represents the catalytic chamber (Löwe et al., 1995; Groll et al., 1997; Baumeister et al., 1998; Unno et al., 2002), in which substrates are degraded into peptides of 3-30 amino acids in length (Kisselev et al., 1998; Groll et al., 1997).

The crystal structure of the CP shows no significant opening that might be large enough to allow a folded polypeptide passage through the proteasome gate (Löwe et al., 1995; Groll et al., 1997; Unno et al., 2002). In the yeast CP, the  $\alpha$  subunits close the entrance gate with several layers of amino acid side chains (Groll et al., 1997). Especially the  $\alpha$ 2,  $\alpha$ 3 and  $\alpha$ 4 subunits are involved in gate closing. The only openings that are present in the CP are small side windows located at the interface between  $\alpha$  and  $\beta$  subunits, but these openings are too small to allow access for polypeptide substrates. However, peptides generated by the proteasome might be released through those pores (Groll et al., 1997).

### 1.6. Proteasome activators

Three classes of proteasome associated proteins or complexes have been identified that activate the peptide hydrolysis activity of the CP. The highly conserved RP is with 700 kDa the largest particle (Udvardy, 1993; DeMartino et al., 1994; Zwickl et al.,

## Introduction

1999). Its structure, function and composition are discussed below in more detail (see section 1.7).

The second class of proteasome activators are the 11S regulators, and like the RP, they bind to the  $\alpha$  rings of the CP. 11S complexes are formed by members of the PA28 protein family. PA28 $\alpha$  and  $\beta$  preferentially form heteroheptameric complexes with each other and function in the immune response (Ahn et al., 1995; Preckel et al., 1999; Khan et al., 2001; Murata et al., 2001). The third member of this family, PA28 $\gamma$ , forms a homoheptameric complex, which was shown to be important for cell division and apoptosis in different organisms (Ahn et al., 1995; Song et al., 1996; Murata et al., 1999; Masson et al., 2001; Khan et al., 2001; Masson et al., 2003). 11S regulators are not found in yeast and will therefore not be discussed in further detail.

The third type of proteasome activator is the protein PA200 or Blm10 in yeast (Ustrell et al., 2002). The structure and function of PA200 and Blm10 are discussed in section 1.8.

Both PA28 and Blm10/PA200 can form with the CP and one RP, a so-called hybrid-proteasome. The function of hybrid proteasomes is not yet understood. It was speculated that PA28 or PA200/Blm10 target RP-CP assemblies to specific locations in the cell. It is also possible that hybrid proteasomes degrade specific substrates more efficiently than 26S or 30S proteasomes (Rechsteiner & Hill, 2005).

### **1.7. The 19S regulatory particle**

The regulatory particle (RP) is a large particle of 700 kDa which binds to the  $\alpha$  rings of the CP. In dividing cells, RPs cap CPs either on one side or on both sides (Eytan et al., 1989; Glickman et al., 1998b; Bajorek et al., 2003). The RP is highly conserved from yeast to higher eukaryotic cell and is also termed PAN in archaeobacteria, PA700 in mammals and the  $\mu$  particle in *Drosophila* (Udvardy, 1993; DeMartino et al., 1994; Zwickl et al., 1999). The RP is the only known proteasome activator that stimulates the protein hydrolysis activity of the CP in addition to the hydrolysis of peptides (Waxman et al., 1987; Rock et al., 1994; Hoffman & Rechsteiner, 1994). Thereby, the RP has to fulfill several functions. First, substrates that are targeted for degradation are recognized by it (Deveraux et al., 1994; Seong et al., 2007; Rosenzweig et al., 2012). After binding to the RP, substrates are unfolded in an ATP-dependent manner and ubiquitin chains are removed by specialized DUBs (Papa & Hochstrasser, 1993;

## Introduction

Park et al., 1997; Amerik et al., 2000; Guterman & Glickman, 2004; Verma et al., 2002). Finally, the RP is involved in the gate opening process of the CP  $\alpha$  rings and is essential for the translocation of the substrate into the CP (Reviewed in Wolf & Hilt, 2004).

Structurally, the 19S RP can be further subdivided into a base and lid complex, which are connected to each other via the N-terminal part of the base subunit Rpn10 (Glickman et al., 1998a). Different functions can be assigned to these subcomplexes. The base in complex with a CP is able to activate peptide hydrolysis and hydrolysis of non-ubiquitylated proteins (Glickman et al., 1998a). Polyubiquitylated proteins, however, are not degraded since their degradation requires the presence of the RP lid (Glickman et al., 1998a). The RP base consists of the subunits Rpt1-6 (regulatory particle triple A protein), Rpn1, Rpn2 and Rpn10 (regulatory particle non ATPase) while the lid complex consists of Rpn3, Rpn5-Rpn9, Rpn11 and Rpn12 (Glickman et al., 1998a; Glickman et al., 1998b).

The crystal structure of the RP by itself or in a complex with the CP has not been solved. However, a model of the human 26S proteasome obtained by cryo-electron microscopy and single particle analysis was proposed recently (da Fonseca et al., 2012; Lander et al., 2013).

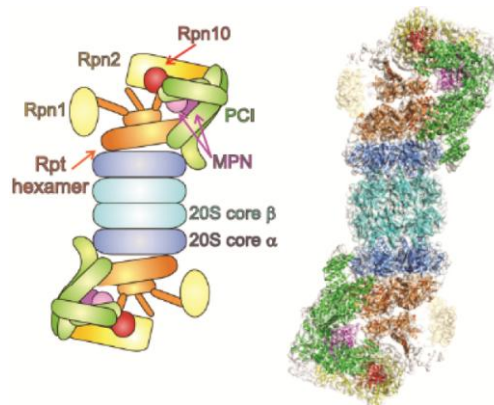


Figure 4: Composition of the 30S proteasome. The 19S RP associates with its hexameric ATPase ring to the CP. The RP can be subdivided into the RP base, consisting of Rpt1-6, Rpn1, Rpn2 and Rpn10, and the RP lid consisting of MPN and CPI subunits (MPN: Rpn8, Rpn11; PCI: Rpn3, Rpn5-7, Rpn9, Rpn12). Figure: da Fonseca et al., 2012.

This model provides insights into the topology of the subunits within the RP. The base associates with its hexameric ring consisting of the six ATPase subunits Rpt1-6 to the ring formed by the seven  $\alpha$  subunits of the CP. This association is mediated by the HbYX motif that is present in the C-terminal regions of Rpt2 and Rpt5 (Gillette et

## Introduction

al., 2008). The binding of Rpt2 and Rpt5 to the  $\alpha$  ring additionally seems to be involved in gate opening since it enhances peptide hydrolysis (Gillette et al., 2008; Rabl et al., 2008). The further RP base subunits Rpn1 and Rpn2 represent with molecular masses of 110 and 104 kDa the largest proteasomal subunits (DeMarini et al., 1995; Hampton et al., 1996; Glickman et al., 1998b). Both seem to function as scaffolding proteins and are structurally related to each other (He et al., 2012). They consist of three domains with their central region consisting of 11 PC (proteasome/cyclosome) repeats of 35-40 residues, a structural element that resembles HEAT (Huntingtin, elongationsfactor 3, protein phosphatase 2A, TOR1) repeats (He et al., 2012). Besides their scaffolding function, Rpn1 and Rpn2 are also involved in the recognition of ubiquitin receptors such as Dsk2, Rad23 and Ddi1 and in the recognition of the transcription activator Rpn4 (Xie & Varshavsky, 2001; Rosenzweig et al., 2012; He et al., 2012). The third non-ATPase subunit of the RP base is Rpn10, which is located at the interface between the base and lid subcomplexes (Glickman et al., 1998b). Rpn10 is involved in the recognition of ubiquitin chains (Deveraux et al., 1994; Elsasser et al., 2004).

The main function of the RP lid is the processing of polyubiquitin chains. All Rpn proteins that are present in the lid can be divided into two groups: subunits which contain the MPN (named after Mpr1 and Pad1) domain and subunits with a PCI (proteasome, COP9, initiation factor3) domain. Both domains are frequently found in subunits of large complexes (Hofmann & Bucher, 1998). The metalloprotease Rpn11 along with Ubp6 is involved in substrate deubiquitination which is required prior to degradation (Yao & Cohen, 2002; Verma et al., 2002; Guterman & Glickman, 2004).

The mechanism of gate opening in the 26S proteasome is still partly unclear. Studies of the archaea RP homologue PAN showed that the binding of the ATPase subunits to the CP induces an opening of the gates formed by the  $\alpha$  subunits (Smith et al., 2007; Rabl et al., 2008). In eukaryotic proteasomes, this process seems to be more complex. In the model of the human 26S proteasome, the gates are not opened completely (da Fonseca et al., 2012). Instead, it was proposed that the gates are either in a disordered state as seen for the proteasome activator Blm10 or that they remain closed (Sadre-Bazzaz et al., 2010; da Fonseca et al., 2012). This finding indicates that additional factors might be involved in gate opening. Previous studies showed that the presence of polyubiquitylated proteins activates the peptidase activity of the CP which indicates that complete gate opening might be achieved during the

processing of substrates (Bech-Otschir et al., 2009; Peth et al., 2009; da Fonseca et al., 2012).

### **1.8. The proteasome activator Blm10**

The yeast protein Blm10 and its orthologue PA200 are after the 19S and the 11S regulators, the third type of known proteasome activators. Like the 11S regulators, their activating function occurs in an ATP-independent manner (Ustrell et al., 2002). Blm10 was identified in the yeast *S. cerevisiae* and its deletion was initially reported to result in an increased sensitivity to the DNA-damaging agent bleomycin. Therefore Blm10 was proposed to function in DNA repair (Febres et al., 2001). PA200 is present in mammals, plants and worms but is not found in other common model organisms like the fission yeast *Schizosaccharomyces pombe* or the fruit fly *Drosophila melanogaster* (Ustrell et al., 2002). The sequence identity between human and mouse PA200 is 90% but only 17% between human PA200 and *S. cerevisiae* Blm10 (Ustrell et al., 2002). Both PA200 and Blm10 are substochiometrically associated to the  $\alpha$  rings of the CP and can either cap the CP on one or both sides (Ortega et al., 2005; Schmidt et al., 2005; Lehmann et al., 2008). Furthermore, as seen for 11S regulators, a hybrid proteasome can form consisting of CP, RP and PA200/Blm10 (Schmidt et al., 2005).

Blm10 is a single-chain protein consisting of 2143 amino acids and has a molecular mass of 246 kDa. It is a non-essential protein and multiple functions have been proposed. First, the hybrid proteasome Blm10-CP-RP is required for the degradation of the transcription factor Sfp1. The role that Blm10 plays in this process is unknown. It might have a targeting function leading the proteasome to its substrate, or it might be involved in substrate recognition (Rechsteiner & Hill, 2005; Lopez et al., 2011). Furthermore, Blm10 is involved in proteasome maturation since the analysis of isolated proteasomal precursor complexes showed that Blm10 can be associated with proteasomal precursor complexes (Fehlker et al., 2003; Li et al., 2007; Marques et al., 2007). The function of Blm10 in CP maturation is to slow the processing of the  $\beta$ 5-propeptide, which allows the complex to mature properly. Deletion of Blm10 therefore results in an acceleration of the propeptide processing and CP maturation (Fehlker et al., 2003). However, this deletion has only a modest effect since the RP was proposed to function partly redundantly (Marques et al., 2007). Blm10 cannot

## Introduction

only bind to proteasomal precursors but also to mature proteasomes to form the CP-Blm10, the Blm10-CP-Blm10 or the hybrid Blm10-CP-RP complexes (Schmidt et al., 2005). Binding of Blm10 to the CP enhances its peptide cleavage activity and therefore Blm10 functions as a proteasome activator (Schmidt et al., 2005; Dange et al., 2011). However, with the exception of the unstructured protein substrate tau-441, the degradation of proteins has so far not been found to be enhanced (Schmidt et al., 2005; Dange et al., 2011). Controversially, Blm10 was also found to participate in the quality control of CPs and to inhibit the activity of proteasomes with prematurely opened gates. Inappropriately opened  $\alpha$  rings are recognized and subsequently closed by Blm10 binding (Lehmann et al., 2008).

New insights into whether Blm10 is an activator or an inhibitor of the proteasome were given by the crystal structure of the Blm10-CP-Blm10 complex (Sadre-Bazzaz et al., 2010).

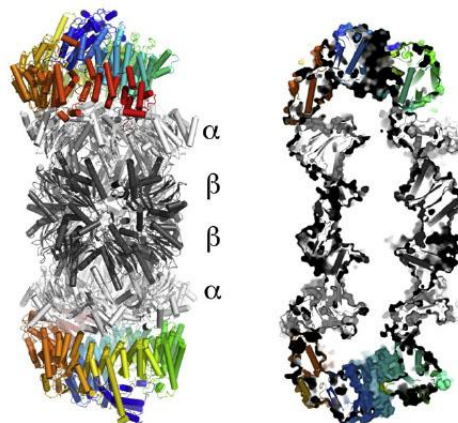


Figure 5: Crystal structure of the Blm10-CP-Blm10 complex. The CP (light and dark grey) is capped on each side by one molecule of Blm10 (colored). Blm10 forms a closed dome on top of the CP and the entrance gates formed by the  $\alpha$  rings are partly opened. Figure: Sadre-Bazzaz et al., 2010.

Blm10 consists of 32 highly variable HEAT-like repeats (Kajava et al., 2004; Sadre-Bazzaz et al., 2010). Each HEAT-like repeat is formed by two helices and a connecting turn. Two repeats are connected with each other by a linker sequence. In the case of Blm10, one helix is 8-35 residues long, the turns are 2-87 residues and the linkers are 1-88 residues. One molecule of Blm10 interacts with all seven  $\alpha$  subunits of one  $\alpha$  ring (Iwanczyk et al., 2006). Therefore, Blm10 forms a closed dome-like structure on top of the CP and only one small opening is detectable at the side of Blm10. This pore is 13 Å by 22 Å and is thought to be too small to allow the passage of a polypeptide, but could allow the passage of peptides (Sadre-Bazzaz et al.,



2010). As observed for all proteasome activators, binding of Blm10 to the CP induces a gate opening of the  $\alpha$  rings. Instead of a fully opened state as observed with the binding of 11S regulators, the gates seem to be in a disordered state when Blm10 is bound (Förster et al., 2003; Förster et al., 2005; Sadre-Bazzaz et al., 2010). The mechanism of gate opening between 11S regulators and Blm10 is nevertheless similar. In the case of Blm10, Pro17 of the  $\alpha$ 5 subunit interacts with the C-terminus of Blm10, which induces the ordering of the Tyr8 and Asp9 residues and results in a disordered gate opening, which is further stabilized by Blm10 (Sadre-Bazzaz et al., 2010).

The published crystal structure of the Blm10-CP-Blm10 complex explains why Blm10 has proteasome activating and inhibiting functions. The function of Blm10 might depend on its stoichiometry with the CP and thus whether the Blm10-CP or the Blm10-CP-Blm10 complex is formed. In the Blm10-CP-Blm10 complex, both entrances to the CP are blocked for protein substrates, in agreement with its proposed function as an inhibitor that recognizes inappropriately opened  $\alpha$  rings (Lehmann et al., 2008). The small pore at the side of Blm10 seems too small for a polypeptide but might allow the passage of peptides. Since the proteasome gates open in a disordered state upon binding of Blm10, peptides entering through the small pore can reach the catalytic chamber and be proteolytically processed in a Blm10-CP complex. Therefore an increase in peptide turnover can be observed (Schmidt et al., 2005; Dange et al., 2011).

### **1.9. Biogenesis of the 20S core particle in yeast**

The expression of genes encoding proteasomal subunits is regulated by the proteasome interacting protein Rpn4. Rpn4 activates transcription by binding to a PACE element (proteasome-associated control element), a nonameric sequence that is located upstream of many genes associated with proteasome function (Mannhaupt et al., 1999). 12 of the 14 different genes encoding subunits of the CP, all genes encoding the ATPase subunits Rpt1-6 and most of the genes encoding non-ATPase subunits contain this sequence element (Mannhaupt et al., 1999). Rpn4 also participates in the regulation of the expression of proteins that are involved in ubiquitylation, such as Ubi4 (Mannhaupt et al., 1999). Proteasomal gene expression is regulated in a negative feedback circuit. The transcription activator Rpn4 induces gene expression,

## Introduction

associates with the RP subunit Rpn2 and is then itself degraded by the proteasome (Xie & Varshavsky, 2001; Wang et al., 2008).

The 20S proteasome is assembled from 28 subunits. The archaeobacterial CP consists only of two different subunits: the  $\alpha$  subunit and the  $\beta$  subunit. Both subunits from *T. acidophilum* can be co-expressed in *E. coli*, which results in the formation of functional proteasome complexes (Zwickl et al., 1994). For eukaryotic proteasomes, the assembly pathway is more complex since 14 different subunits have to be orchestrated in order to find their exact position in the nascent complex.

The assembly of the eukaryotic CP starts with the formation of the  $\alpha$  subunit ring. In contrast to the archaeobacteria proteasome, eukaryotic proteasomes require assistance from chaperones since the individual subunits do not recognize their respective position in the nascent  $\alpha$  ring (Gerards et al., 1997; Gerards et al., 1998). Two pairs of chaperones are responsible for the formation of correctly assembled  $\alpha$  rings. In yeast they were found to be Pba1-Pba2 (PAC1-PAC2 in mammals) and Pba3-Pba4 (PAC3-PAC4 in mammals; Hirano et al., 2005; Le Tallec et al., 2007; Yashiroda et al., 2008; Kusmierczyk et al., 2008). Pba1-Pba2 is involved in early steps of  $\alpha$  ring assembly (Hirano et al., 2005). During  $\alpha$  ring assembly, Pba3-Pba4 associates with the nascent precursor to orchestrate late stages of  $\alpha$  ring formation and to initiate  $\beta$  ring formation (Hirano et al., 2006; Kusmierczyk et al., 2008; Yashiroda et al., 2008). At this stage, an intermediate complex called 15S precursor consisting of all  $\alpha$  subunits,  $\beta$ 2,  $\beta$ 3 and  $\beta$ 4 plus the chaperones Pba1-Pba2, Ump1 or Blm10 can be isolated from yeast (Nandi et al., 1997; Li et al., 2007). The small maturase Ump1 associates with the nascent proteasomal precursor during  $\beta$  ring formation and is required for late steps of proteasome maturation (Ramos et al., 1998; Li et al., 2007). The next isolated intermediate complex is the so called half-CP consisting of the same subunits as the 15S complex and additionally containing the subunits  $\beta$ 1,  $\beta$ 5 and  $\beta$ 6 (Li et al., 2007). After the incorporation of  $\beta$ 7, two half-CPs form a short-lived intermediate, the so-called pre-holo-CP (Li et al., 2007).

Five of seven  $\beta$  subunits ( $\beta$ 1,  $\beta$ 2,  $\beta$ 3,  $\beta$ 4 and  $\beta$ 5) are synthesized with propeptides, which prevent the formation of premature catalytically active complexes (Groll et al., 1997; Groll et al., 1999). Additionally, these propeptides seem to be of importance for the assembly of the CP *per se* since the presence of the  $\beta$ 5-propeptide has been

shown to be essential for the incorporation of the subunit into the nascent CP (Chen & Hochstrasser, 1996). After the pre-holo-CP has formed, the propeptides are cleaved off autocatalytically (Seemüller et al., 1996). Ump1 and Blm10 have been shown to participate in  $\beta$ -propeptide processing (Fehlker et al., 2003; Ramos et al., 1998). The role of Blm10 is thought to slow  $\beta$ 5-propeptide processing (Fehlker et al., 2003; see also section 1.8 for details on the function of Blm10). Ump1 plays a critical role in propeptide processing as its deletion causes a premature processing of the propeptides (Ramos et al., 1998). After the association of two half-CPs, Ump1 is trapped inside the catalytic chamber of the proteasome. When the autocatalytic cleavage of the propeptides is completed, the catalytically active subunits degrade Ump1 (Ramos et al., 1998).

### **1.10. Proteasome localization in yeast**

The proteasome was found to be essential for cell cycle progression and to participate in protein degradation such as ERAD (ER Associated Degradation). To fulfill both of these functions, it is necessary that it localizes both to the nucleus as well as to the cytoplasm, and that the intracellular distribution can be regulated. In yeast, proteasome localization can be easily monitored by direct fluorescence microscopy (Enenkel et al., 1999). Yeast genes are easily manipulated by homologous recombination techniques (Orr-Weaver et al., 1981; Sikorski & Hieter, 1989), which allows the replacement of endogenous proteasome subunits with GFP-tagged versions which were shown to be fully incorporated into proteasomes (Wendler et al., 2004; Lehmann et al., 2008; Laporte et al., 2008). Subsequently, the localization of GFP-tagged proteasomes can be examined by direct fluorescence microscopy.

In yeast cells, the localization of proteasomes is dependent on the growth phase of the cells (Laporte et al., 2008). In dividing yeast cells, approximately 80% of all proteasomes are found to be localized to the nucleus or to the nuclear envelope and the majority of CPs in this growth phase is associated with one or two RPs (Enenkel et al., 1998; Russell et al., 1999; Bajorek et al., 2003). The localization of the proteasomes to the nucleus suggests that its function there is primarily to degrade short-lived proteins and to regulate cell cycle progression. Yeast proteasomes are imported from the cytosol into the nucleus as inactive precursor complexes and maturation is completed there (Lehmann et al., 2002).

## Introduction

When yeast cells reach quiescence, the localization of their proteasomes changes significantly (Laporte et al., 2008). Nuclear proteasomes first move to the nuclear periphery. Later, they are translocated out of the nucleus and concentrated in dot-like structures that are localized close to the nucleus. In prolonged quiescence, these granules move further away from the nucleus and only a small portion of proteasomes remains localized to the nuclear periphery (Laporte et al., 2008). CPs and RPs show colocalization in all growth phases (Laporte et al., 2008). The proteasome-containing granules were named PSGs (proteasome storage granules). Importantly, these highly motile structures are not surrounded by a membrane and do not contain aggregated proteins. When cells leave quiescence after the addition of fresh glucose to the media and start dividing again, PSGs dissolve within a few minutes.

In quiescent yeast cells, different dot-like structures can be found. PSGs are therefore not identical to actin-containing bodies or P-bodies, which contain RNA and RNA modifying proteins (Laporte et al., 2008). The trigger for PSG formation was identified as a lack of glucose in the media and subsequent decrease of intracellular ATP levels and increase of AMP levels (Laporte et al., 2008; Laporte et al., 2011). A recently published study proposed that the lack of glucose causes a decrease in the intracellular pH during quiescence, which functions as the main trigger for PSG formation (Peters et al., 2013). The reason for PSG formation is not understood very well, but two possibilities were proposed previously. PSGs might, as suggested by the name, serve the storage of mature proteasomes in quiescence to avoid an energy- and time-consuming proteasomal *de novo* synthesis when cells leave quiescence and resume proliferation (Laporte et al., 2008). PSG formation might thereby also protect proteasomes against autophagocytosis (Peters et al., 2013). A second study proposed that the granules represent a major site of protein degradation (Kaganovich et al., 2008). The latter study identified two different kinds of granules in yeast and mammalian cells in which proteasomes were inhibited, resulting in cell cycle arrest. The granules were called JUNQ (juxtanuclear quality control compartment) and IPOD (insoluble protein deposit) and contain misfolded proteins. In JUNQs, the misfolded proteins were soluble and proteasomes were recruited to them, suggesting they might represent the same structures as PSGs. Colocalizing proteasomes were thought to degrade misfolded polyubiquitylated proteins in these structures (Kaganovich et al., 2008).

## Introduction

In higher eukaryotes, proteasome localization differs within the organism. Isolations of proteasomes derived from different tissues and cell compartments revealed that the proteasome localizes both to the nucleus and the cytosol, but, dependent on the cell type, in different ratios (Tanaka et al., 1990). Furthermore, studies in *Drosophila* embryos showed that the localization of proteasomes changes within a cell during different stages of development (Haass et al., 1989). A correlation between proteasome localization and function was given by the examination of proteasome localization in neuronal cells. Upon depolarisation, proteasomes were shown to move from dendritic shafts to dendritic spines with the purpose of moving their degradative capacity to a different area in the cell (Bingol & Schuman, 2006).

### 1.11. Nuclear transport

The nuclear envelope (NE) is the barrier that separates the cytoplasm from the nucleoplasm. It is formed by a double membrane in which the nuclear pore complexes (NPCs) are embedded. NPCs form the connective portals between the cytosol and the nucleus. Their main function is on the one hand to guarantee free diffusion of small molecules such as water, small metabolites, ions or peptides between the cytoplasm and the nucleus, and on the other hand to exclude macromolecules from non-specific translocation into or out of the nucleus. The size limit of molecules that can pass through NPCs by diffusion is either 40 kDa or 5 nm. Cargoes that are above that limit have to be specifically transported through nuclear pores. The size limit for this specific transport is 39 nm.

NPCs are cylindrical complexes with an overall octagonal structure. They are 100-150 nm in diameter and 50-70 nm in width. The central pore is 50 nm long and 30 nm in diameter (reviewed in Wentz & Rout, 2010). In yeast, one NPC consists of approximately 30 different proteins, but since NPCs exist in eightfold symmetry and each protein is present in multiple copies, one NPC is formed by approximately 400 proteins (Rout et al., 2000). The shape of the NPC is determined by a so-called core complex formed by four rings, which function as scaffolds and also provide stability for the whole complex. In yeast, the two inner rings are formed by the Nup170 complex and the two outer rings by the Nup84 complex (Aitchison et al., 1995; Siniosoglou et al., 1996). Structurally, core proteins have related secondary structures. They consist mostly of  $\beta$ -propeller folds,  $\alpha$ -solenoid folds or a mixture of both

## Introduction

(Devos et al., 2006). The core complex is attached to the luminal ring formed by integral membrane proteins, which anchor the NPC in the double membrane (Nehrbass et al., 1996; Alber et al., 2007). Filamentous proteins are attached to the core complex, which form a basket-like structure on the nuclear side (Stoffler et al., 2003). Attached to the inner rings is furthermore a ring formed by linker nucleoporins. Linker nucleoporins are the main binding site for a group of proteins called FG-Nups (Alber et al., 2007). FG-Nups are nucleoporins that contain natively unfolded regions which are enriched in phenylalanine (F) and glycine (G) residues (Radu et al., 1995b; Denning et al., 2003).

The translocation of macromolecules larger than 5 nm or 40 kDa requires specific interactions with the NPCs. Cargoes thereby associate to soluble transport factors that interact themselves with FG-Nups (Adam et al., 1990). These transport factors are also termed karyopherins, transportins and importins or exportins. Importins and exportins identify their cargo with the aid of sequence motifs that are located in it (Imamoto et al., 1995). NLSs (Nuclear Localization Sequences) ensure the import of a protein into the nucleus and the artificial fusion of an NLS to a protein is sufficient for its translocation. Amino acid sequences of NLSs in proteins are variable, and for most importins, it is unknown which sequences they potentially recognize (Wente & Rout, 2010). The cNLS (classical Nuclear Localization Sequences) was the first NLS to be recognized. It consists of the short amino acid motif KKKRK (Goldfarb et al., 1986). The so-called bi-partite NLS consists of two sequence motifs of basic amino acids that are separated by a roughly 10 amino acid long spacer sequence (Dingwall et al., 1988). The presence of a NES (nuclear export signal) in a protein provides its export out of the nucleus. NES are leucine-rich sequences and the amino acid sequence of the classical NES is LXXXLXXLXL. The presence of both a NLS and a NES causes the cyclic import and export (Wente & Rout, 2010). Currently, many different import and export signals have been identified, and some of them have only weak similarity with the classical import and export signals.

When a cargo is translocated, the importin binds to the cargo and transports it to the NPC. At the NPC, the importin interacts with FG-Nups and mediates the translocation through the NPC. Several models for the mechanism of the translocation process are currently proposed (reviewed in Macara, 2001; Wente & Rout, 2010). In one model, the FG-Nups seem to function as 'polymer brushes' that keep macromolecules from translocation by sweeping them away. Importins interact with the FG-Nups and

## Introduction

thereby facilitate the translocation (Rout et al., 2000). In a second model, FG-Nups form a dense network and the binding of the importin partially destroys this network allowing the passage of the importin-cargo complex (Lim et al., 2007). In the 'saturated' or 'hydrophobic gel' model, the side chains of the phenylalanines in the FG-Nups are proposed to be cross-linked, and interaction of the importin with the FG-Nups destroys these cross-links (Frey et al., 2006; Ribbeck & Görlich, 2002). Prove was found for all proposed models, so that a combination of the models is conceivable (Wente & Rout, 2010).

The nuclear import cycle starts with the binding of the importin to the NLS of its cargo. The importin subsequently mediates the contact to and the translocation through the NPC by interacting with Nups. After the translocation into the nucleus, the small protein Ran (Ras-related nuclear protein) binds to the importin-cargo complex. Ran is a GTPase that is found in the nucleus mainly in its GTP-bound form and in the cytosol in its GDP-bound form. Binding of Ran-GTP to the importin-cargo complex reduces the affinity of the importin to its cargo resulting in its release (Moore & Blobel, 1993; Rexach & Blobel, 1995; Floer & Blobel, 1996). The dimeric Ran-GTP-importin complex is then exported into the cytoplasm, where the RanGAP (GTPase activating protein) together with a RanBP (Ran binding protein) activates the GTPase activity of Ran. The hydrolysis of GTP to GDP dissociates Ran-GDP and the importin and Ran-GDP is subsequently recycled to the nucleus. Back in the nucleus, a RanGEF (Ran guanine nucleotide exchange factor) exchanges the GDP with a GTP and the translocation cycle can re-start.

## Introduction

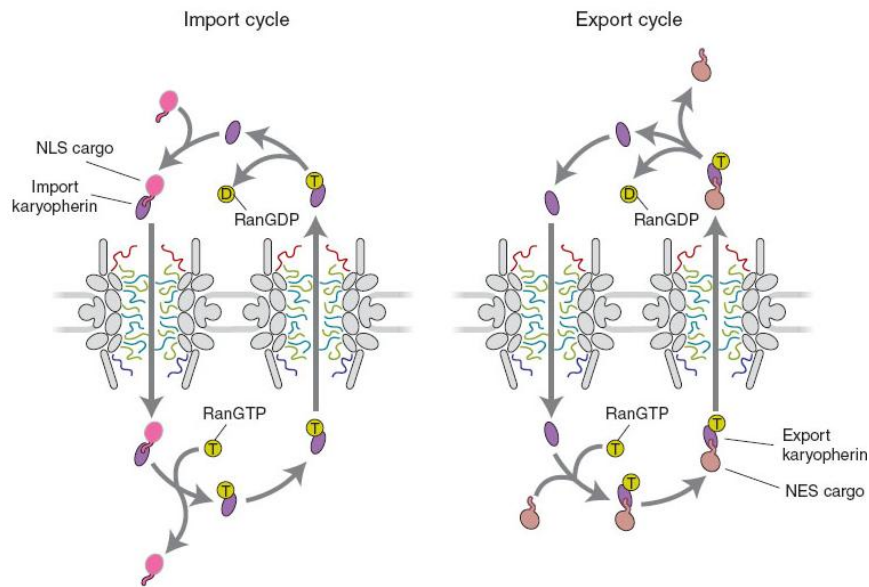


Figure 6: The nuclear import (left) and export (right) cycle. The import cargo (pink) binds to its importin (purple) and the dimeric complex is translocated through the NPC. The translocation is mediated by the interaction of the importin with components of the NPC. In the nucleus, Ran-GTP (yellow) binds to the complex and causes the release of the cargo. The Ran-GTP-importin complex is transported out of the nucleus, where GTP is hydrolyzed to GDP and importin and Ran-GDP dissociate. Export cargoes (dark pink) form in the nucleus a trimeric complex with their exportin and Ran-GTP. The complex is translocated and GTP is hydrolyzed in the cytosol, which results in the dissociation of the complex. Figure: Wentz & Rout, 2010.

The Ran-GTP-Ran-GDP gradient ensures the directionality of nuclear transport (Richards et al., 1997). The maintenance of the gradient is only possible because Ran has by itself a very low GTPase activity and nucleotide exchange rate so that almost no nucleotide hydrolysis occurs in the nucleus and no nucleotides are exchanged in the cytosol (Klebe et al., 1995a; Klebe et al., 1995b). The spatial separation of the RanGAP in the cytosol and the RanGEF in the nucleus is necessary to increase these activities drastically and thereby to maintain the gradient (Klebe et al., 1995b).

In yeast, two homologues of Ran, Gsp1 and Gsp2, exist. Gsp1 and Gsp2 have 97% sequence identity with each other, but only Gsp1 is essential for cell viability (Belhumeur et al., 1993). The essential protein Prp20 functions as RanGEF (Amberg et al., 1993), Rna1 as RanGAP (Becker et al., 1995) and Yrb1 is the homologue of the human RanBP1 (Butler & Wolfe, 1994).

Proteins with a classical mono- and bipartite NLS are not imported by one importin, but by a complex formed by the importins  $\alpha$  and  $\beta$  (Radu et al., 1995a). Importin  $\alpha$  thereby represents an adaptor that associates to the cargo and to importin  $\beta$  (Görlich et al., 1995; Moroianu et al., 1995). Importin  $\beta$  itself does not interact with the cargo



## Introduction

but holds all other functions of importins, namely the interaction with the NPC and Ran-GTP (Radu et al., 1995a).

The nuclear export cycle occurs in a similar fashion as the import cycle. In the nucleus, the exportin recognizes its cargo via a NES located in the cargo and forms with the cargo and Ran-GTP the trimeric Ran-GTP-exportin-cargo complex (Kutay et al., 1997; Askjaer et al., 1998). In contrast to the import cycle, Ran-GTP association with the exportin increases the affinity of the exportin to its cargo (Kutay et al., 1997). The trimeric complex is subsequently translocated into the cytosol, where Ran-bound GTP is hydrolyzed to GDP resulting in the dissociation of Ran-GDP, the cargo and the exportin.

In budding yeast 14 different transportins, but only one adaptor protein, named Kap60, Srp1 or karyopherin  $\alpha$  were identified (Enenkel et al., 1995; Fries et al., 2007). Importins share only weak sequence identity, but a common feature of their structure is a tandem HEAT repeat fold with antiparallel helices that are connected by a turn (Wente & Rout, 2010). Analyses of proteins that function as importins revealed strong heterogeneity in their Ran binding sites and, aside from an acidic cluster and an N-terminally located CRIME region, no conserved and invariant residues or sequences involved in Ran-GTP binding could be identified (Enenkel et al., 1996; Görlich et al., 1997; Vetter et al., 1999a; Macara, 2001). Therefore, the identification of new importins based on their primary structure is difficult (Macara, 2001; Wozniak et al., 1998). Binding of Ran-GTP to the importin occurs with different affinities, ranging from interactions that are hard to detect to interactions with high affinities (Macara, 2001). Most importins in yeast are non-essential genes, indicating that cargo specificity between different importins may be overlapping (Marelli et al., 1998).

### **1.12. Nuclear transport of proteasomes**

The localization of proteasomes is dynamic and it changes with the metabolic state of the cell (Laporte et al., 2008). In dividing yeast cells, the CP mainly localizes to the nucleus (Enenkel et al., 1998; Russell et al., 1999). Newly synthesized CPs are imported as inactive precursor complexes from the cytosol into the nucleus where the final steps in maturation occur (Lehmann et al., 2002). Proteasomal precursor complexes are too large to be translocated by diffusion and furthermore their translocation has to be regulated strictly. Therefore, two different conformational states were

proposed: one in which proteasomes are capable of being transported through nuclear pores, and one in which they are not (Tanaka et al., 1990). The capability to be transported is located in the N-termini of the  $\alpha$  subunits.  $\alpha$  subunits derived from different species show a conserved extension in which a cNLS is located (Tanaka et al., 1990; Zwickl et al., 1992). This cNLS is accessible in proteasomal precursor complexes, but is masked in mature CPs due to conformational changes that occur during maturation (Tanaka et al., 1990; Lehmann et al., 2002). The import of precursor complexes occurs via the classical import pathway using the transport receptors importin  $\alpha$  and importin  $\beta$ . In contrast, the masked cNLS in mature CPs are not recognized by the transport receptor complex importin  $\alpha\beta$  (Lehmann et al., 2002).

In the case of the RP, functional cNLS recognized by importin  $\alpha$  were identified in Rpn2 and Rpt2. However, only deletion of the cNLS in Rpn2 resulted in mislocalization of the RP base at elevated temperatures, indicating that this cNLS might be mainly responsible for RP base import. At lower temperatures, deletion of this NLS could be compensated, therefore it was suggested that the function of the cNLSs is redundant (Wendler et al., 2004). In contrast to the RP base, the lid itself is not recognized by importin  $\alpha$ . Most likely, its import occurs with the assistance of adaptor proteins. In *S. cerevisiae*, Sts1 associates with Rpn11 and with its NLS with importin  $\alpha$  (Chen et al., 2011). Similarly, Yin6 mediates the contact of the lid subunit Rpn5 and importin  $\alpha$  in *S. pombe* (Yen et al., 2003a; Yen et al., 2003b).

### 1.13. Thesis Rationale

The discovery of the formation of PSGs in quiescent yeast cells opened a new field in the research on proteasomes, and showed that proteasome localization is not static but a dynamic process (Laporte et al., 2008). At the beginning of this study, it was unknown how proteasome CPs and RPs are transported into PSGs and how they are re-imported into the nucleus after PSG dissolution.

This study can be separated into three parts:

- To study the PSG formation
- To further determine the function of PSGs
- To investigate the mechanism of CP re-import

## Introduction

To address the first question, it was examined whether the proteasome activator Blm10 was involved in PSG formation. Direct fluorescence microscopy was used to reveal whether its mutation or deletion affected CP and RP export or sequestration.

Two controversial hypotheses on the function of PSGs were proposed previously. One study suggested a simple storage function for PSGs, whereas the second study brought PSGs in context with protein degradation (Laporte et al., 2008; Kaganovich et al., 2008). To further investigate the function of PSGs, the configuration of proteasomes sequestered to PSGs was analyzed by native PAGE in this study. Additionally, the degradation of the cytosolic substrate  $\Delta$ ss-CPY\* was examined in a wildtype strain and in a strain with disturbed PSG formation.

The main part of this work focused on the proteasome activator Blm10 and its potential role in CP re-import. Due to structural similarities between Blm10 and importins, Blm10 was previously brought in context with protein transport or targeting (Glickman & Raveh, 2005). Fluorescence microscopy revealed that deletion of *BLM10* resulted in a delay in the import of the mature CP. Therefore the main objective of this work was to examine the hypothesis that Blm10 might function as importin for mature CPs. To achieve this, it was tested in a collaborative project whether Blm10 induces CP uptake into reconstituted *Xenopus* egg nuclei. Additionally, the major steps of the CP re-import were experimentally reconstructed using *in vivo* and *in vitro* methods to examine whether Blm10 meets common criteria of importins.



## 2. Material and methods

### 2.1. Material

#### 2.1.1. Antibodies

Table 1: List of antibodies used in this work

Antibody	Used dilution	Source
Mouse $\alpha$ -GFP (JL-8)	1:1000	Clontech
Mouse $\alpha$ -HA 16B12	1:10.000	Covance
Mouse $\alpha$ -His	1:1000	Abgent
Mouse $\alpha$ -Myc	1:1000	Sigma
Mouse $\alpha$ -Penta-His	1:1000	Qiagen
Mouse $\alpha$ -PGK	1:10.000	Molecular Probes, Eugene, USA
Rabbit $\alpha$ - $\beta$ 7	1:5000	W. Heinemeyer
Rabbit $\alpha$ -Blm10	1:20.000	C. Enenkel
Rabbit $\alpha$ -Kar2	1:10.000	R. Schekman
Rabbit $\alpha$ -Ran	1:5000	E. Hurt
Rabbit $\alpha$ -Rpt1	1:20.000	W. Heinemeyer
Goat $\alpha$ -rabbit, HRPO conjugated	1:10.000	Dianova, Hamburg, Deutschland
Goat $\alpha$ -mouse, HRPO conjugated	1:10.000	Dianova, Hamburg, Deutschland
Goat $\alpha$ -rabbit, HRPO conjugated	1:5000	Jackson Immuno Research
Rabbit $\alpha$ -mouse, HRPO conjugated	1:5000	Jackson Immuno Research

#### 2.1.2. Enzymes

*Bam*H1: Thermo Fisher Scientific

*Pst*I: Thermo Fisher Scientific

*Xho*I: Thermo Fisher Scientific

T4-DNA-Ligase: Thermo Fisher Scientific

Phusion High-Fidelity DNA Polymerase: Thermo Fisher Scientific

Phusion High-Fidelity DNA Polymerase: New England Biolabs

Apyrase: Sigma

Biotinylated Thrombin: EMD Millipore

## Material and methods

TEV protease: Roboklon

All enzymes were used with the buffers and at the reaction conditions recommended by the manufacturer.

### **2.1.3. Ladders and standards**

#### DNA ladder

1kb ladder: Carl Roth GmbH

GeneRuler™ 1kb Plus DNA Ladder: Thermo Fisher Scientific

TrackIt™ 1 Kb Plus DNA Ladder: Invitrogen

#### Protein ladder

PageRuler™ Prestained Protein Ladder: Thermo Fisher Scientific

### **2.1.4. Kits**

ECL™ Western Blotting-Kit mit Hyperfilm ECL (Amersham, Little Chalfont, UK)

GeneJET™ Plasmid Miniprep Kit (Thermo Fisher Scientific)

MasterPure™ Yeast DNA Purification Kit (Epicentre Biotechnologies)

NucleoSpin® Extract II kit (Macherey-Nagel, Düren, Deutschland)

Pierce® ECL Western Blotting Substrate (Thermo Fisher Scientific)

Protein Assay (Bio-Rad Laboratories)

QIAprep® Spin Miniprep Kit (Qiagen)

QIAquick® PCR Purification Kit (Qiagen)

Thrombin Cleavage Capture Kit (EMD Millipore)

## 2.1.5. Chemicals and consumables

Table 2: List of chemicals and consumables used in this work

<b>Chemical</b>	<b>Manufacturer</b>
Ampicillin	Carl Roth GmbH
Ampicillin	BioShop Canada
Bacto™ Pepton	BD
Bacto™ Trypton	BD
Bio-Spin® Disposable Chromatography Columns	Bio-Rad Laboratories
BioTrace™ NT Nitrocellulose Blotting Membrane	Pall Life Sciences
BioTrace™ PVDF Blotting Membrane	Pall Life Sciences
Complete Protease Inhibitor Cocktail	Roche
Cycloheximide	Sigma
Desthiobiotin	Sigma
Ethidium bromide	Roth
Ethidium bromide	BioShop
Glutathione-Agarose	Sigma
Glutathione Sepharose 4B	GE Healthcare
HABA	Sigma
HisPur™ Ni-NTA Resin	Thermo Fisher Scientific
IgG Sepharose™ 6 Fast Flow	GE Healthcare
IPTG	BioShop
LB broth Lennox	BioShop
MG-132	Abmole
Ni-NTA Agarose	Qiagen
Nurseothricin	Werner BioAgents
Peptone	BioShop Canada
Phleomycin	Santa Cruz Biotech
Poly-Prep® Chromatography Columns	Bio-Rad Laboratories
RedSafe™ Nucleic Acid Staining Solution	Intron
Strep-Tactin® matrix	IBA BioTAGnology
Yeast extract	BD, Sparks, USA
Yeast extract	BioShop Canada
Yeast nitrogen base w/o aa	Invitrogen

All common chemicals and consumables were obtained from typical suppliers.

All amino acids were obtained from Sigma.

**2.1.6. Instruments and software**

Table 3: List of instruments used in this work

<b>Instrument</b>	<b>Manufacturer</b>
Amicon <sup>®</sup> Ultra-4 Centrifugal Filter Units	Millipore
Avanti J-26 XP	Beckman Coulter
Axio Imager.Z1 fluorescence microscope	Carl Zeiss
Centrifuge 5417R	Eppendorf
Centrifuge 5810R	Eppendorf
DMR Fluorescence microscope	Leica
EnSpire <sup>™</sup> 2300 Multilabel Reader	PerkinElmer
French <sup>®</sup> Pressure Cell Press	SLM Instruments
French <sup>®</sup> Pressure Cell Press	Thermo Spectronic
Gel Doc 2000	Bio-Rad Laboratories
Gene Pulser	Bio-Rad Laboratories
L8-70M Ultracentrifuge	Beckman Coulter
MiniCycler <sup>™</sup>	MS Research
Mini-Protean <sup>®</sup> Tetra Electrophoresis System	Bio-Rad Laboratories
Mini-Sub <sup>®</sup> Cell GT Cell DNA Electrophoresis	Bio-Rad Laboratories
Mini Trans-Blot <sup>®</sup> Cell	Bio-Rad Laboratories
Novaspec II Photometre	Pharmacia, Uppsala, Schweden
Objective 100x	PL Fluostar
Objective Plan-Apochromat 100x/1.4 Oil DIC	Carl Zeiss AG
Optimax TR Film Developer	MS Laborgeräte
ORCA-ER camera	Hamamatsu Photonics
Owl HEP-1	Thermo Fisher Scientific
PowerPac <sup>®</sup> Basic Power Supply	Bio-Rad Laboratories
PowerPac <sup>®</sup> HC High Current Power Supply	Bio-Rad Laboratories
Rotor JLA-8.1	Beckman Coulter
Rotor SS-34	Thermo Fisher Scientific
Rotor SW40	Beckman Coulter
Sorvall <sup>®</sup> RC 5C Plus	Thermo Fisher Scientific
Sorvall <sup>®</sup> RC 6 <sup>™</sup> Plus	Thermo Fisher Scientific
SRX-101A Film Developer	Konica Minolta
Thermomixer comfort	Eppendorf
Typhoon Trio	GE Healthcare



## Material and methods

Ultrospec	LKB Biochrom
Volocity <sup>®</sup> Software	Improvision
X- Cite <sup>®</sup> Series 120 mercury lamp	EXFO

### 2.2. Media and strains

All media used for *E. coli* or yeast cell cultures and all buffers used in this work were prepared with Milli-Q ultrapure water. All media were autoclaved at 121.5°C for 25 min prior to usage.

Solid media additionally contained 2% agar.

#### 2.2.1. Media for cultivation of *E. coli*

##### LB broth

pH 7.5	
1%	Yeast extract
1%	Bacto peptone
0.5%	NaCl

Alternatively, premixed LB powder (LB broth Lennox) was used as recommended by the manufacturer (Bioshop Canada).

Cells containing a plasmid encoding for an ampicillin resistance gene were grown in media supplemented with 100 µg/ml ampicillin.

##### SOC-Medium (Super Optimal Broth)

pH 7.4	
0.5%	Yeast extract
2%	Bacto tryptone
0.4%	D-Glucose
10 mM	NaCl
2.5 mM	KCl
10 mM	MgCl <sub>2</sub>
10 mM	MgSO <sub>4</sub>

## Material and methods

### 2.2.2. Growth media for *S. cerevisiae*

#### Rich Medium (YPD medium)

pH 5.5	
1%	Yeast extract
2%	Peptone
2%	D-Glucose

#### Complete minimal medium (CM medium)

pH 5.6	
0.17%	Yeast nitrogen base w/o amino acids
0.5%	(NH <sub>4</sub> ) <sub>2</sub> SO <sub>4</sub>
2%	D-Glucose
0.17%	Dropout powder

For an induction with Galactose, 2% D-(+)-Galactose instead of 2% D-Glucose were used.

#### Dropout powder

40 µg/ml	Adenine (hemisulfate salt)
20 µg/ml	L-arginine (HCl)
100 µg/ml	L-asparatic acid
100 µg/ml	L-glutamic acid (monosodium salt)
30 µg/ml	L-lysine (mono-HCl)
20 µg/ml	L-methionine
50 µg/ml	L-phenylalanine
375 µg/ml	L-serine
200 µg/ml	L-threonine
30 µg/ml	L-tyrosine
150 µg/ml	L-valine

Dropout powder did not contain L-histidine, L-leucine, L-tryptophan and L-uracil. For the selection of an auxotrophy marker, the following amino acid had to be supplemented separately.

## Material and methods

50 µg/ml	L-histidine
60 µg/ml	L-leucine
40 µg/ml	L-tryptophan
50 µg/ml	L-uracil

For selection of yeast cells containing the resistance gene *natMX*, 100 µg/ml nourseothricin was added to the media.

### 2.2.3. *S.cerevisiae* strains

Table 4: List of *S. cerevisiae* strains used in this work

Strain	Genotype	Source
WCGa Wt	<i>MATa his3-11,15 leu2-3,112 ura3-52 can GAL</i>	Heinemeyer et al., 1993
Wt β5-GFPS HTA2-cherry	<i>MATa his3-11,15 leu2-3,112 ura3-52 can GAL HTA2-RFP-natMX PRE2-GFPS-HIS3-URA3</i>	J. Jando
Wt β5-GFPS	<i>MATa his3-11,15 leu2-3,112 ura3-52 can GAL PRE2-GFPS-HIS3-URA3</i>	Lehmann et al., 2008
WCGa <i>blm10Δ</i>	<i>MATa his3-11,15 leu2-3,112 ura3-52 can GAL blm10Δ::HIS3</i>	Fehlker et al., 2003
<i>blm10Δ</i> β5-GFPS	<i>MATa his3-11,15 leu2-3,112 ura3-52 can GAL blm10Δ::HIS3 PRE2-GFPS-HIS3-URA3</i>	Lehmann et al., 2008
Wt Rpn1-GFPS	<i>MATa his3-11,15 leu2-3,112 ura3-52 can GAL RPN1-GFPS-HIS3-URA3</i>	C. Enenkel
<i>blm10Δ</i> Rpn1-GFPS	<i>MATa his3-11,15 leu2-3,112 ura3-52 can GAL blm10Δ::HIS3 RPN1-GFPS-HIS3-URA3</i>	C. Enenkel
Wt Rpn11-GFPS	<i>MATa his3-11,15 leu2-3,112 ura3-52 can GAL RPN11-GFPS-HIS3-URA3</i>	C. Enenkel
<i>blm10Δ</i> Rpn11-GFPS	<i>MATa his3-11,15 leu2-3,112 ura3-52 can GAL blm10Δ::HIS3 RPN11-GFPS-HIS3-URA3</i>	C. Enenkel
<i>ump1Δ</i> Blm10-GFPHA	<i>MATa his3-11,15 leu2-3,112 ura3-52 can GAL ump1Δ::LEU2 Blm10-GFPHA-URA3-HIS3</i>	M. Fehlker
Wt β5-GFPS Ump1-HA	<i>MATa his3-11,15 leu2-3,112 ura3-52 can GAL PRE2-GFPS-HIS3-URA3 ump1::Ylplac128-UMP1-HA</i>	Lehmann et al., 2010

## Material and methods

<i>blm10Δ</i> β5-GFPS Ump1-HA	<i>MATa his3-11,15 leu2-3,112 ura3-52 can GAL</i> <i>blm10Δ::HIS3 PRE2-GFPS-HIS3-URA3</i> <i>ump1::Ylplac128-UMP1-HA</i>	Lehmann et al., 2010
<i>srp1-49</i> β5-GFPS	<i>MATa ade2-1 his3-11,15 leu2-3,112 ura3-1 trp1-Δ63</i> <i>can1-100 srp1-49 PRE2-GFPS-HIS3-URA3</i>	Weberruss et al., 2013
<i>srp1-49</i> β5-GFPS	<i>MATa ade2-1 his3-11,15 leu2-3,112 ura3-1 trp1-Δ63</i> <i>can1-100 srp1-49 BLM10-GFPHA-HIS3-URA3</i>	Weberruss et al., 2013
<i>blm10Δ</i> α4-HA- TAP	<i>MATa his3-11,15 leu2-3,112 ura3-52 can GAL</i> <i>blm10Δ::HIS3 PRE6-HA-Tev-PROA-HIS3-URA3</i>	C. Enenkel
<i>gsp1-1</i> Blm10- GFPHA	<i>MATα his3Δ200 leu2Δ1 trp1Δ63 ura3-52 gsp1-1 Blm10-</i> <i>GFPHA-URA3-HIS3</i>	J. Jando
Wt α4-HA-TAP	<i>MATa his3-11,15 leu2-3,112 ura3-52 can GAL PRE6-</i> <i>HA-Tev-PROA-HIS3-URA3</i>	C. Enenkel
<i>blm10Δ</i> α4-HA- TAP Leu	<i>MATa his3-11,15 leu2-3,112 ura3-52 can GAL</i> <i>blm10Δ::HIS3 PRE6-HA-Tev-PROA-LEU2</i>	C. Enenkel

### 2.2.4. *E. coli* strains

Table 5: List of *E. coli* strains used in this work

Strain	Genotype	Source
DH5α	F <sup>-</sup> endA1, <i>hsdR17</i> (r <sub>k</sub> -m <sub>k</sub> +), <i>glnV44</i> , <i>thi-1</i> , <i>recA1</i> , <i>gyrA</i> (Nal <sup>r</sup> ), <i>relA1</i> , Δ( <i>lac ZYA-argF</i> )U169, <i>deoR</i> , θ80 <i>lacZΔM15</i> + pGEX-Hul5 360-635	IBC, Stuttgart
XL10 Gold	<i>Tetr D(mcrA)183 D(mcrCB-hsdSMR-mrr)173</i> <i>endA1 supE44 thi-1 recA1 gyrA96 relA1 lac Hte</i> [F' <i>proAB lacIqZDM15 Tn10</i> (Tetr) Amy Cam <sup>r</sup> ]	Stratagene, La Jolla, USA
BL21 (DE3)	F <sup>-</sup> <i>ompT gal dcm lon hsdS<sub>B</sub></i> (r <sub>B</sub> <sup>-</sup> m <sub>B</sub> <sup>-</sup> ) λ(DE3 [ <i>lacI</i> <i>lacUV5-T7 gene 1 ind1 sam7 nin5</i> ])	IBC, Stuttgart

## 2.3. Oligonucleotides

Table 6: List of oligonucleotides used in this work

Name	Sequence
Blm10 CT fwd	AAA GGA TTC GGT CGC TAA ACT ATT GAC GAC C
Blm10 CT rev	AAA CTC GAG GGC ATA GTA ACT TCT CCA TAG
Blm10 $\Delta$ C fwd	CAT GGT GGT TGC CTG CAG TCG
Blm10 $\Delta$ C rev	AAA CTC GAG CTA GGT CGT CAA TAG TT

## 2.4. Plasmids

Table 7: List of plasmids used in this work

Name	Plasmid	Source
p $\Delta$ ssCPY*GFP	pRS316 [ $\Delta$ ssCPY*-GFP]	Park et al., 2007
p $\Delta$ ssCPY*LeuMyc	pRS316 [ $\Delta$ ssCPY*-Leu2Myc]	Park et al., 2007
YCp- <i>BLM10</i>	YCplac111 [ <i>BLM10</i> ]	C. Enenkel
pTF155	pTF155 [GAL-His12-Blm10]	Iwanczyk et al., 2006
pGEX-Nup53	pGEX [GST-Nup53]	Marelli et al., 1998
pGEX-4T-1	pGEX [GST]	GE Healthcare
pGEX-Gsp1Q71L	pGEX [GST-Gsp1Q71L]	Maurer et al., 2001
pGEX-Gsp1	pGEX [GST-Gsp1]	Maurer et al., 2001
pQE30	pET21b [6His]	Qiagen
pMW1	pET21b [6His-Blm10 1804-2143]	This work
pMW2	pTF155 [GAL-His12-Blm10 $\Delta$ 1804-2143]	This work
pGEX-Blm10 1749-2143	pGEX [GST-6His-Blm10 1749-2143]	T. Bissinger
pGEX-Blm10 1749-2143 W2021A	pGEX [GST-6His-Blm10 1749-2143 W2021A]	T. Bissinger
pGsp1G21V-FLAG	YEp351[GAL-FLAG-GSP1-G21V-LEU2]	Hellmuth et al., 1998
pQE-6His-Gsp1	pQE [6His-Gsp1]	Schlenstedt et al., 1995

## **2.5. Cell culture and cell-biological methods**

To supply cells with the optimum amount of oxygen, the volume of flasks used was chosen to be five times as large as the volume of the liquid culture. Liquid cultures were incubated in a shaker at 200 rpm.

### **2.5.1. Growth conditions for *E. coli* cultures**

All *E. coli* cultures were generally grown at 37°C if not mentioned differently. In cell cultures that were used for later protein purification, growth temperature and induction temperature are mentioned in the respective purification protocol. If ampicillin was used for the selection of a plasmid, a concentration of 100 µg/ml was added to the media.

### **2.5.2. Growth conditions for *S. cerevisiae* cultures**

All yeast cultures were incubated at 30°C unless mentioned differently. Precultures were inoculated from single colonies derived from agar plates, incubated over night in testing tubes and then transferred into the respective flask for the main culture.

Cells grown to logarithmic phase were diluted from precultures in fresh YPD media and grown for 8 h or ON. To confirm that cells were in logarithmic phase, the optical density of the culture was measured using a photometer. Cultures in logarithmic phase have an OD<sub>600</sub> in the range of 0.4-2.5. Cells grown to stationary phase were used 4 to 5 days after inoculation in YPD.

### **2.5.3. Measurement of cell growth**

To determine in which growth phase a culture was the optical density was measured using a photometer at 600 nm. Reference for all measurements was the respective media. Cell cultures were diluted in media until the measured OD<sub>600</sub> was between 0.1 and 0.5 and the measured value was adjusted according to the dilution. In yeast cultures, an OD<sub>600</sub> of 1.0 corresponds to  $2 \times 10^7$  cells per ml.

#### **2.5.4. Glycerol stocks of *E. coli* and *S. cerevisiae* strains**

Glycerol stocks were used for long-time storage of all *E. coli* and *S. cerevisiae* strains. Over night cultures of *E. coli* or yeast were mixed with equal volumes of sterile 80% glycerol and immediately frozen and stored at -80°C.

#### **2.5.5. Direct fluorescence microscopy**

For direct fluorescence microscopy, the Axio Imager.Z1 (Carl Zeiss AG) equipped with the mercury lamp X-Cite<sup>®</sup> Series 120 (EXFO) was used. Images were captured using the camera ORCA-ER (Hamamatsu Photonics) and the software Volocity<sup>®</sup> (Improvision). For microscopy of yeast cells, an objective with a magnification of 100x was used (Objective Plan-Apochromat 100x/1.4 Oil DIC, Carl Zeiss AG).

Right before microscopy, 1 ml of a yeast culture was centrifuged and the cell pellet was washed with ddH<sub>2</sub>O. The green fluorescence of GFP was observed with an excitation wavelength of 488 nm and at an emission of 520 nm. For RFP, 595 nm and 615 nm were used.

For the determination of the ratio of the intranuclear and cytosolic fluorescence intensities the software ImageJ was used. Intranuclear and cytosolic fluorescence intensities of 10 nuclei per strain were measured and the ratio and SEM (standard error of the mean) were calculated.

### **2.6. Molecular biological Methods**

#### **2.6.1. Isolation of plasmid DNA from *E. coli***

For the isolation of plasmid DNA from *E. coli*, the GeneJET™ Plasmid Miniprep Kit (Thermo Fisher Scientific) or the QIAprep Spin MiniPrep Kit (Qiagen) were used. Plasmid isolations were performed according to the instructions of the manufacturer. All isolated plasmids were tested by a restriction digestion.

#### **2.6.2. Easy Plasmid Miniprep**

This method is an alternative method for plasmid isolations. In contrast to commercially available kits using columns, this method can be used to monitor numerous

## Material and methods

transformants at low costs. The result of this method is a plasmid preparation of less purity that can be used for control restriction digestion.

2 ml of an *E. coli* overnight culture were harvested by centrifugation (14000 rpm; 1 min). The cell pellet was resuspended in 40  $\mu$ l Easy prep buffer, the suspension then incubated at 95°C for 2 min and finally cooled on ice for 1 min. After centrifugation (15 min, 14000 rpm), plasmid DNA was present in the supernatant. 0.5  $\mu$ l to 1  $\mu$ l were used for control restriction digestion.

### Easy prep buffer

10 mM	Tris/HCl, pH 8.0
1 mM	EDTA
15%	Sucrose
2 mg/ml	Lysozyme
0.2 mg/ml	RNase
0.1 mg/ml	BSA

### **2.6.3. Isolation of genomic DNA from *S. cerevisiae***

To isolate genomic DNA from yeast, the MasterPure™ Yeast DNA Purification Kit (Epicentre Biotechnologies) was used according to the manual of the manufacturer.

### **2.6.4. Polymerase chain reaction (PCR)**

Amplification reactions were performed in 30 cycles, each consisting of a heat denaturation step at 95°C, a primer annealing step at a temperature specific for the pair of primers, and an elongation step at 72°C.

Plasmid template DNA was diluted 1:100 prior to PCR, genomic DNA was diluted 1:10.



## Material and methods

### Composition of a PCR reaction

1 $\mu$ l	Template DNA
1 $\mu$ l	Primer forward (50 $\mu$ M)
1 $\mu$ l	Primer reverse (50 $\mu$ M)
10 $\mu$ l	Buffer 5x
1 $\mu$ l	dNTP mix (10 mM)
0.5 $\mu$ l	Phusion High Fidelity DNA Polymerase
Ad 50 $\mu$ l	ddH <sub>2</sub> O

PCR products were controlled by agarose gel electrophoresis and purified using the QIAquick<sup>®</sup> PCR Purification Kit (Qiagen) prior to further usage.

### **2.6.5. Restriction digestion of plasmid DNA**

Enzymes were used according to the manufacturer's instructions and in the buffer and at the temperature recommended.

#### Analytical digestion

Analytical restriction digestions were used to control isolated plasmid DNA. In a 10  $\mu$ l sample, 0.5  $\mu$ l to 2  $\mu$ l of isolated plasmid DNA solution were incubated with 1  $\mu$ l of 10x buffer and 3-5 U of each enzyme used. Digestion was performed for 1 h.

#### Preparative digestion

A preparative digestion was performed before a ligation reaction. Vector DNA and PCR products were used as samples.

For the digestion of vector DNA, 3-10  $\mu$ l of plasmid, 5 U of each enzyme and the recommended buffer were used. The DNA solutions were digested for 2 h and then purified using the QIAquick<sup>®</sup> PCR Purification Kit (Qiagen).

Insert DNA was derived from PCR. 20  $\mu$ l of purified PCR product was incubated with 5 U of each enzyme and the recommended buffer. The digestion reaction was performed for 2 h at the recommended temperatures. Before the ligation with the vector, the DNA was purified using the QIAquick<sup>®</sup> PCR Purification Kit (Qiagen).

### **2.6.6. Agarose gel electrophoresis**

This method was used for the separation of DNA molecules. In this work, 0.8% and 1% agarose gels were used. For the visualization of the DNA molecules either

## Material and methods

ethidium bromide (final concentration in gels 0.5 µg/ml) or RedSafe™ Nucleic Acid Staining Solution was used. The horizontal electrophoresis was performed at constant voltage at 120 V for 30 min to 45 min in 1x TAE buffer. 6x DNA loading buffer was added to the samples. Afterwards, the gel was photographed under UV light (302 nm) using the Gel Doc 2000.

### Agarose gels

0,8% or 1% agarose were dissolved in 1x TAE. 0.5 µg/ml ethidium bromide or 1x RedSafe™ were added.

### 1x TAE buffer

pH 7.5	
40 mM	Tris/acetate, pH 7.5
2 mM	EDTA

### DNA loading buffer

pH 8.0	
49.8%	Glycerol
50%	1x TAE
0.2%	Bromophenol blue

### **2.6.7. Extraction of DNA fragments out of agarose gels**

For the extraction of DNA fragments out of agarose gels, the NucleoSpin® Extract II-Kit (Macherey-Nagel) was used according to the instructions of the manufacturer. Since the isolated DNA fragments were used for a subsequent ligation reaction, the bands were excised at low UV radiation intensities.

### **2.6.8. Ligation of DNA fragments**

Before the ligation of the vector and the insert, a preparative restriction digestion was performed. For the ligation reaction, the linearized vector and the insert were used in a 1:3 ratio. The ligation reaction was carried out at room temperature for 1 h with the T4 DNA Ligase (Thermo Fisher Scientific) using the manufacturer's buffer. Ligated DNA was transformed in *E. coli*.

### **2.6.9. Construction of pMW1 and pMW2**

pMW1 encodes for the C-terminal 339 amino acids of Blm10 tagged with 6xHis. The background of the plasmid is the pET21b vector. A restriction digestion of the vector was performed using the enzymes *Bam*HI and *Xho*I. The insert encoding for the C-T of Blm10 was amplified with PCR using the primers Blm10 CT fwd and rev. Blm10 CT fwd added a *Bam*HI restriction site and Blm10 CT rev added a *Xho*I restriction site. The PCR product was purified using the QIAquick PCR purification kit and digested with *Bam*HI and *Xho*I. The digested vector and insert were purified with the QIAquick PCR purification kit and then used for ligation.

pMW2 encodes for 12xHis-Blm10  $\Delta$ 1804-2143. pTF155 was digested with the restriction enzymes *Pst*I and *Xho*I. The restriction digestion resulted in two DNA fragments: the longer one was pTF155 lacking the C-terminal 414 amino acids of Blm10. This fragment served as background for pMW2. Since a construct lacking only 339 amino acids was required, PCR was used to amplify this part out of pTF155. For the PCR, the primers Blm10  $\Delta$ C fwd and rev were used. The reverse primer added a *Xho*I restriction site to the PCR product that allowed the ligation with the vector. The PCR product was purified (QIAquick PCR purification kit) and digested with *Pst*I and *Xho*I. Digested vector and insert were purified and ligated.

### **2.6.10. Transformation of *E. coli***

50  $\mu$ l of a frozen suspension of chemical competent *E. coli* were thawed on ice. The DNA solution was added afterwards to the cell suspension. After 30 min incubation on ice, a heat shock was performed by incubating the cells at 42°C for 1 min. The cells were cooled subsequently on ice and 500  $\mu$ l of SOC media was added. The cells were recovered for 30 min to 1 h at 37°C and plated on selective media containing 100  $\mu$ g/ml ampicillin. The transformants were verified by plasmid isolation and restriction digestion.

### **2.6.11. Transformation of *S. cerevisiae* with lithium acetate**

50 ml of a yeast culture grown to logarithmic phase were harvested and the cell pellet was washed first with 10 ml ddH<sub>2</sub>O, then with 1 ml ddH<sub>2</sub>O and finally with 1 ml LiOAc/TE/H<sub>2</sub>O. The pellet was then resuspended in 200  $\mu$ l LiOAc/TE/H<sub>2</sub>O. 50  $\mu$ l of this suspension of competent cells were used for each transformation. To the compe-

## Material and methods

tent cells, 5 µl of pre-boiled and chilled ssDNA, 10 µl of PCR product and 300 µl of LiOAc/TE/PEG were added and the sample was carefully mixed. After 30 min incubation at 30°C, heat shock was performed by incubating the cells for 15 min at 42°C. For transformations in which low transformation efficiencies were expected, 37 µl of DMSO was added prior to incubation at 42°C. To cool the cells after the heat shock, 800 µl of ddH<sub>2</sub>O was added to the mix. To achieve a higher efficiency in homologous recombination, the cells were recovered in 3 ml of YPD media for 2-3 h and plated afterwards on selective media. The plates were incubated at 30°C for 3-4 days.

### TE/LiOAc/H<sub>2</sub>O

10 mM	Tris
1 mM	EDTA
100 mM	LiOAc

### TE/LiOAc/PEG

10 mM	Tris
1 mM	EDTA
100 mM	LiOAc
40%	PEG 3350 (w/v)

### 10x TE

100 mM	Tris/HCl, pH 7.5
10 mM	EDTA, pH 8.0

### 10x LiOAc

1M	LiOAc
----	-------

## **2.6.12. Plasmid transformation in *S. cerevisiae***

This method is based on the lithium acetate method, but is faster and only suitable for the transformation of plasmids. The cell pellet of 1 ml of an ON yeast culture was washed in 1 ml ddH<sub>2</sub>O. The pellet was then resuspended in 100 µl LiOAc/TE/H<sub>2</sub>O. 50 µl of this suspension were used per transformation. 5 µl of preboiled and chilled ssDNA, 2 µl of plasmid DNA and 300 µl of LiOAc/TE/PEG were added to the competent cells and the sample was carefully mixed. After a 30 min incubation at 30°C, a heat shock was performed by incubating the cells for 15 min at 42°C. The cells were directly plated on selective media after the heat shock.

### **2.6.13. Transformation of *S. cerevisiae* by electroporation**

15 ml of a yeast culture grown to logarithmic phase were harvested and the cell pellet was first washed with 10 ml ddH<sub>2</sub>O, then with 5 ml of a 1M sorbitol solution and finally with 1.5 ml ice cold sorbitol. The cell pellet was resuspended in 100  $\mu$ l sorbitol. 40  $\mu$ l of this cell suspension were used per transformation and therefore pipetted into a precooled transformation cuvette. After addition of 2  $\mu$ l plasmid solution or 3.5  $\mu$ l PCR product, respectively, the cuvette was shortly incubated on ice. The electroporation was performed at 1.5 kV, 25  $\mu$ F and 200  $\Omega$ . The optimal range of the time constant was between 4.4 and 4.6 ms. After the impulse, 1 ml of sorbitol was added quickly and the cells plated on selective media.

## **2.7. Methods in protein biochemistry**

### **2.7.1. Cycloheximide chase analysis**

Cycloheximide (CHX) is an antibiotic isolated from *Streptomyces griseus*, which inhibits the binding of the aminoacyl tRNA to the ribosomes in eukaryotic cells and therefore blocks protein synthesis. In this work, CHX chase analysis was used to examine the protein degradation of yeast cells grown to stationary phase.

20 OD<sub>600</sub> of yeast cells grown to stationary phase were used. 2 OD<sub>600</sub> were harvested at each time point. CHX (10 mg/ml, 150  $\mu$ l per 10 OD<sub>600</sub> of cells) was added directly after taking of the sample at time point 0 min. The following time points were taken: 0 min, 30 min, 60 min and 90 min. All samples were immediately incubated for 30 min on ice with equal volumes of ice cold 30 mM NaN<sub>3</sub>. All samples were analyzed by cell disintegration and protein precipitation, followed by SDS-PAGE and immunoblotting.

### **2.7.2. Protein purifications**

#### CP

Proteasome CPs were purified from yeast strains in which the endogenous  $\alpha$ 4 subunit was replaced by an  $\alpha$ 4-HA-Tev-ProA ( $\alpha$ 4-HA-TAP). This protein tag allows the purification of CPs with IgG Sepharose (GE Healthcare). To release bound CPs from the sepharose, two methods can be used. Tev protease cleaves between the HA-tag and the protein A tag resulting in native CP preparations with an HA-tag. For the se-

## Material and methods

cond method, IgG sepharose with bound proteasomes is incubated with 0.5 M AcOH resulting in a non-native preparation.

For CP purifications, Wt and *blm10Δ* strains were grown in YPD. For a CP preparation with little associated RP, the culture was incubated for 3 d instead of over night. Yeast cells were harvested and the pellet resuspended in lysis buffer. Cell lysis was performed using the French pressure cell press. To further reduce the amount of RP in the preparation, 5  $\mu$ l of apyrase was added to the lysate to degrade remaining ATP. The lysate was cleared from cell debris by centrifugation (rotor SS-34, 14000 rpm, 4°C, 20 min) and the cleared lysate was incubated with IgG sepharose for 2 h or over night at 4°C. After the binding, the sepharose was washed with washing buffer, whereby the volume of the washing buffer was approximately 50x of the volume of the sepharose. For native purifications, the CP was cleaved off with Tev protease (Roboklon) for 1 h at RT and subsequently overnight at 4°C. 5  $\mu$ l of Tev protease were used for 1 ml of sepharose.

### Lysis buffer

20 mM Tris, pH 7.5

150 mM NaCl

### 10x Washing buffer (10x PBS)

220 mM Na<sub>2</sub>HPO<sub>4</sub>

28 mM NaH<sub>2</sub>PO<sub>4</sub>

1.5 M NaCl

### CP-GFPS

CP-GFPS were purified from *blm10Δ* strains with a  $\beta$ 5-GFPS tag allowing the native purification of the GFP-tagged proteasome with Strep-Tactin<sup>®</sup> beads (IBA BioTAGnology). Yeast cells were grown in YPD for 36 h, subsequently harvested and the pellet resuspended in buffer W (ratio 3:1). Cell lysis was performed using the French pressure cell press. Cell lysate was cleared from cell debris by centrifugation (rotor SS-34, 14000 rpm, 4°C, 20 min) and the pH of the cleared lysate was adjusted to pH 8. The cleared lysate was incubated with equilibrated Strep-Tactin<sup>®</sup> beads ON at 4°C. After binding, beads were washed with buffer W, whereby the volume of the washing buffer was approximately 100x of the volume of the matrix. CP-GFPS was eluted at RT with 3 column volumes of buffer E (30 min) and the beads regenerated with buffer R.

## Material and methods

### Buffer W

100 mM	Tris pH 7.5
1 mM	EDTA
150 mM	NaCl

### Buffer E

100 mM	Tris pH 7.5
1 mM	EDTA
5 mM	Desthiobiotin
150 mM	NaCl

### Buffer R

100 mM	Tris pH 7.5
1 mM	EDTA
1 mM	HABA
150 mM	NaCl

### 12xHis-Blm10

12xHis-Blm10 was purified from a *blm10*Δ strain transformed with the plasmid pTF155 as described before (Iwanczyk et al., 2006). Cells were cultured for growth over night in CM media lacking uracil. The cells were then harvested, the pellet washed three times with ddH<sub>2</sub>O and transferred into CM media lacking uracil and glucose but supplemented with galactose for induction. The purification protocol and used buffers were described in Iwanczyk et al., 2006.

### 12xHis-Blm10 Δ1804-2143

A *blm10*Δ strain was transformed with pMW2, a plasmid which encodes for 12xHis-Blm10 Δ1804-2143. Cell culture and protein purification were performed as described for 12xHis-Blm10 (see above and Iwanczyk et al., 2006). Purified 12xHis-Blm10 Δ1804-2143 turned out to be a highly unstable protein.

### Blm10 1804-2143

Blm10 1804-2143 was purified from *E. coli* BL21 transformed with pMW1. Cell culture was in LB+amp. The main culture was inoculated 1:30 from a preculture grown over night. Cells were incubated at 30°C for 5 h and then induced with 1.5 mM IPTG for 1.5 h. The cells were harvested, resuspended in lysis buffer and lysed with the French pressure cell press. The lysate was cleared from cell debris by centrifugation

## Material and methods

(rotor SS-34, 14000 rpm, 4°C, 20 min) and the cleared lysate was incubated with NiNTA agarose for 1 h at 4°C. After binding, the sepharose was washed with washing buffer 1 and washing buffer 2, whereby the volume of each washing buffer was approximately 20x of the volume of the sepharose. The protein was eluted using elution buffer and rebuffered in PBS so that the final concentration of imidazol was less than 5 mM. All buffers used for the preparation were described in Iwanczyk et al., 2006.

### Blm10 1749-2143 and Blm10 1749-2143 W2021A

The purification of Blm10 1749-2143 was performed as described before (Studienarbeit T. Bissinger). The purification of Blm10 1749-2143 W2021A was performed in the same way. The GST-tag was cleaved off using thrombin.

### GST-Gsp1 and GST-Gsp1Q71L

The purification of GST-Gsp1 and GST-Gsp1Q71L was performed from *E.coli* BL21 transformed with the respective plasmid (pGEX-Gsp1; pGEX-Gsp1Q71L). Cell culture was performed at 30°C for 4 h starting from an OD<sub>600</sub> of 0.1. The expression of the protein was induced with 1.5 mM IPTG for 1.5 h at 30°C. Cells were then harvested, resuspended in lysis buffer and lysed with the French pressure cell press. The lysate was cleared from cell debris by centrifugation (rotor SS-34, 14000 rpm, 4°C, 20 min) and the cleared lysate was incubated with glutathione sepharose (Sigma; GE Healthcare) for 1.5 h at 4°C. After the binding, the sepharose was washed with washing buffer, whereby the volume of each washing buffer was approximately 50x of the volume of the sepharose. The fusion protein was eluted with elution buffer (2x 15 min, 4°C).

#### Lysis buffer

20 mM Tris, pH 7.5

150 mM NaCl

#### 10x Washing buffer (10x PBS)

220 mM Na<sub>2</sub>HPO<sub>4</sub>

28 mM NaH<sub>2</sub>PO<sub>4</sub>

1.5 M NaCl



## Material and methods

### Elution buffer

50 mM	Tris, pH 8.0
15 mM	Glutathione reduced

### GST-Nup53

GST-Nup53 was purified as described before (Marelli et al., 1998). GST-Nup53 was not eluted for the binding assays but remained bound on the sepharose.

### GST

Purification of GST was performed from *E.coli* BL21 transformed with pGEX-4T-1. Cell culture was performed at 30°C for 4 h starting from an OD<sub>600</sub> of 0.1. Protein expression was induced with 0.5 mM IPTG for 1.25 h at 30°C. Cells were then harvested, resuspended in lysis buffer and lysed with the French pressure cell press. Cell lysate was cleared from cell debris by centrifugation (rotor SS-34, 14000 rpm, 4°C, 20 min) and the cleared lysate was incubated with glutathione sepharose (Sigma; GE Healthcare) for 1.5 h at 4°C. After binding, the sepharose was washed with washing buffer, whereby the volume of each washing buffer was approximately 50x of the volume of the sepharose. GST was eluted with elution buffer (2x 15 min, 4°C).

### Lysis buffer

20 mM	Tris, pH 7.5
150 mM	NaCl

### 10x Washing buffer (10x PBS)

220 mM	Na <sub>2</sub> HPO <sub>4</sub>
28 mM	NaH <sub>2</sub> PO <sub>4</sub>
1.5 M	NaCl

### Elution buffer

50 mM	Tris, pH 8.0
15 mM	Glutathione reduced

### **2.7.3. Solution binding assays**

All solution binding assays performed in this study were based on the method described in Hahn & Schlenstedt, 2011.

## Material and methods

### Binding of Blm10 to GST-Nup53 and GST

GST-Nup53 was purified from *E. coli*. Since GST-Nup53 contains natively unfolded regions, it was not eluted from glutathione sepharose but remained bound. To test for a possible binding of Blm10, approximately 50 µg of 12xHis-Blm10 were added to 30 µl glutathione sepharose on which GST-Nup53 or GST had been immobilized. The samples were incubated on ice for 30-60 min to allow a possible association and then washed 3x with 1 ml PBSKMT buffer. Samples were analyzed by SDS-PAGE, Coomassie blue staining and immunoblotting against 12xHis-Blm10.

#### PBSKMT

25 mM	Sodium phosphate, pH7.3
150 mM	NaCl
3 mM	KCl
1 mM	MgCl <sub>2</sub>
5 mM	2-mercaptoethanol
0.1%	Tween 20

### Binding of Blm10-CP and CP to GST-Nup53

GST-Nup53 was purified from *E. coli* as described above. 30 µl glutathione sepharose with immobilized GST-Nup53 were incubated with equal amounts of purified CP or Blm10-CP (approx. 100 µg). Both samples were incubated on ice for 30-60 min to allow the association and then washed 3x with 1 ml precooled PBSKMT buffer. Samples were analyzed by SDS-PAGE and immunoblotting against 12xHis-Blm10 and  $\alpha$ 4-HA.

### Binding of Blm10 to GST-Gsp1Q71L-GTP, GST-Gsp1-GDP and GST

GST-Gsp1Q71L, GST-Gsp1 and GST were purified as described above. Equal amounts (approx. 15 µg) were immobilized on 30 µl of glutathione sepharose. 50 µl of PBSKMT was then pipetted on the sepharose. To ensure that GST-Gsp1Q71L was in the GTP bound and GST-Gsp1 in the GDP bound state, they were pre-loaded with 2 mM GTP or GDP, respectively. To each sample 25 µg of Blm10 was added and incubated on ice for 30 min. Unbound proteins were washed off with PBSKMT. The binding of Blm10 was analyzed by SDS-PAGE and immunoblotting against 12xHis-Blm10.

#### Binding of Blm10 1804-2143 and Blm10 $\Delta$ 1804-2143 to GST-Gsp1Q71L-GTP

The binding of 6xHis-Blm10 1804-2143 and 12xHis-Blm10  $\Delta$ 1804-2143 to GST-Gsp1Q71L-GTP was performed as described for 12xHis-Blm10. Purification of 12xHis-Blm10  $\Delta$ 1804-2143 resulted in a highly unstable protein. Therefore, it was confirmed by immunoblotting that the amount of undegraded 12xHis-Blm10  $\Delta$ 1804-2143 was comparable to 6xHis-Blm10 1804-2143.

#### Binding of Blm10 1749-2143 and Blm10 1749-2143 W2021A to GST-Gsp1Q71L-GTP and GST

The binding of 6xHis-Blm10 1749-2143 and 6xHis-Blm10 1749-2143 W2021A to GST-Gsp1Q71L-GTP and GST was performed as described for 12xHis-Blm10.

#### **2.7.4. Thrombin cleavage**

Thrombin cleavage was performed for the GST-fusion protein GST-Gsp1Q71L. GST-Gsp1Q71L was purified as described above and remained bound to glutathione sepharose. Cleavage was performed in thrombin cleavage buffer with biotinylated thrombin for 2 h at RT or ON at 4°C (Thrombin Cleavage Capture Kit, EMD Millipore). Thrombin was removed from the preparation using the supplemented agarose.

#### **2.7.5. Reconstitution of CP import into reconstituted *Xenopus* egg nuclei**

The reconstitution of the *Xenopus* egg nuclei was performed by A. Savulescu as previously described (Savulescu et al., 2011). Nuclei were reconstituted by mixing *Xenopus* egg membrane vesicles and cytosolic fractions at a 1:20 ratio. A system for ATP regeneration and sperm chromatin was added. Prior to the import experiment, it was confirmed that nuclear and NPC assembly had been successful.

Reconstitution reactions were diluted with 3 volumes of 1xELBS. Yeast CP was purified from *blm10* $\Delta$  cells and subsequently labeled with Oregon Green 488 succinimidyl ester (Molecular Probes). 12xHis-Blm10 was purified from yeast (Iwanczyk et al., 2006). For Blm10-CP complexes, 0.2  $\mu$ g Oregon Green labeled CP were incubated with 0.4  $\mu$ g Blm10 in PBS for 30 min in the dark. Nuclear import reaction was subsequently performed with Blm10-OG-CP and OG-CP. The nuclei were subsequently fixed and analyzed by confocal microscopy.

## Material and methods

Quantification of the rim-like and intranuclear fluorescence intensities was achieved with the software ImageJ. Intranuclear and rim-like fluorescence were quantified for 30 nuclei from three independent experiments analyzed by epifluorescence microscopy. Error bars indicate SEM.

### **2.7.6. Cell disintegration and protein precipitation by Yaffe and Schatz**

The cell pellet of 1 ml of an ON yeast culture was resuspended in 1 ml ddH<sub>2</sub>O. After the addition of 160 µl 1.85 M NaOH solution and 85 µl 2-mercaptoethanol, the sample was incubated for 10 min on ice. To precipitate all proteins, 160 µl of a 50% TCA solution was added and the sample was incubated on ice for 10 min. To pellet precipitated proteins, the sample was centrifuged (5 min; 14.000 rpm; 4°C). The protein pellet was washed with 500 µl of ice cold acetone and after the complete evaporation of the acetone, 50-100 µl of 1x SDS sample buffer was added to the sample. The sample was shortly mixed by vortex before it was boiled at 95°C for 5 min for protein extraction. The sample was centrifuged for 3 min at 14.000 rpm prior to SDS-PAGE. This method was also used for the samples of the CHX chase analysis.

#### 5x SDS sample buffer

187.5 mM	Tris/HCl, pH 6.8
25%	Glycerol
7.5%	SDS
12.5%	2-mercaptoethanol
	Bromophenol blue

### **2.7.7. Protein precipitation**

This method was used for the precipitation and analysis of purified proteins. 1/10<sup>th</sup> of the sample volume of a 0.015% sodium desoxycholate solution and of a 72% TCA solution were added to the sample and mixed. The mixture was incubated on ice for 10 min, then centrifuged (10 min; 14000 rpm, 4°C) and washed with 500 µl of ice cold acetone. The protein pellet was resuspended in 50-100 µl of 1x SDS sample buffer.

### **2.7.8. Native glass bead cell disintegration**

This method for cell disintegration was used to obtain native proteins or protein complexes out of a small volume of yeast cultures. Cells were harvested and the cell pel-

## Material and methods

let was washed with 1 ml ddH<sub>2</sub>O. Cell pellet was then resuspended in TB buffer in a ratio of 1:3 and glass beads were added to the suspension. The mixture was 5x mixed by vortex for 1 min each. Between the individual vortex steps, the cells were allowed to cool on ice for 2 min. After the last vortex step, the mixture was centrifuged (10 min; 4°C; 14000 rpm). The supernatant of this preparation contained soluble native proteins that were used for native PAGE.

### TB buffer

20 mM	Hepes/KOH, pH 7.4
110 mM	KOAc
2 mM	MgCl <sub>2</sub>
1 mM	EGTA
2 mM	DTT
2 mM	ATP

### **2.7.9. Cell disintegration by French Pressure Cell press**

This method for cell lysis was used for *E. coli* and yeast cell pellets with a volume larger than 1 ml. Cell pellets were resuspended in the respective lysis buffer. A typical ratio of cell pellet to lysis buffer is 1:3. 10 µg/ml of DNase was added to *E. coli* suspensions to reduce sample viscosity prior to lysis. The cells were lysed twice in the precooled steel cylinder to ensure that the lysis was efficient.

### **2.7.10. Native polyacrylamide gel electrophoresis**

Native polyacrylamide gel electrophoresis (native PAGE) was used for the separation of different proteasome configurations. To achieve the best results, gels with an acrylamide gradient ranging from 3.5%-6% were used.

## Material and methods

Table 8: Composition of a 1.5 mm 3.5%-6% native gel

Component	Volume [ $\mu$ l] 3.5%	Volume [ $\mu$ l] 6%
ddH <sub>2</sub> O	3670.0	1720.0
5x native running buffer	1100.0	1100.0
Glycerol	-	1500.0
ATP (200 mM)	27.5	27.5
DTT (200 mM)	27.5	27.5
30% Acrylamide	641.0	1100.0
10% APS	27.0	22.0
TEMED	2.7	2.2

5x native sample buffer was added to all samples prior to electrophoresis. Native PAGE was performed in 1x native buffer ON at 4°C and 45 V.

### 5x Native running buffer

0.45 M	Tris
4.45 M	Boric acid
10 mM	MgCl <sub>2</sub>

### 5x Native sample buffer

50%	Glycerol
Bromophenol blue	

### **2.7.11. Analysis of native gels by phosphofluoroimaging**

In this work, GFP-tagged proteasomes of different configurations were separated by native PAGE. After the electrophoresis, the gels were analyzed by phosphofluoroimaging using the Typhoon Trio (GE Healthcare). The following settings were used: Emission 520 nm, absorption 488 nm, normal sensitivity, 400-700 V, 100  $\mu$ m resolution. After phosphofluoroimaging the gels could be blotted using a semi dry blotter.

### **2.7.12. SDS polyacrylamide gel electrophoresis (SDS PAGE)**

Prior to SDS PAGE, all samples were mixed with 1x SDS sample buffer and were boiled at 95°C for 5 min and centrifuged for 3 min at 14000 rpm. The composition and volumes listed in the tables below show the volumes for one 1 mm gel.

## Material and methods

Table 9: Composition of 5 ml separating gel

<b>Separating gel</b>			
	<b>7.5%</b>	<b>10%</b>	<b>12%</b>
<b>Component</b>	Volume [ml]	Volume [ml]	Volume [ml]
ddH <sub>2</sub> O	2.4	2.0	2.3
30% Acrylamide	1.3	1.7	1.4
1.5 M Tris pH 8.8	1.3	1.3	1.3
10% SDS	0.050	0.050	0.050
10% APS	0.025	0.025	0.025
TEMED	0.003	0.003	0.003

Table 10: Composition of 4 ml stacking gel (5%)

<b>Stacking gel</b>	
<b>Component</b>	<b>Volume [ml]</b>
ddH <sub>2</sub> O	1.6
30% Acrylamide	0.3
0.5 M Tris pH 6.8	0.7
10% SDS	0.027
10% APS	0.013
TEMED	0.003

Electrophoresis was performed in 1x SDS running buffer at constant amperage (30 mA per gel) with a maximum voltage set to 250 V. Electrophoresis was stopped as soon as the bromophenol blue band reached the end of the gel. 1.5 µl of PageRuler™ Prestained Protein Ladder (Thermo Fisher Scientific) were used as protein ladder.

### 10x SDS running buffer

250 mM	Tris
1.92 M	Glycine
1%	SDS

### **2.7.13. Western blot**

In this study, two different methods for western blotting were used, namely the semi dry blot and the wet blot method.

## Material and methods

Subsequent to blotting, proteins on the membranes were stained with Ponceau S solution for 10 min and subsequently destained with ddH<sub>2</sub>O in order to verify that the blotting procedure was successful.

### Ponceau S (0.2%)

0.4 g	Ponceau S
198 ml	ddH <sub>2</sub> O
2 ml	Acetic acid

### Semi dry blot

Semi dry blot was performed for blotting of proteins separated by native PAGE. PVDF membranes were used. Prior to usage, the membranes were shortly incubated in methanol for their activation. Semi dry western blotting for native gels was performed at constant amperage of 400 mA for 15 min using the Owl HEP-1 (Thermo Fisher Scientific) semi dry blotter.

### Semi dry western blotting buffer

25 mM	Tris
192 mM	Glycine
0.1%	SDS
20%	Methanol

### Wet blot

Wet blotting was used for transfer of proteins from an SDS gel onto nitrocellulose (NC) membranes. Transfer was generally performed for 90 min at 300 mA. The transfer of Blm10 was either performed for 4 h at 200 mA using standard wet blot buffer containing 10% methanol or over night at 33V using 'Blm10 wet blot buffer'. Additional cooling was required in both case.

For wet blotting, the Mini Trans-Blot Cell (Bio-Rad) was used.

### 1x Blotting buffer

25 mM	Tris
192 mM	Glycine
0.02%	SDS
10-20%	Methanol



## Material and methods

### Blm10 wet blotting buffer

12.5 mM	Tris
96 mM	Glycine
0.05%	SDS
1%	Methanol

### **2.7.14. Immuno detection**

Subsequent to western blotting, immuno detection was performed. Therefore, the membranes were first incubated for 30 min to 2 h with blocking buffer. Incubation with primary antibody occurred for 2 h at RT or alternatively ON at 4°C. After the incubation with primary antibody, the membranes were washed 3x for 10 min with blot washing buffer and subsequently incubated with the HRPO conjugated secondary antibody for 2 h at RT. Prior to incubation with ECL solutions for 1 min (ECL™ Western Blotting-Kit, Amersham; Pierce® ECL Western Blotting Substrate, Thermo Fisher Scientific), the membranes were washed again. Signal detection occurred by exposure on an X-ray film and subsequent development of the film.

A table of all antibodies used in this study with the corresponding manufacturers and dilutions can be found in Table 1.

### Blocking buffer

30 mM	Tris/HCl, pH 7.5
150 mM	NaCl
5%	Skim milk powder
0.1%	Tween 20

### Blot washing buffer

30 mM	Tris/HCl, pH 7.5
150 mM	NaCl
0.1%	Tween 20

### **2.7.15. Inhibition of the proteasomal activity with MG-132**

To inhibit the activity of purified proteasomes specifically, CP preparations were incubated with 200 µM MG-132 for 2 h on ice. MG-132 was dissolved in DMSO. To verify that the activity was sufficiently inhibited, peptide cleavage assays were performed.

### **2.7.16. Centrifugation in a glycerol density gradient**

The density gradient was established using a gradient mixer. 5.7 ml of 10% glycerol buffer and 5.9 ml of 40% glycerol buffer were used for the gradient. The gradient was poured into a Beckman centrifuge tube suitable for SW40 rotor and stored at 4°C. The sample was pipetted on top of the gradient. Centrifugation was performed for 16 h at 4°C and 40000 rpm. After centrifugation, 600 µl fractions were collected by pipetting them from the top of the centrifugation tube.

#### 10% glycerol buffer

20 mM	Tris/HCl, pH 7.5
150 mM	NaCl
10%	Tween 20

#### 40% glycerol buffer

20 mM	Tris/HCl, pH 7.5
150 mM	NaCl
40%	Tween 20

### **2.7.17. Measurement of proteasomal activity with fluorogenic substrates (peptide cleavage assay)**

100 µl of substrate buffer were pipetted into a black 96 well plate. 10 µl of the sample was added to the substrate buffer and mixed by pipetting. The plate was covered with the lid and aluminium foil and incubated at 37°C for 30 min. The activity was measured using the Enspire™ 2300 Multilabel Reader with the following settings: 390 nm excitation and 460 nm emission. Suc-Leu-Leu-Val-Tyr-AMC (Tyr substrate) was used as a substrate for chymotryptic protease activity.

#### Substrate buffer

50 mM	Tris/HCl, pH 7.5
5 mM	MgCl <sub>2</sub>
100 µM	Tyr substrate

### **2.7.18. Test for phleomycin sensitivity**

To test wt and *blm10Δ* cells for their potential sensitivity for the DNA damaging agent phleomycin, cells were grown to logarithmic or stationary phase. Equal amounts of

## Material and methods

cells were harvested and treated with 1  $\mu\text{g/ml}$  phleomycin or mock-treated with ddH<sub>2</sub>O. Cells were subsequently spotted on YPD plates in serial dilutions and the plates were incubated at 30°C for 2 d.



### 3. Results

#### 3.1. Blm10 is involved in the sequestration of proteasomes into PSGs

##### 3.1.1. Blm10 is required for the sequestration of the CP into PSGs

The localization of proteasomes in yeast cells is highly dynamic and was recently shown to be dependent on the metabolic state of the cell (Laporte et al., 2008; Laporte et al., 2011). In dividing cells, 80% of all proteasomes are localized to the nucleus (Enekel et al., 1998; Russell et al., 1999). When yeast cells enter quiescence, CPs and RPs are first transported to the nuclear periphery and later out of the nucleus, where they are sequestered into motile cytosolic proteasome storage granules (PSGs) (Laporte et al., 2008). To confirm the localization of proteasomes in dividing and non-dividing cells, a wt strain was created with GFP-labeled CP. As a nuclear marker, HTA2 was labeled with RFP. Cells were grown in YPD to logarithmic or stationary phase and CP and HTA2 localization were monitored by direct fluorescence microscopy (Figure 7: upper lane: logarithmic phase; lower lane: stationary phase).

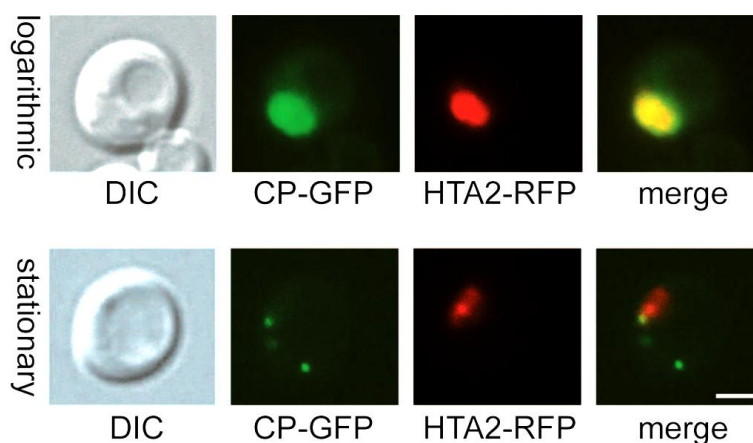


Figure 7: CP localization in logarithmic and stationary phase. In a wt strain, the CP subunit  $\beta 5$  was chromosomally tagged with GFP and the histone HTA2 with a mCherry tag (RFP). Cells were cultivated in YPD media to logarithmic or stationary phase. Samples of the culture were analyzed by direct fluorescence microscopy. Red and green channels were merged by the software Improvision. Bar: 2  $\mu\text{m}$ .

Consistent with previous data, the CP colocalized with the nuclear marker in dividing cells and was sequestered into cytosolic PSGs in stationary phase.

## Results

The mechanism for proteasome sequestration is unknown, but a candidate which could participate in this process is the protein Blm10. Its overall structure is similar to importin  $\beta$ , which previously led to the hypothesis that Blm10 might have an unknown function as a transport factor (Glickman & Raveh, 2005; Huber & Groll, 2012). To test whether Blm10 participates in proteasome dynamics when yeast cells enter quiescence, proteasome localization was analyzed in wt and *BLM10* deletion cells grown to logarithmic (Figure 8A) or stationary phase (Figure 8B). The  $\beta 5$  subunit of the CP was chromosomally tagged with GFP in both strains, and the localization of GFP-CP was monitored by direct fluorescence microscopy.

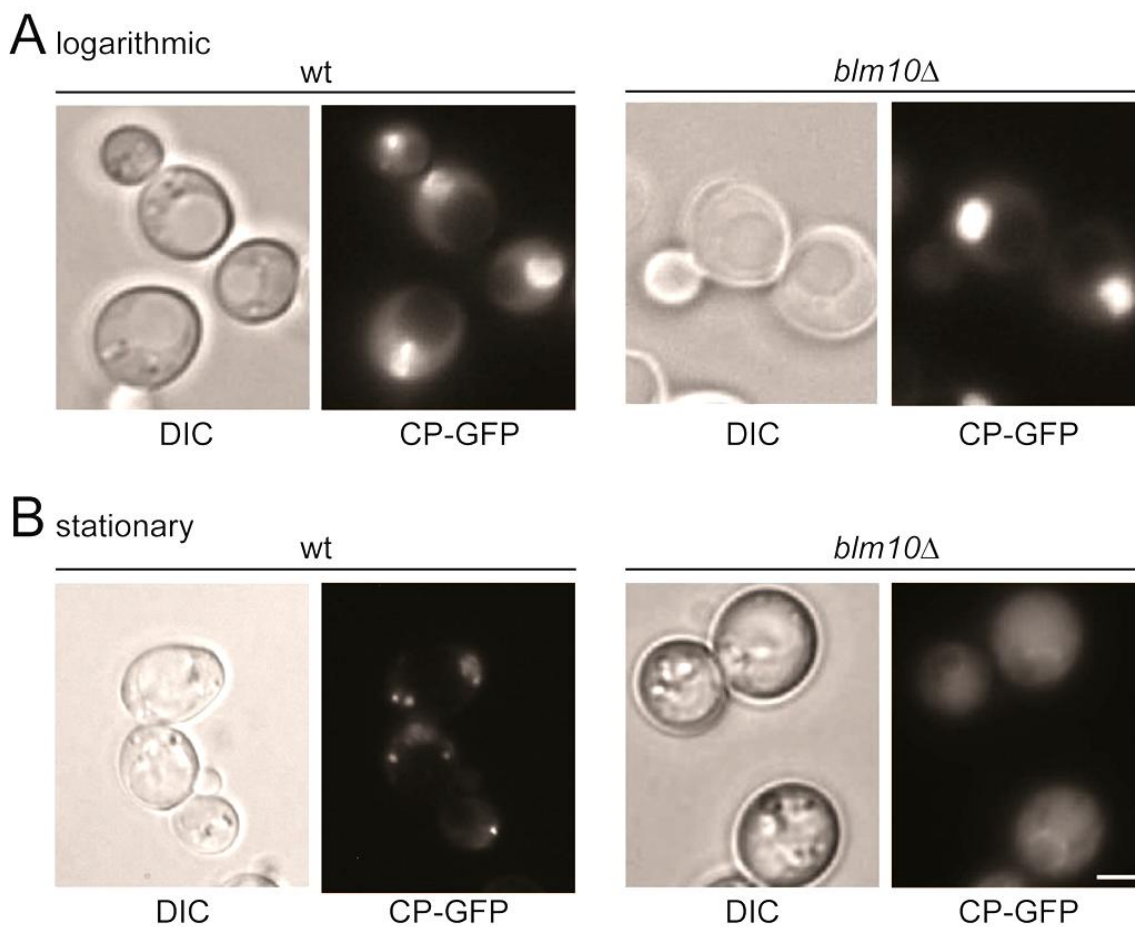


Figure 8: *BLM10* deletion prevents the sequestration of the CP into PSGs in stationary phase. A wt and a *blm10* $\Delta$  strain in which the CP subunit  $\beta 5$  was tagged with GFP were grown to logarithmic (A) and stationary phase (B) in YPD media. Samples of the culture were analyzed by direct fluorescence microscopy using filters for GFP. Bar: 2  $\mu$ m.

In logarithmic phase, the CP is mainly localized to the nucleus in both strains, as described before (Figure 8A; Russell et al., 1999; Fehlker et al., 2003). In stationary phase however, the intracellular distribution of the CP differed drastically between the wt and the *blm10* $\Delta$  strains. Consistent with previous data, the CP was sequestered

## Results

into PSGs in wt cells (Figure 8B, left panel; Laporte et al., 2008). In contrast to that, no sequestration was observed in non-dividing *blm10* $\Delta$  cells and the CP showed un-specific cytosolic localization (Figure 8B, right panel). The fact that the CP was found in the cytoplasm in both strains suggests that Blm10 is not required for the nuclear export of the CP, but rather for the sequestration of CPs into the PSGs. A faint signal could be detected in the nuclear periphery of both strains, which indicates that a small fraction of the CP still localized there.

### **3.1.2. The sequestration of the RP into PSGs is independent of Blm10**

Like the CP, the RP base and lid are sequestered into PSGs in stationary phase (Laporte et al., 2008). To analyze whether their sequestration is also affected by deletion of *BLM10*, the localization of RP base and lid was tested as described for the CP (see 3.1.1). Instead of a GFP-tagged  $\beta 5$  subunit however, the RP base subunit Rpn1 (Figure 9A) or the RP lid subunit Rpn11 (Figure 9B) were chromosomally tagged with GFP. RP base and lid localization were analyzed in cells grown to logarithmic and stationary phase using direct fluorescence microscopy.

## Results

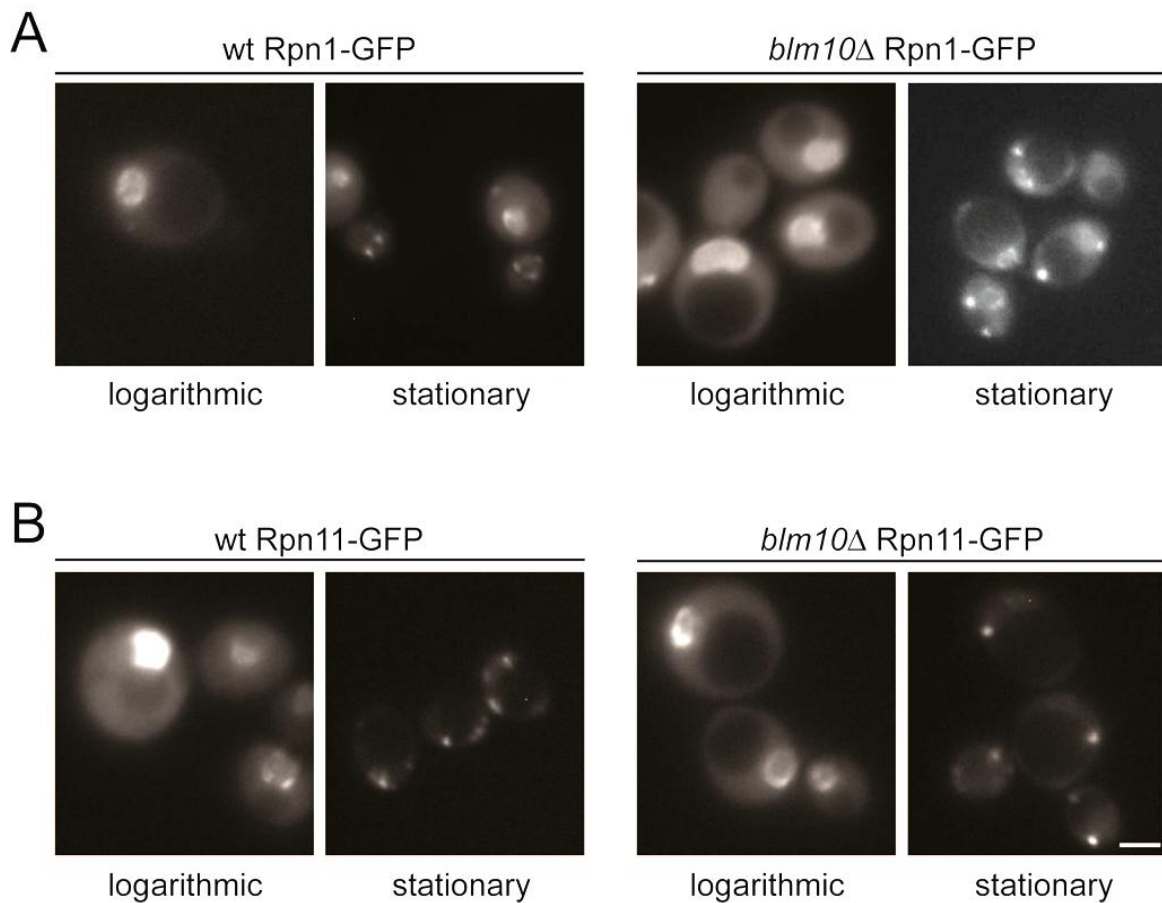


Figure 9: Sequestration of RP base and lid is not dependent on Blm10. Wt and *blm10*Δ cells, in which the RP base subunit Rpn1 or the RP lid subunit Rpn11 were tagged with GFP, were grown in YPD to logarithmic and stationary phase. Localization of the RP base and lid were monitored by direct fluorescence microscopy. Bar: 2  $\mu$ m.

Analysis of RP localization by fluorescence microscopy revealed that RP base and lid were mainly nuclear in logarithmic phase and were sequestered into PSGs in stationary phase in both the wt and the *blm10*Δ strains. This result suggests that Blm10 is only required for CP sequestration but not for RP base and lid sequestration and it indicates that the mechanism for RP and CP sequestration may differ from each other.

### 3.1.3. Blm10 localizes to PSGs in stationary phase

Blm10 was found to associate with precursor complexes (Fehlker et al., 2003; Marques et al., 2007; Li et al., 2007) as well as mature CPs to form Blm10-CP, Blm10-CP-Blm10 and the hybrid Blm10-CP-RP complex (Schmidt et al., 2005; Lehmann et al., 2008). Consistently, Blm10 was previously shown to colocalize with the proteasome in logarithmic phase (Fehlker et al., 2003; Schmidt et al., 2005). The lo-60



## Results

calization of Blm10 in cells grown to stationary phase is currently unknown, but since CP sequestration is dependent on Blm10, it is plausible to assume that Blm10 is like the CP sequestered into PSGs. To test this hypothesis, Blm10 was chromosomally tagged with GFP in an *ump1Δ* strain. Deletion of *UMP1* results in an increased expression of Blm10, which enhances the signal from Blm10-GFP for direct fluorescence microscopy. Blm10 localization was monitored in cells grown to logarithmic and stationary phase by direct fluorescence microscopy (Figure 10).

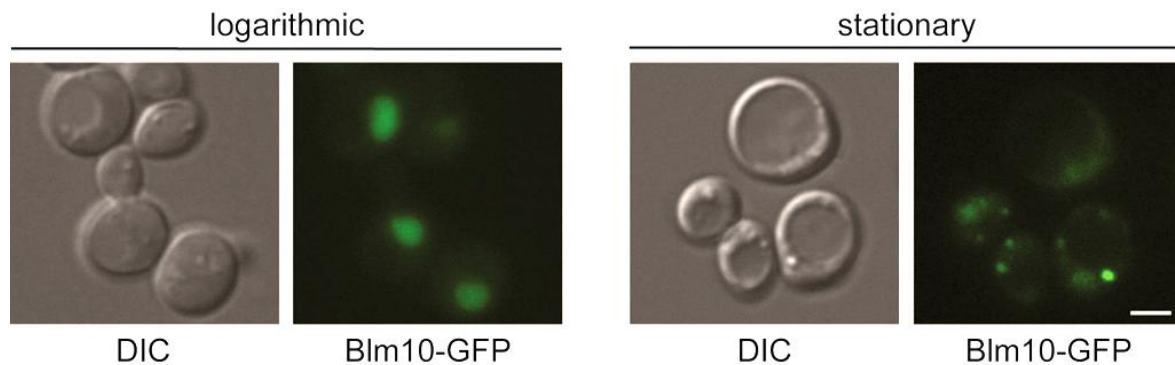


Figure 10: Blm10 localization in logarithmic and stationary phase. Blm10 localization was monitored with direct fluorescence microscopy in dividing and non-dividing *ump1Δ* cells, in which Blm10 was chromosomally tagged with GFP. Bar: 2  $\mu$ m.

As previously described, Blm10 localized mainly to the nucleus in dividing cells (Fehlker et al., 2003; Schmidt et al., 2005). In stationary phase however, it is sequestered into the PSGs as observed for the proteasome CP and RP (see Figure 8 and Figure 9).

### 3.2. PSGs function as stocks for mature proteasomal particles

#### 3.2.1. Analysis of proteasome configuration in non-dividing cells

In dividing cells, most CPs are associated with either one or two RPs (Glickman et al., 1998b; Bajorek et al., 2003). The association of the CP with the RP is required for the degradation of polyubiquitylated substrates, including regulators of the cell cycle. Quiescent cells are non-dividing, and RP and CP still colocalize. However, instead of the nuclear localization observed in dividing cells, RPs and CPs are sequestered into PSGs in quiescence (Laporte et al., 2008). In contrast to logarithmic phase, RP-CP complexes were previously found to dissociate in stationary phase (Bajorek et al., 2003).

## Results

The function of the PSG formation is not understood very well, but two possibilities were proposed. First, PSGs might, as suggested by the name, serve as proteasome stocks (Laporte et al., 2008), second, they might represent a major site of protein degradation (Kaganovich et al., 2008; see also introduction). In the latter case, it is absolutely necessary that the RP and CP are associated. In order to examine what configurations sequestered proteasomes have in PSGs, native PAGE was performed. In wt and *blm10* $\Delta$  strains, the CP subunit  $\beta$ 5 was chromosomally tagged with GFP and the maturase Ump1 was tagged with HA. Lysates of these two strains, which were grown in YPD to either logarithmic (Figure 11A) or to stationary phase (Figure 11B), were analyzed by native gradient PAGE. All complexes containing CP-GFP were visualized using phosphofluoroimaging and immunoblotting against HA, Blm10, and the RP base subunit Rpt1.

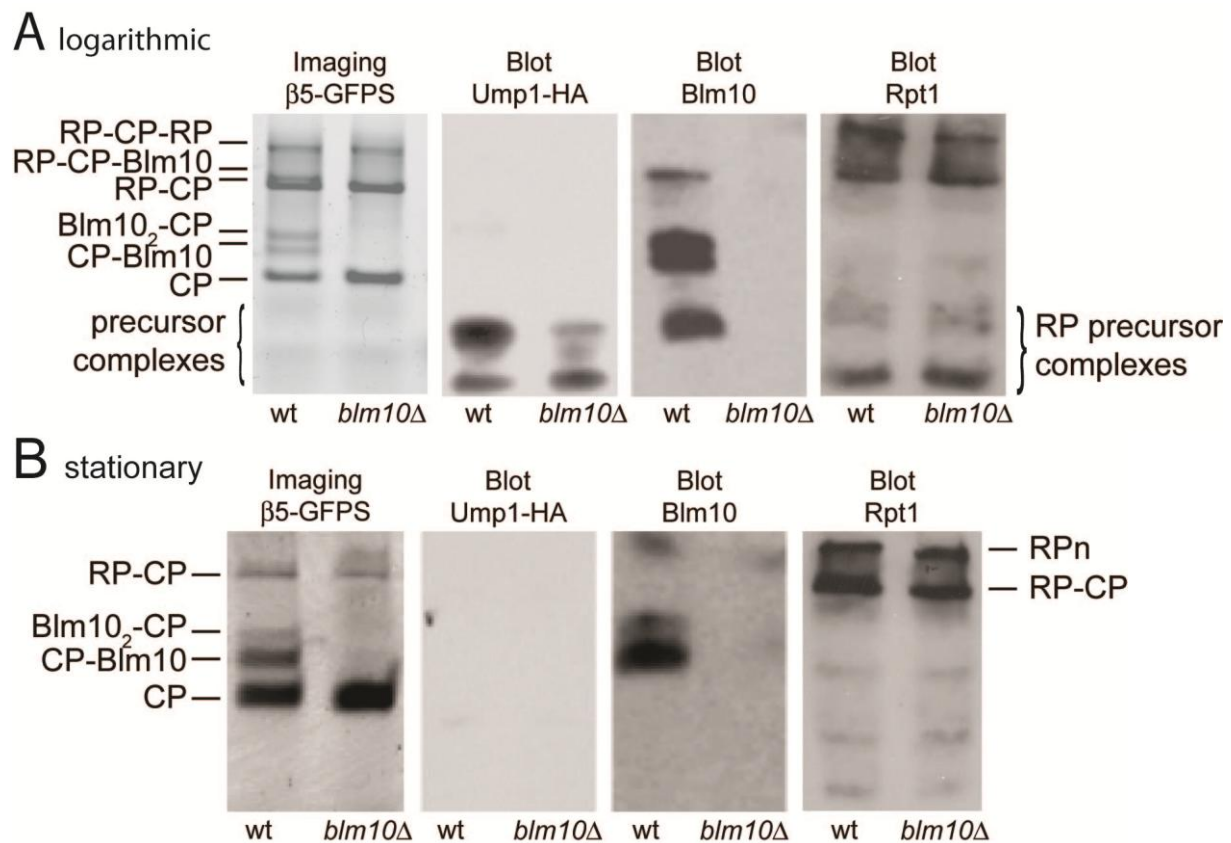


Figure 11: Analysis of proteasome configurations. Wt and *blm10* $\Delta$  strains with a GFP-tagged  $\beta$ 5 subunit and a HA-tagged Ump1 were grown in YPD to logarithmic (A) or stationary phase (B). Lysates of these cells were subjected to native gradient PAGE. CP-GFP containing complexes were visualized by phosphofluoroimaging, precursor complexes by immunoblotting against HA-tagged Ump1, RP complexes by immunoblotting against Rpt1 and Blm10 containing complexes by immunoblotting against Blm10.

In logarithmic phase, phosphofluoroimaging revealed seven previously described complexes containing CP-GFP (Figure 11A; Schmidt et al., 2005; Lehmann et al.,

## Results

2008). For both wt and *blm10Δ* cells, the majority of CPs were capped with at least one RP, forming the 30S complex RP-CP-RP, the 26S complex RP-CP and in case of the wt, the hybrid RP-CP-Blm10. The association of the RP to the CP was verified by immunoblotting against the RP base subunit Rpt1. Furthermore some free CP was detectable. In lysates derived from wt cells, the Blm10 associated complexes Blm10-CP, Blm10-CP-Blm10 and the hybrid Blm10-CP-RP were additionally identified. Blm10 association was verified by immunoblotting against Blm10. Proteasomal precursor complexes were found in the phosphofluoroimage as well as in the immunoblot against the HA-tag of the precursor associated maturase Ump1. Consistent with previous studies, which assigned Blm10 a role in proteasome maturation, Blm10 was associated with the precursor complexes (Figure 11A, blot Blm10; Fehlker et al., 2003; Li et al., 2007) and deletion of *BLM10* resulted in a slightly changed precursor pattern.

The major difference in proteasome configurations between cells grown to logarithmic (Figure 11A) and to stationary phase (Figure 11B) was that the ratio of RP-associated CP to free CP was notably changed. Lysate derived from cells grown to stationary phase contained mostly free CP, and in case of the wt strain, CP associated with one or two molecules of Blm10. Only a very faint signal was detected in the phosphofluoroimage for RP-CP complexes and no RP-CP-RP complexes were detectable at all (Figure 11B, phosphofluoroimage). Furthermore, proteasomal precursor complexes were depleted completely, as shown by the absence of a band in the immunoblot against Ump1-HA and the lack of faster migrating complexes in the phosphofluoroimage. While the RP was mostly not associated with the CP in stationary phase, it did not exist as a single particle or dissociate into the RP base and lid subcomplexes in stationary phase. Instead, immunoblotting against Rpt1 showed two bands, one representing the remaining RP-CP complexes while the second migrated the same distance as RP-CP-RP complexes. However, since the respective band was not present in the phosphofluoroimage, the RP formed a different complex lacking CPs. RPs purified in the absence of ATP form so-called  $RP_n$  complexes that were shown to co-migrate with RP-CP-RP in native PAGE experiments (Kleijnen et al., 2007).  $RP_n$  stands for a RP that is not competent to associate with a CP (Kleijnen et al., 2007). Comparably, intracellular ATP levels decrease in stationary phase and AMP levels rise (Laporte et al., 2011) indicating that the unidentified band found in the immunoblot against Rpt1 might represent  $RP_n$  complexes.

## Results

In summary, RP and CP colocalize to PSGs, but the two particles are not associated with each other. Additionally, cells do not synthesize new proteasomes in quiescence as seen by the complete depletion of proteasomal precursor complexes.

### **3.2.2. Analysis of the degradation of the model substrate $\Delta$ ss-CPY\* in non-dividing *blm10* $\Delta$ cells**

PSGs/JUNQ were proposed to be major sites for proteasomal degradation (Kaganovich et al., 2008; see section 4.2 for a discussion of the terminology of JUNQ and PSG). According to this hypothesis, substrates like polyubiquitylated proteins are sequestered into PSGs in order to concentrate them in one spot of the cell and the subsequent recruitment of proteasomes to these structures was thought to facilitate their degradation (Kaganovich et al., 2008). In a *blm10* $\Delta$  strain, PSGs are generally formed in stationary phase, as seen by the formation of dot-like structures for the GFP-labeled RP base and lid (see Figure 9). However, CP sequestration is prevented by the deletion of Blm10 and CPs localized instead diffusely to the cytoplasm (see Figure 8B). If proteasomal substrates but not CPs are sequestered to PSGs in a *blm10* $\Delta$  strain and PSGs serve as degradation sites, the degradation of these substrates should be drastically delayed in *blm10* $\Delta$  cells compared to wt cells. Importantly, while Blm10 is classified as a proteasome activator, binding of Blm10 to the CP results only in an enhanced hydrolysis of model peptide substrates (Schmidt et al., 2005) but not in an enhanced degradation of polypeptides (Ustrell et al., 2002; Fehlker et al., 2003). Consistent with this, experiments using pulse chase analysis showed that *BLM10* deletion does not affect the degradation of polyubiquitylated substrates (Doctoral thesis M. Fehlker).

To test whether the degradation of substrates that are localized to PSGs is slowed in a *blm10* $\Delta$  strain grown to stationary phase, the degradation of a derivative of the model ERAD substrate CPY\* was assayed. In the sequence of the *PRC1* gene, encoding for carboxypeptidase Y (CPY), a point mutation was introduced resulting in the misfolded protein CPY\* that is degraded by ERAD (Hiller et al., 1996). In the derivative used in this work, the signal sequence of CPY\* was deleted resulting in its cytosolic localization (Park et al., 2007).

To confirm that the chosen substrate localized to PSGs, a plasmid encoding for the GFP-tagged version  $\Delta$ ssCPY\*-GFP was transformed into wt and *blm10* $\Delta$  strains.

## Results

Cells were grown in selective media to stationary phase and the localization of  $\Delta$ ssCPY\*-GFP was monitored using direct fluorescence microscopy (Figure 12A).

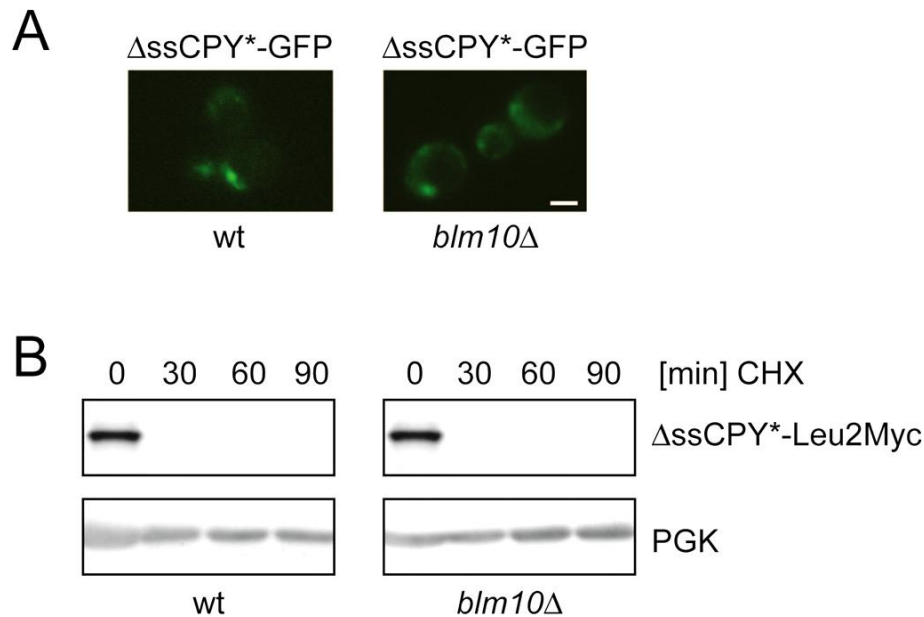


Figure 12: The degradation of  $\Delta$ ssCPY\*-Leu2Myc is not delayed in *blm10Δ* cells. Wt and *blm10Δ* cells were transformed with plasmids encoding  $\Delta$ ssCPY\*-GFP (A) or  $\Delta$ ssCPY\*-Leu2Myc (B) and grown in selective media to stationary phase. (A) To confirm that the chosen substrate is sequestered into cytosolic granules in both strains, direct fluorescence microscopy was performed with the GFP-tagged version of the substrate. Bar: 2  $\mu$ m. (B) The degradation of the reporter substrate was analyzed by performing a CHX chase experiment. CHX was added to the cells at time point '0 min'. Samples were taken at the indicated time points and analyzed by SDS-PAGE and immunoblotting against Myc, and PGK as loading control.

Similar to the substrate VHL-GFP (Weberruss et al., 2013),  $\Delta$ ssCPY\*-GFP was concentrated in cytosolic granules in cells grown to stationary phase (Figure 12A). Deletion of *BLM10* had no effect on its localization.

For the degradation study, a plasmid encoding  $\Delta$ ssCPY\*-Leu2Myc was transformed into wt and *blm10Δ* strains. Cells were grown in selective media to stationary phase and a degradation assay using CHX was performed (Figure 12B). CHX is an antibiotic isolated from *Streptomyces griseus* that blocks the binding of aminoacyl-tRNAs to ribosomes and functions as an inhibitor of *de novo* protein synthesis in eukaryotic cells. CHX was added to the cells after the '0 min' sample was taken and the degradation of  $\Delta$ ssCPY\*-Leu2Myc was studied in a time frame of 90 min, with samples taken every 30 min. All samples were analyzed by immunoblotting using  $\alpha$ Myc antibodies for the substrate and  $\alpha$ PGK antibodies as a loading control.

Analysis of the CHX chase experiment revealed no difference in the degradation of  $\Delta$ ssCPY\*-Leu2Myc for both strains (Figure 12B) and the substrate was degraded ef-

## Results

ficiently within 30 min, although in the case of the *blm10* $\Delta$  strain, no CP was recruited to PSGs. This result suggests that the sequestration of proteasome CPs is not required for the degradation of this substrate.

### **3.3. The re-import of mature CPs into the nucleus is dependent on Blm10**

#### **3.3.1. Nuclear uptake of mature CPs is dependent on Blm10**

PSGs were identified as highly motile clusters located in the cytosol of yeast cells. The composition of PSGs and participating proteins are not known. However, it is known that they do not contain insoluble proteins (Laporte et al., 2008; Kaganovich et al., 2008). The trigger for PSG formation was found to be a lack of carbon source in the media and a subsequent decrease of intracellular ATP levels and increase of AMP levels (Laporte et al., 2008; Laporte et al., 2011). In the case of YPD media, glucose is the limiting factor. Aside from the change in the ATP and AMP levels, the intracellular pH also decreases upon glucose depletion (Peters et al., 2013). Consequently, the dissolution of PSGs is dependent on the metabolic state of the cell. Addition of glucose results in an increase in intracellular ATP levels and PSGs are dissolved simultaneously (Laporte et al., 2008). Previous work using direct fluorescence microscopy showed that this dissolution of PSGs and the nuclear import of proteasomes that were stored there occurred in less than 15 minutes (Laporte et al., 2008). Importantly, the increase of nuclear proteasomes is not due to novel proteasome synthesis, since it can also be observed in cells in which *de novo* protein synthesis was repressed by the translation inhibitor CHX (Laporte et al., 2008).

The mechanism of how mature proteasomes are re-imported into nuclei is unknown. Since Blm10 was identified in this work to be involved in the sequestration of the CP into PSGs and as there are structural similarities between Blm10 and importins (Glickman & Raveh, 2005; Huber & Groll, 2012), the question arose of whether Blm10 also participates in the dissolution of PSGs and the re-import of proteasomes into the nucleus. To examine this possibility, wt and *blm10* $\Delta$  strains were created with a GFP-labeled  $\beta 5$  subunit. Both strains were grown in YPD to stationary phase and it was verified by direct fluorescence microscopy that PSG formation had occurred in the wt strain and that the CP was localized diffusely in the cytosol of the *blm10* $\Delta$

## Results

strain (Figure 13A, time point '0 min'). Subsequently, the cells were transferred into fresh YPD media, samples were taken at the indicated time points (Figure 13A, '5 min', '15 min', '30 min', '60 min' and '120 min') and CP localization was immediately analyzed at each time point by direct fluorescence microscopy (Figure 13A; upper lane wt, lower lane *blm10* $\Delta$ ).

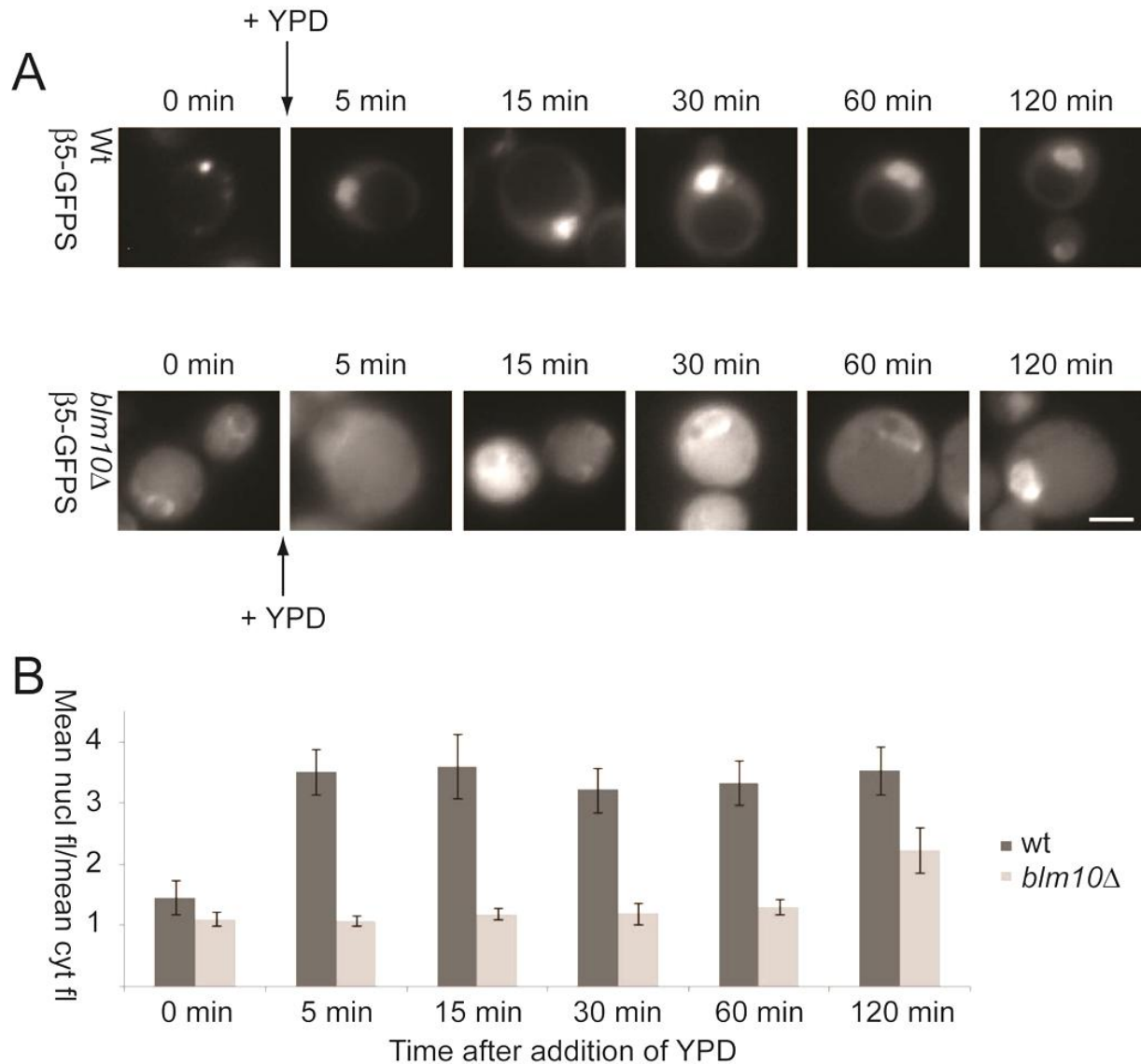


Figure 13: The re-import of the CP into the nucleus is dependent on Blm10. (A) In wt and *blm10* $\Delta$  cells, the CP subunit  $\beta 5$  was chromosomally tagged with GFP. Cells were grown in YPD to stationary phase ('0 min') and then transferred into fresh YPD media. The localization of the CP was examined by direct fluorescence microscopy at the indicated time points. Bar: 2  $\mu$ m. (B) The mean nuclear and cytosolic fluorescence intensities of 10 cells were determined using the software Image J and presented as a ratio of mean nuclear over mean cytosolic fluorescence. Error bars indicate SEM.

As described before, the dissolution of PSGs and the subsequent re-import of the CP into the nucleus of the yeast cells occurred quickly in wt cells and were completed within 5 min after the addition of fresh media (Figure 13, upper lane; Laporte et al.,

## Results

2008). When *BLM10* is deleted, the re-import of the CP was substantially slowed. Before time point '120 min', no notable increase in the intranuclear GFP signal was detectable and the nuclear envelope was only faintly decorated with CPs. Only after 120 min, was the nucleus decorated with CPs again. Therefore, the re-import of the CP is approx. 2 h delayed in *blm10Δ* cells in comparison to the wt.

To further quantify this delay, the ratio of the mean nuclear and cytosolic fluorescence intensities of 10 cells was determined with the software ImageJ (Figure 13B). In wt cells, the mean nuclear and cytosolic intensities were approximately equal at time point '0 min'. 5 min after the addition of fresh YPD, the mean nuclear intensity was 4-fold greater than the cytosolic intensity, which can be explained by the quick nuclear import of the CP.

Similar to the wt strain, the ratio of the mean nuclear to the mean cytosolic fluorescence intensity was approx. 1 at time point '0 min' for the *blm10Δ* strain. Due to the reduced rate of import, the ratio of the mean nuclear and cytosolic fluorescence intensities raised only after 120 min. Since the mean cytosolic fluorescence intensities at '0 min' and '120 min' were found to be approx. the same in the *blm10Δ* strain, the increase in the intranuclear GFP signal after 120 min is therefore presumably at least partly due to resumed proteasomal synthesis

Together, these results suggest that Blm10 participates not only in CP sequestration into PSGs but also in the re-import of mature CPs into the nucleus.

### **3.3.2. The nuclear uptake of the RP base and lid is independent of Blm10**

Like the CP, sequestered RP complexes were shown to be re-imported into the nucleus within 15 min after the cells were transferred into fresh YPD (Laporte et al., 2008). Since the CP and the RP are not associated in cells grown to stationary phase (see Figure 11B), it is possible that the mechanism for the re-import is distinct for these two particles. It is also possible that RP and CP associate prior to the nuclear transport and that they are imported in form of the hybrid complex Blm10-CP-RP. To study these possibilities, the re-import experiment described in section 3.3.1 was repeated using chromosomally GFP-tagged Rpn1 (RP base; Figure 14A) or Rpn11 (RP lid; Figure 14B). RP base or lid localization was monitored immediately after the samples were taken by direct fluorescence microscopy.



## Results

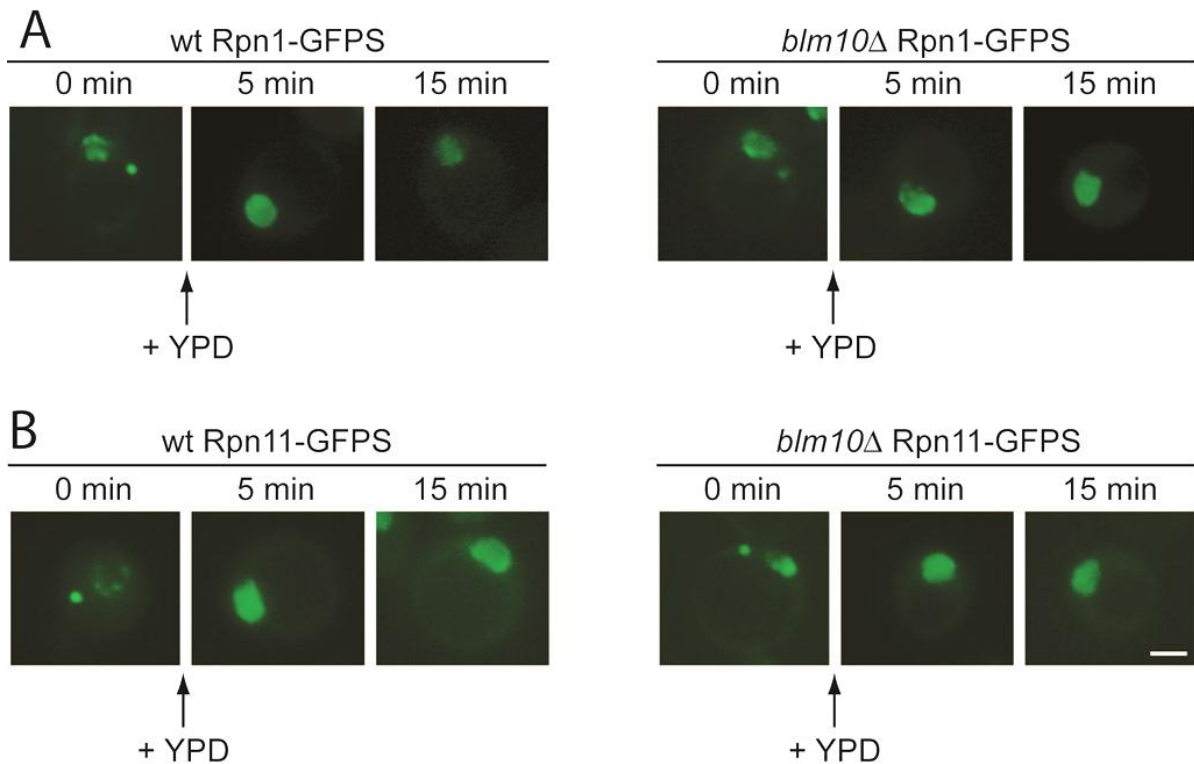


Figure 14: The re-import of RP base and lid is not dependent on Blm10. In wt and *blm10*Δ cells, the RP base subunit Rpn1 (A) or the RP lid subunit Rpn11 (B) were tagged with GFP. Cells were grown in YPD to stationary phase ('0 min') and then transferred into fresh YPD media. At the indicated time points, the localization of the RP base or lid was examined by direct fluorescence microscopy. Bar: 2  $\mu$ m.

As expected, RP base and RP lid were sequestered into PSGs in wt and *blm10*Δ cells at time point '0 min'. Consistent with previous studies (Laporte et al., 2008), RP base and lid were re-imported into the nucleus within 5 min after the cells were transferred into fresh YPD media. Deletion of *BLM10* had neither an effect on PSG dissolution or on the re-import of the RP base and lid. This finding suggests that the re-import of the CP and the RP are distinct processes. In case of the CP, Blm10 is crucial for its sequestration as well as for its re-import into the nucleus. In case of the RP, Blm10 is neither required for the sequestration into PSGs or for the re-import into the nucleus.

### 3.3.3. The recovery of nuclear RP-CP complexes is delayed in *blm10*Δ cells

When cells grown to stationary phase are transferred into fresh media, they leave quiescence and resume cell division after a lag phase. The cell cycle is a process whose regulation is dependent on proteasomal proteolysis and requires nuclear as-

## Results

sociated RP-CP complexes. In stationary phase, RP and CP complexes are located in PSGs but dissociated from each other (see Figure 11; Bajorek et al., 2003; Laporte et al., 2008). Since RP and CP are not associated in PSGs and only CP re-import is dependent on Blm10 (see Figure 13 and Figure 14), RPs and CPs are presumably translocated separately into the nucleus. In wt cells, the re-import of both complexes into the nucleus is accomplished in less than 5 min. Currently, it is unknown, however, how long the required time for a subsequent RP-CP reassociation is. In contrast to wt cells, CP re-import is drastically delayed in a *BLM10* deletion strain (Figure 13). Therefore it is plausible to assume that *blm10* $\Delta$  cells additionally show a delay in the reassociation of RP and CP complexes. To monitor the kinetics of the association of RPs and CPs upon PSG dissolution, native PAGE experiments were performed. The  $\beta$ 5 subunit of the CP was chromosomally tagged with GFP in wt and *blm10* $\Delta$  strains and cells were grown in YPD media to stationary phase. Before the cells were transferred into fresh media, a sample was taken ('0 min'). Further samples were taken at the indicated time points. The cells were lysed with glass beads and the lysates analyzed on a native gradient gel. CP-GFP containing complexes were detected by phosphofluoroimaging of the GFP tag (Figure 15).

## Results

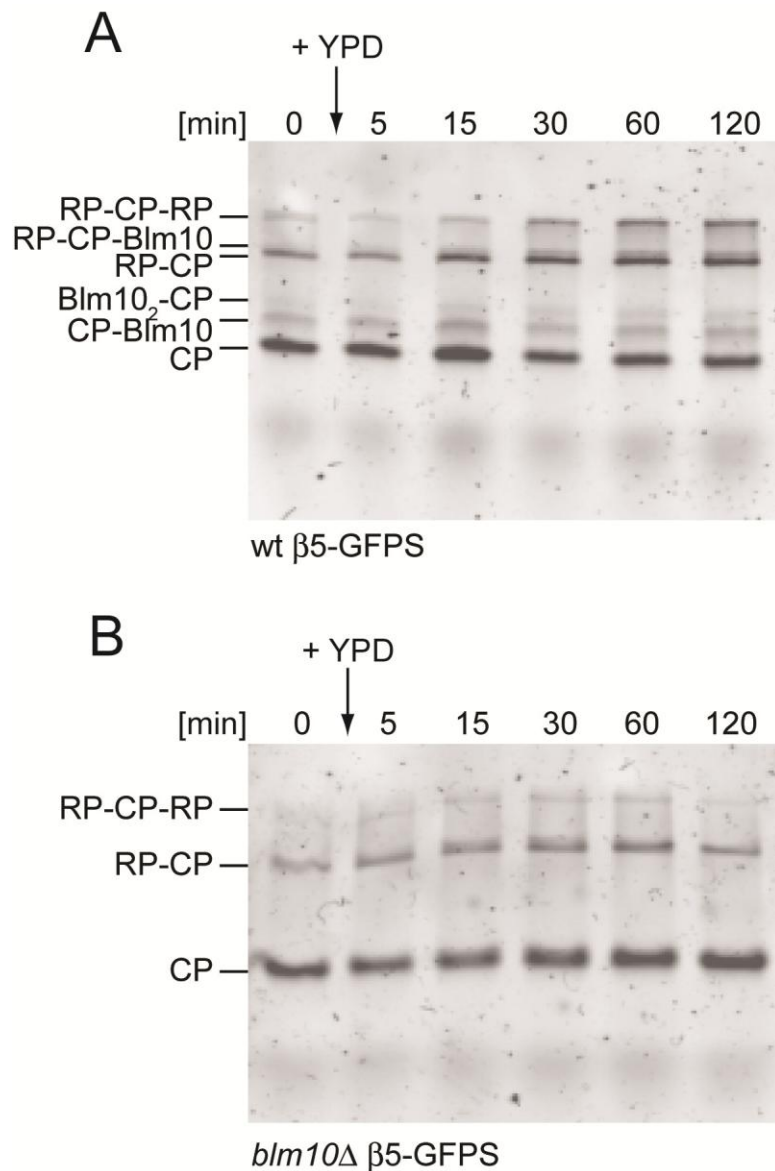


Figure 15: Recovery of associated RP-CP complexes is delayed by *BLM10* deletion. To monitor the reassociation of RP and CP complexes, native PAGE experiments were performed. The  $\beta 5$  subunit of the CP was chromosomally tagged with GFP in wt and *blm10*Δ strains. Cells were grown in YPD media to stationary phase. Before the cells were transferred into fresh media, a sample was taken ('0 min'). Further samples were taken at the indicated time points. Cells were lysed with glass beads and proteasome configurations analyzed by native PAGE. CP complexes were detected by phosphofluoroimaging of the GFP tag

Consistent with previous findings, the majority of CPs were not associated with RPs in stationary phase (time point '0 min'; see also Figure 11). After the cells were transferred into fresh YPD media, a quick reassociation of RP and CP complexes could be observed for wt cells (Figure 15A). 15 min after the transfer into new media the amount of associated RP-CP complexes increased notably, and after 30 min the amount of RP-CP-RP complexes had increased in comparison to stationary phase

## Results

('0 min'). No further increase in RP and CP association was detectable between time points '60 min' and '120 min' indicating that the cells had reached a steady state.

Deletion of *BLM10* had a drastic effect on the association of RP and CP. Direct fluorescence microscopy had previously revealed that CP, but not RP, import is delayed by 120 min in *blm10Δ* cells. Consequently, this also affected the reassociation of the RP and CP. 120 min after these cells were transferred into fresh YPD media, no increase in RP-CP complexes was detectable.

### **3.3.4. Non-dividing *blm10Δ* cells are sensitive to phleomycin**

Initially, it was reported that Blm10 is involved in DNA repair and that its deletion results in cells that are sensitive to the DNA damaging agent bleomycin (Febres et al., 2001). This finding is in conflict with later studies that did not determine a sensitivity of *blm10Δ* cells to DNA damaging agents (Iwanczyk et al., 2006). To test whether the sensitivity against DNA damaging agents is dependent on the growth phase of the cells, a wt strain was transformed with the empty vector YCplac111 (YCp) and a *blm10Δ* strain with YCplac111 (YCp) or YCplac111-*BLM10* (YCp-*BLM10*). YCp-*BLM10* expresses Blm10 under its endogenous promoter and is expected to complement the deletion of *BLM10*. All strains were grown in YPD to logarithmic or stationary phase and equal amounts of cells were harvested, treated with or without 1 µg/ml phleomycin, a derivative of bleomycin. Afterwards, the cells were spotted in serial dilutions on YPD plates and incubated at 30°C. After two days, the growth of the spotted cells originated from logarithmic (Figure 16A) or stationary cultures (Figure 16B) was analyzed.

## Results

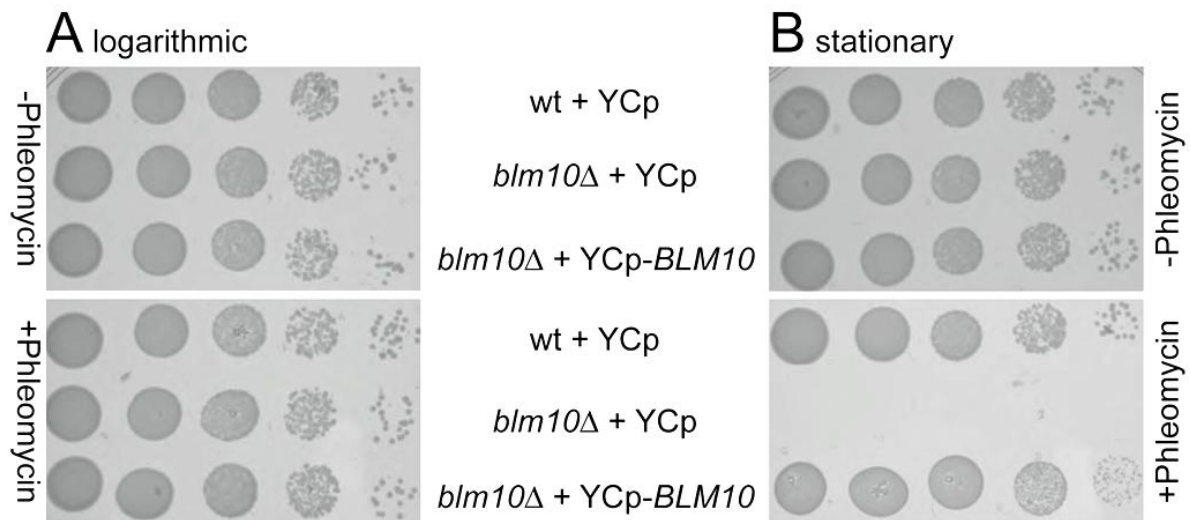


Figure 16: Quiescent *blm10Δ* cells are sensitive against phleomycin. A wt strain was transformed with the empty vector YCplac111 (YCp) and a *blm10Δ* strain with YCplac111 (YCp) and YCplac111-*BLM10* (YCp-*BLM10*). The three strains were grown in YPD to logarithmic (A) or stationary phase (B) and equal amounts of cells were harvested, resuspended in ddH<sub>2</sub>O and incubated for 3 h at 30°C with or without 1 μg/ml phleomycin. The cells were afterwards spotted in serial dilutions on YPD plates and incubated at 30°C for two days. Figure: C. Enenkel.

All spotted wt and *blm10Δ* cells that were derived from cultures grown to logarithmic phase grew to comparable extents with or without phleomycin treatment (Figure 16A). This finding is consistent with a previous study that showed that *BLM10* deletion did not result in sensitivity to bleomycin and phleomycin (Iwanczyk et al., 2006). In contrast, phleomycin treatment of quiescent *blm10Δ* cells transformed with the empty vector YCp resulted in their complete failure to grow on YPD plates, whereas the wt transformed with YCp and *blm10Δ* transformed with YCp-*BLM10* grew to a similar extent as cells without treatment (Figure 16B). These findings indicate that quiescent *blm10Δ* are highly sensitive to the DNA damaging agent phleomycin.

### 3.4. Blm10 acts as importin for mature CPs

At the beginning of this study, it was unknown how mature proteasomes are imported into the nucleus after dissolution of PSGs. Fluorescence microscopy performed in this study showed that deletion of *BLM10* delayed the re-import of mature CPs and the subsequent growth out of stationary phase (see section 3.3). The reason for the delayed CP import in *blm10Δ* cells was unknown. Blm10 could on the one hand directly be responsible for CP re-import and therefore represent its importin. On the other hand, Blm10 could also function as an adaptor protein to which an additional importin can bind.

## Results

Blm10 consists of 32 HEAT-like repeats (Sadre-Bazzaz et al., 2010), a structural motif that is also found in importins. Importantly however, the existence of HEAT repeats does not represent a criterion for the identification of importins, since these motifs are also found in proteins that are not associated with nuclear transport. In addition to the secondary structure, the overall structure of Blm10 is similar to the one of importins, so that it was previously speculated whether Blm10 might function in nuclear transport (Glickman & Raveh, 2005; Huber & Groll, 2012).

The properties listed below are commonly found in importins and additionally allow a differentiation between an importin and an adaptor:

- The importin and the cargo associate with each other, which promotes the nuclear transport of the formed importin-cargo complex.
- Subsequent to the formation of the importin-cargo complex, the importin mediates the contact of the complex to proteins of the NPC. This interaction facilitates the translocation through the nuclear pore. Therefore, the affinity of the cargo to Nups is enhanced when it is associated with its importin.
- The nuclear import of the importin and the importin-cargo complex is dependent on Ran and on a functional Ran-GTP-Ran-GDP gradient.
- In the nucleus, Ran-GTP associates with the importin-cargo complex which results in the dissociation of the complex into the cargo and the Ran-GTP-importin complex.
- Ran-GTP and the importin form a complex which is exported into the cytosol, where GTP hydrolysis occurs resulting in the dissociation of the importin from Ran-GDP.
- The affinity of the importin for Ran-GDP is significantly lower than for Ran-GTP.

In order to examine if Blm10 is the importin for the mature CP, the criteria mentioned above have to be fulfilled.

### **3.4.1. Blm10 facilitates the uptake of yeast CP into reconstituted *Xenopus* egg nuclei**

The association of the cargo with its importin is required for the translocation of the complex through the NPC, whereas the cargo by itself is not transported. In the case of Blm10, it was shown previously that it is capable of associating with its potential

## Results

cargo, the mature CP, to form Blm10-CP, Blm10-CP-Blm10 and Blm10-CP-RP complexes (see native PAGE in Figure 11; Fehlker et al., 2003; Schmidt et al., 2005; Lehmann et al., 2008).

The formation of the importin-cargo complex promotes its nuclear transport. Data obtained from fluorescence microscopy of living yeast cells showed that the rapid re-import of mature CPs out of PSGs is dependent on Blm10 (see section 3.3.1). To find further evidence showing that Blm10 facilitates the import of mature CPs into nuclei, a different experimental strategy was chosen. Recently, the nuclear import of mature proteasomes from *Xenopus laevis* was studied using a cell free import assay (Savulescu et al., 2011). In this assay, functional nuclei of *Xenopus* oocytes were reconstituted out of egg extracts and the import of different proteasome species derived from *Xenopus* extracts was studied (Savulescu et al., 2011). Free CP and RP-CP complexes were found not to be translocated into reconstituted *Xenopus* egg nuclei, a result, which is consistent with studies in yeast (Lehmann et al., 2002). Eggs from *Xenopus* and yeast cells grown to stationary phase are both non-dividing cells in which the proteasome is not located in the nucleus. After fertilization of the egg or addition of fresh medium, it is crucial that proteasomes are rapidly imported into the nucleus to resume cell division. In order to examine whether association of Blm10 to the yeast CP is required for CP import into reconstituted *Xenopus* egg nuclei, the above described import assay was performed in collaboration with A. Savulescu (Technion, Haifa, Israel). The localization of fluorescently labeled yeast CP was studied with confocal and epifluorescence microscopy. Since GFP-labeled CP resulted in insufficient fluorescence signals, yeast CP was purified from *blm10* $\Delta$  cells and subsequently labeled with the fluorescence dye Oregon Green 488 succinimidyl ester (OG; Oregon green labelling was performed by A. Savulescu). Prior to the reconstitution experiment, native PAGE analysis and peptide cleavage activity assays were performed to test whether OG-labeled CP (OG-CP) was able to bind to Blm10. OG-CP was incubated with or without purified 12xHis-Blm10, run on a native PAGE gel and OG-CP configuration was analyzed by phosphorimaging (Figure 17A). Binding of an excess of Blm10 to OG-CP should result in reduced peptide cleavage activity since binding of Blm10 to the CP caps the proteasome's entrance pores formed by the  $\alpha$  rings. To test this, OG-CP was incubated with and without an excess of Blm10. To separate unbound Blm10, CP and Blm10-CP-Blm10, density gradient centrifugation was performed. Peptide cleavage activity of each fraction was meas-

## Results

ured by usage of Suc-Leu-Leu-Val-Tyr-AMC as substrate. Absolute activities are shown relative to the maximum cleavage activity (Figure 17B).

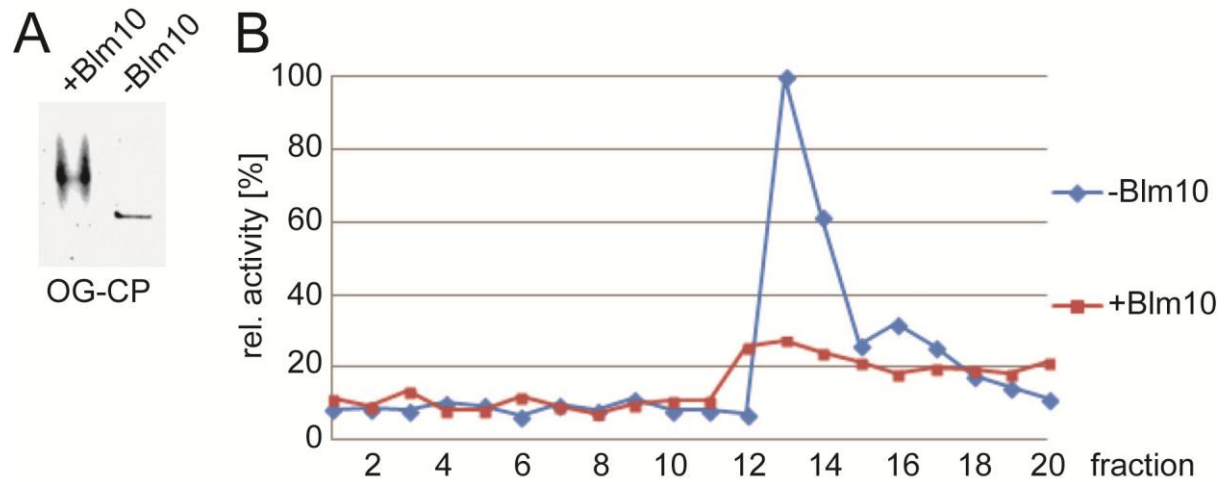


Figure 17: Blm10 binds to OG labeled yeast CP. (A) OG-CP was incubated with or without Blm10. The samples were subsequently analyzed on a native gradient gel and OG-CP was visualized using phosphorimaging. (B) The peptide cleavage activity for the substrate Suc-Leu-Leu-Val-Tyr-AMC was measured for OG-CP and OG-CP pre-incubated with Blm10 after density gradient centrifugation (10%-40% glycerol gradient). Fraction 1 represents 10% glycerol and fraction 20, 40%. The measured absolute activities are shown relative to the maximum cleavage activity.

Incubation of OG-CP with Blm10 resulted in the formation of a slower migrating complex in the native gel. Furthermore, the analysis of the peptide cleavage activity showed that pre-incubation of OG-CP with Blm10 reduced the maximum cleavage activity by 73% in relation to Blm10-free CP. This is consistent with previous data, showing that incubation of the CP with an excess of Blm10 reduces the activity by 80% (Fehlker et al., 2003). Both results show that OG-labeling of the yeast CP does not affect its binding to Blm10.

To test the effect of Blm10 on the import of OG-CP into reconstituted *Xenopus* egg nuclei, OG-CP was incubated with or without Blm10 to allow the formation of OG-CP-Blm10 complexes. After the incubation, samples were added to the reconstituted nuclei, which were subsequently fixed and analyzed by confocal microscopy. In Figure 18A, three nuclei per condition ('-Blm10', '+Blm10'; nuclei I-III) are shown, with three 0.37  $\mu\text{m}$  thick slices taken of the middle of each nucleus. The intranuclear and the rim-like fluorescence were quantified for 30 nuclei from epifluorescence images using the software Image J. The histogram is shown in Figure 18B. This experiment was performed by A. Savulescu.



## Results

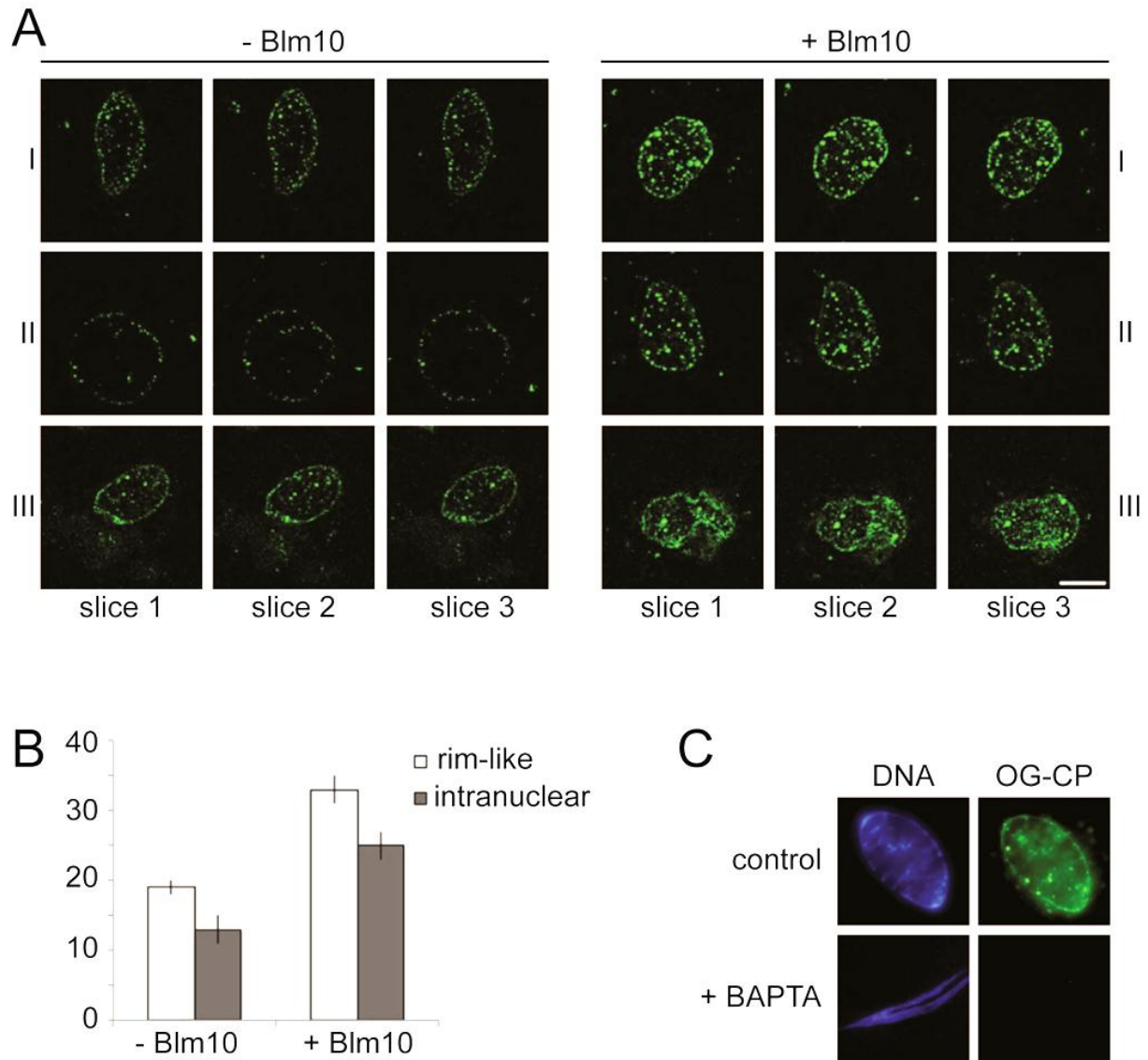


Figure 18: Blm10 facilitates the uptake of yeast CP into reconstituted *Xenopus* egg nuclei. (A) OG-CP was incubated with or without Blm10 and the samples were added to reconstituted nuclei. The fixed nuclei were analyzed by confocal microscopy. Three nuclei per condition (I-III) each with three 0.37  $\mu\text{m}$  thick slices taken of the middle of the nucleus are shown. Bar: 10  $\mu\text{m}$ . (B) The intranuclear and the rim-like fluorescence for 30 nuclei were quantified from epifluorescence images using the software Image J. Error bars indicate SEM. (C) Yeast CP associates specifically with NPCs and not with nuclear membranes. Addition of BAPTA during nuclear reconstitution of *Xenopus* egg nuclei inhibits early steps in nuclear assembly resulting in pore-less nuclei. Yeast CP was incubated with functional (control) or pore-less nuclei (+ BAPTA) and the localization of the CP was monitored by epifluorescence microscopy. This experiment (A-C) was performed by A. Savulescu.

In the absence of Blm10, only weak rim-like staining at the nuclear membranes and weak intranuclear fluorescence were detected. The incubation of Blm10 with OG-CP facilitated its import into the reconstituted nuclei. Quantification of the intranuclear and rim-like signals showed that in the presence of Blm10, intranuclear fluorescence intensity increased by a factor of 1.9 while the rim-like fluorescence intensity increased by a factor of 1.8. Therefore, the association of Blm10 to OG-CP clearly re-

## Results

sulted in a recruitment of the OG-CP-Blm10 complex to the nuclear membranes and a subsequent translocation through the NPCs.

Control experiments showed that no rim-like signal for OG-CP was observed in nuclei treated with BAPTA (Figure 18C). BAPTA treatment during early stages of nuclear assembly results in nuclei without nuclear pores, thus the recruitment of OG-CP was specific to NPCs and not to nuclear membranes in general.

Taken together, this experiment provided further evidence that the nuclear import of mature CPs is enhanced by Blm10 association.

### **3.4.2. Re-import of mature CPs and Blm10 is independent of Srp1/importin $\alpha$**

Previous studies showed that CP precursor complexes are imported via the classical import receptor complex importin  $\alpha\beta$  in dividing yeast cells. In contrast, mature CPs are not recognized by importin  $\alpha\beta$  (Lehmann et al., 2002). To test whether the re-import of the CP and Blm10 upon PSG dissolution is dependent on importin  $\alpha$ , fluorescence microscopy was performed with a strain expressing a temperature sensitive mutant of Srp1 (*srp1-49*), the yeast homologue of importin  $\alpha$  (Yano et al., 1992; Enenkel et al., 1995). In this strain, nuclear transport depending on importin  $\alpha$  is disturbed at non-permissive temperature. The re-import was examined in *srp1-49* strains, in which Blm10 (Figure 19, right panel) or the CP subunit  $\beta 5$  (Figure 19, left panel) were chromosomally tagged with GFP. Both strains were grown at non-permissive temperature to stationary phase ('0 min') and subsequently transferred into fresh YPD media. Samples were taken at the indicated time points ('5 min' or '15 min') and CP or Blm10 localization was immediately analyzed by direct fluorescence microscopy.

## Results

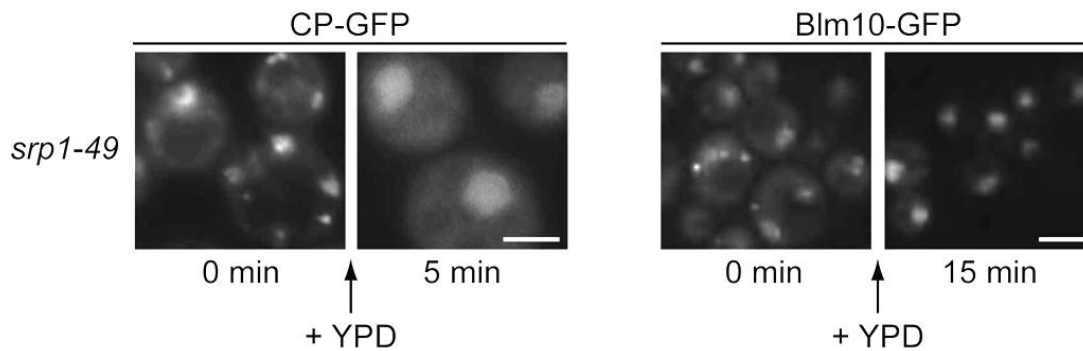


Figure 19: The import of mature CP and Blm10 is not dependent on importin  $\alpha$ . The CP or Blm10 were chromosomally tagged with GFP in *srp1-49* strains. Cells were grown at restrictive temperature in YPD to stationary phase ('0 min') and then transferred into fresh YPD media. At the indicated time points, the localization of the CP or Blm10 was examined by direct fluorescence microscopy. Bar: 2  $\mu$ m (CP) or 4  $\mu$ m (Blm10). Figure: C. Enenkel.

As seen for wt cells, Blm10 and the CP were sequestered into PSGs in *srp1-49* cells grown at non-permissive temperature to stationary phase. Transfer of the cells into fresh YPD media resulted in the rapid re-import of Blm10 and the CP into the nuclei suggesting that the re-import occurred independently of importin  $\alpha$ . This result is consistent with previous data showing that mature CPs are not recognized by importin  $\alpha\beta$  (Lehmann et al., 2002). The results shown in this work indicate that also the import of Blm10 is not dependent on importin  $\alpha$ .

### 3.4.3. Blm10 interacts with Nup53 and enhances binding of CPs to Nup53

After the association of the importin with the cargo, the importin functions as mediator for the translocation through the NPC by interacting with proteins of the nuclear pore, so-called Nups. To test for a potential interaction between Blm10 and Nups, Nup53 was chosen as representative protein of the NPC as it was previously shown to function in protein import by interacting with the importins Pse1/Kap121 and Kap95/importin  $\beta$ , but not with exportins (Marelli et al., 1998; Fahrenkrog et al., 2000; Tetenbaum-Novatt et al., 2012). Nup53 belongs to the class of FG-Nups since it contains regions that are enriched in phenylalanine (E) and glycine (G) repeat motifs. To analyze a possible binding of Blm10 to Nup53 *in vitro*, solution binding assays were performed. Briefly, the proteins of interest were purified and subsequently tested for their potential association in solution. Nup53 was purified as GST fusion protein from *E. coli* (Figure 20A, load; Coomassie blue stained gel) and 12xHis-Blm10 was purified from yeast (Figure 20A, left lane; Coomassie blue stained gel). To exclude the possibility of unspecific binding of Blm10 to the affinity beads or to the GST-tag of the

## Results

fusion protein, GST was purified from *E. coli* (Figure 20A, load; Coomassie blue stained gel). GST-Nup53 and GST were immobilized on glutathione sepharose beads and incubated with equal amounts of Blm10 (Figure 20A, load, top lane; Coomassie blue stained gel). After thorough washing of the affinity beads, bound proteins were analyzed by SDS-PAGE and Coomassie blue staining (Figure 20B: bound; top). The presence of Blm10 was verified by immunoblotting against the 12xHis-tag of Blm10 (Figure 20B: bound; bottom).

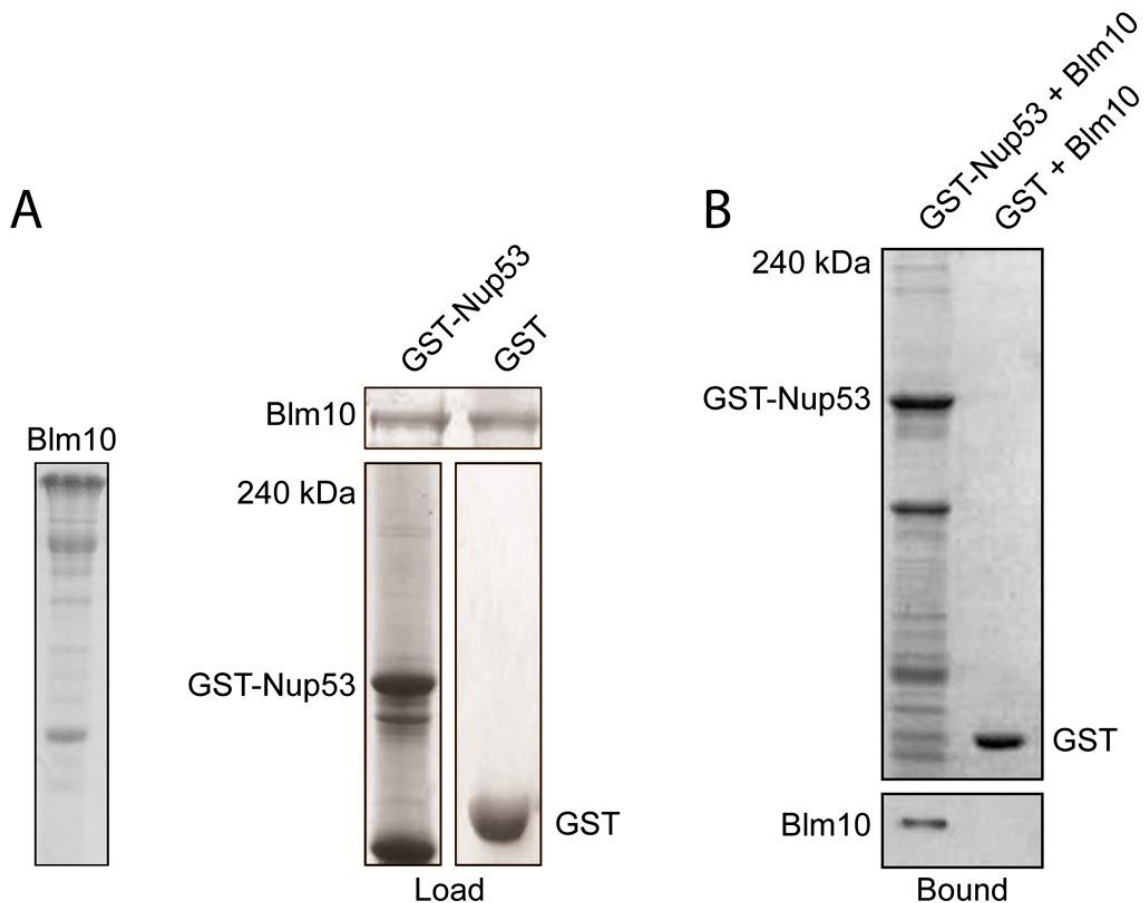


Figure 20: Blm10 interacts with GST-Nup53. Solution binding assays were performed with GST-Nup53 and GST purified from *E. coli* (A, load) and 12xHis-Blm10 purified from yeast (A). GST-Nup53 and GST were immobilized on glutathione sepharose and incubated with equal amounts of 12xHis-Blm10 (A, load, top lane, Coomassie Blue stained). After washing of the beads, bound proteins were analyzed by SDS-PAGE and Coomassie Blue staining (B, bound: top panel). The presence of Blm10 was verified by immunoblotting against the 12xHis-tag of Blm10 (B, bound: bottom panel).

The binding of Blm10 to GST-Nup53 or GST was first analyzed by Coomassie Blue staining. In the sample, in which 12xHis-Blm10 was incubated with GST-Nup53, an additional band of 240 kDa was detected. Since no band was visible at this molecular mass for purified GST-Nup53 (Figure 20A, load), it assumingly represented bound Blm10. This assumption was verified by immunoblotting against the 12xHis-tag of Blm10 (Figure 20B, bound). Blm10 did not bind to GST alone.

## Results

A crucial property of an importin is that it increases the affinity of the cargo for the NPC to facilitate its translocation. Blm10-CP complexes should therefore have higher affinity for Nups than the CP by itself. To test this, solution binding assays were performed. Free CPs were purified from a culture of uninduced *blm10* $\Delta$  cells transformed with an inducible plasmid overexpressing 12xHis-Blm10. Blm10-capped CP was purified from the same culture after induction. In both strains the  $\alpha$ 4 subunit was chromosomally tagged with a HA-TevProA tag, which allowed affinity purification of free CP or Blm10-CP with IgG sepharose beads. CP and Blm10-CP were cleaved off the affinity beads using Tev protease. As before, GST-Nup53 was used as a representative protein for the NPC. Since the hydrophobic FG repeats of Nup53 are natively unfolded and disordered, they could potentially serve as substrate for free CPs. Binding assays could therefore show a signal that is not due to a relevant interaction between the proteins, but rather due to the CP degrading the unfolded structures. To minimize this false positive signal, the proteolytic activity of the proteasome was inhibited using the specific proteasome inhibitor MG-132. To ensure that the activity was inhibited, peptide cleavage assays were performed prior to solution binding assays showing a 90% inhibition of the proteasomal activity. As shown above, GST-Nup53 was immobilized on glutathione sepharose beads (Figure 21A, load, bottom lane; Coomassie blue stained gel) and incubated with equal amounts of CP or Blm10-CP. To confirm that equal amounts of proteasome were used, the loads were separated by SDS-PAGE, and the gel was subsequently stained with Coomassie blue and immunoblotted against the HA-tag of  $\alpha$ 4 (Figure 21A, load). To test for the presence of 12xHis-Blm10 in the CP preparations, immunoblotting against Blm10 was performed. Blm10 was detectable in the induced culture, although not visible by Coomassie blue staining (Figure 21A, load). After the incubation of GST-Nup53 with the CP or Blm10-CP, the sepharose beads were washed and bound CP and Blm10 were analyzed by immunoblotting against  $\alpha$ 4-HA and 12xHis-Blm10 (Figure 21B, bound).

## Results

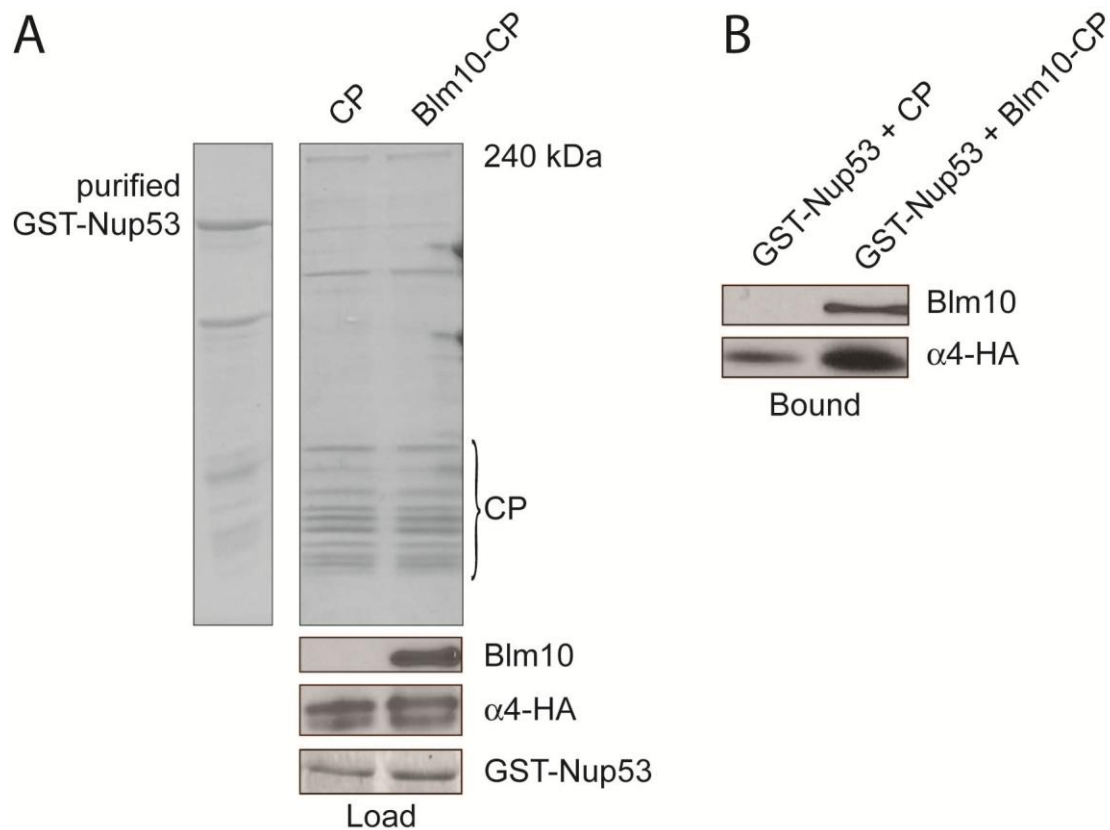


Figure 21: Blm10 enhances the affinity of the CP to GST-Nup53. GST-Nup53 was purified from *E. coli* (A, left lane; Coomassie blue stained gel) and immobilized on glutathione sepharose beads (A, load, bottom panel; Coomassie blue stained gel). CP and Blm10-CP were purified from yeast (A, load, top panel; Coomassie blue stained gel). Both proteasome preparations were blotted against  $\alpha$ 4-HA and 12xHis-Blm10 (A, load). GST-Nup53 was incubated with equal amounts of CP or Blm10-CP. Prior to the incubation of the CP or Blm10-CP with GST-Nup53, the proteolytic activity of the CP was inhibited with MG-132. After washing, bound proteins were analyzed by immunoblotting against  $\alpha$ 4-HA and 12xHis-Blm10 (B).

The analysis of the bound proteins showed that Blm10-CP complexes had a higher affinity for GST-Nup53 in comparison to free CPs. As anticipated for importins, Blm10 mediated the contact of the CP to Nups.

In summary, Blm10 was found to interact with proteins of the NPC and its association with the CP additionally increased the affinity of the CP to Nup53, which is specific for an importin and essential for the translocation of the cargo.

### 3.4.4. The import of Blm10 is dependent on the Ran cycle

The classical nuclear import and export cycle is dependent on a functional Ran-GTP-Ran-GDP gradient established and maintained by multiple enzymes. Briefly, in the nucleus the level of Ran-GTP is high whereas the level of Ran-GDP is low. The reverse is true in the cytosol. In yeast, two homologues of Ran were identified, Gsp1 and Gsp2, but only Gsp1 is essential (Wong et al., 1997). Ran and Gsp1 are

## Results

highly homologous proteins that share 90% sequence identity (Wong et al., 1997). To examine whether the Gsp1-GTP-Gsp1-GDP gradient is required for the nuclear import of Blm10 from the cytosolic PSGs, a strain was used that expresses a temperature sensitive mutant of Gsp1 (*gsp1-1*). At elevated temperatures, this mutant shows a temperature sensitive phenotype caused by a disrupted Gsp1 gradient (Wong et al., 1997). The *BLM10* gene in the *gsp1-1* strain was chromosomally tagged with GFP and Blm10 localization was monitored by direct fluorescence microscopy at the indicated conditions (Figure 22).

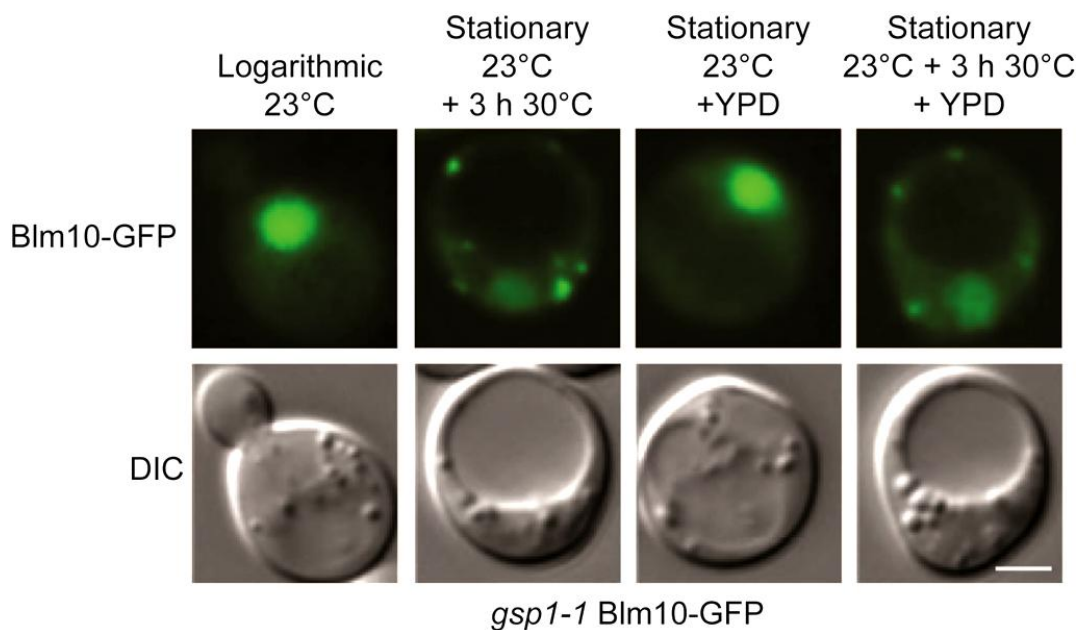


Figure 22: The import of Blm10 is dependent on a functional Gsp1 gradient. Blm10 was chromosomally tagged with GFP in the *gsp1-1* strain. Localization of Blm10 was monitored by direct fluorescence microscopy at the indicated conditions. Figure: C. Enenkel.

The localization of Blm10 in cells grown to logarithmic phase is mainly nuclear, as published before (logarithmic, 23°C; see also section 3.1.3; Fehlker et al., 2003; Schmidt et al., 2005; Doherty et al., 2012). To monitor the localization of Blm10 in stationary phase, the cells were grown at the permissive temperature of 23°C to stationary phase. Blm10 localized to PSGs (not shown) that rapidly dissolved after addition of fresh YPD media (stationary + YPD, 23°C). To test whether the disruption of the Gsp1 gradient affects the import of Blm10, stationary cells were incubated for 3 h at non-permissive temperature (30°C). Blm10 still localized to PSGs (stationary, 23°C + 3 h 30°C). However, transfer of these cells into new YPD medium resulted in no nuclear import of Blm10 (stationary, 23°C + 3 h 30°C + YPD). This finding indicates that the disturbance of the Gsp1 gradient prevented the import of Blm10, and conse-

## Results

quently, that the import of Blm10 out of the PSGs is dependent on the established Gsp1-GTP-Gsp1-GDP gradient.

### **3.4.5. Analysis of the interaction of Blm10 and Gsp1-GTP**

A classical feature of importins is their ability to bind to Ran-GTP in the nucleus. The formed Ran-GTP-importin complex is subsequently exported out of the nucleus into the cytosol, where GTP hydrolysis occurs resulting in the dissociation of Ran-GDP and the importin (Moore & Blobel, 1993; Rexach & Blobel, 1995; Floer & Blobel, 1996). Therefore, importins have a significantly lowered affinity for Ran-GDP than for Ran-GTP. To test whether Blm10 can bind to Gsp1-GTP and to test whether its affinity for Gsp1-GDP is lower than for Gsp1-GTP, solution binding assays were performed. This assay was used previously to determine interactions between Ran-GTP and importins (Maurer et al., 2001; Hahn & Schlenstedt, 2011). A point mutant of Gsp1 (Gsp1Q71L), which stabilizes the GTP bound form of Gsp1, and wt Gsp1 were purified as GST fusion proteins from *E. coli*. 12xHis-Blm10 was purified from yeast (Figure 23A, left lane; Coomassie blue stained gel). Prior to the immobilization on glutathione sepharose beads, GST-Gsp1Q71L was loaded with GTP and wt GST-Gsp1 with GDP. GST served as a negative control (Figure 23A, load; Coomassie Blue stained gel). Equal amounts of Blm10 (Figure 23A, load, bottom lane; Coomassie blue stained gel) were incubated with the immobilized proteins and bound proteins were analyzed by SDS-PAGE and immunoblotting against the 12xHis-tag of Blm10 (Figure 23A, right panel).



## Results

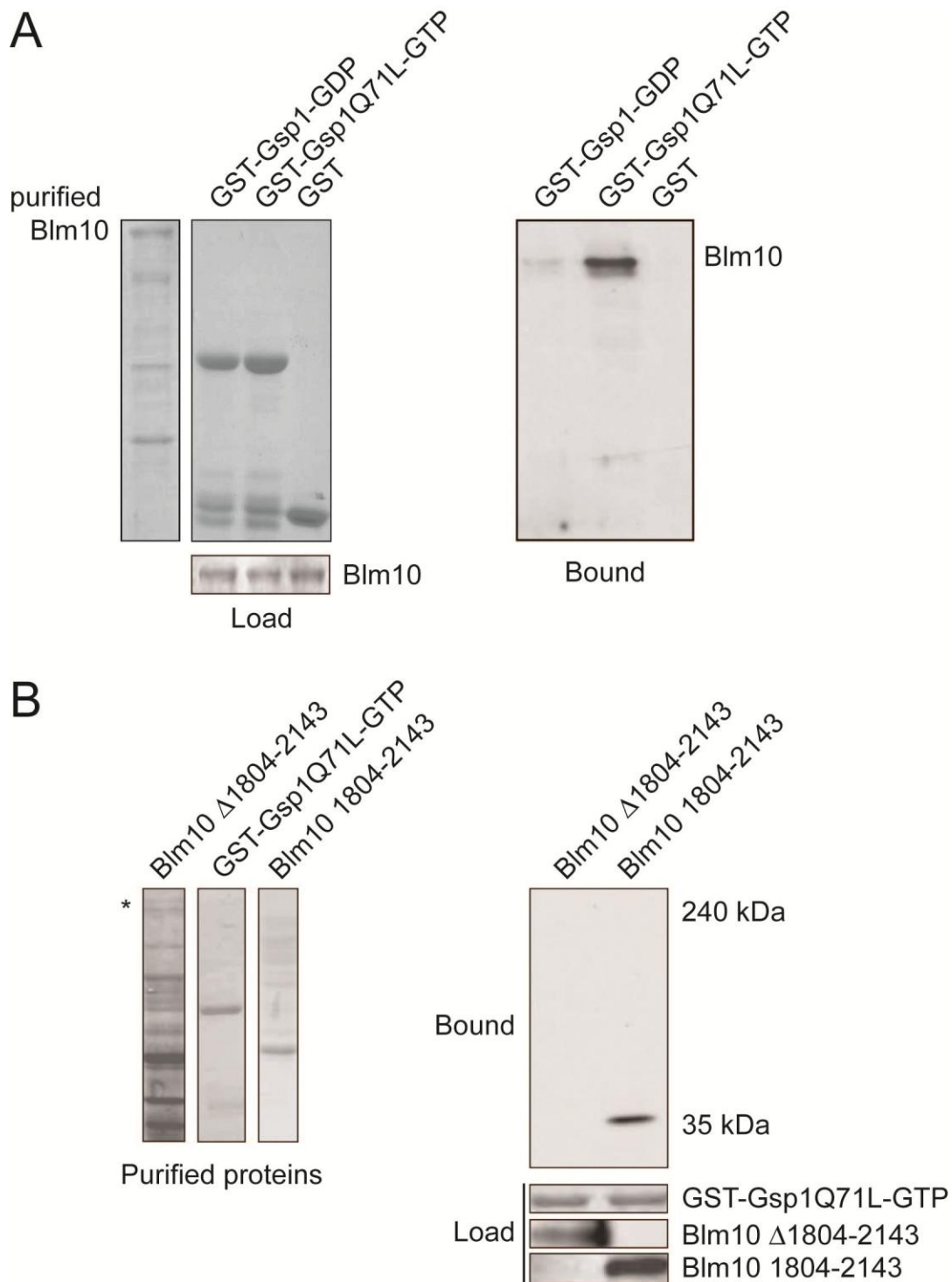


Figure 23: Blm10 interacts with Gsp1-GTP with its C-terminal region. (A) Solution binding assays were performed to examine the affinity of Blm10 for Gsp1-GTP, Gsp1-GDP and GST. GST-Gsp1Q71L, GST-Gsp1 and GST were purified from *E. coli* and 12xHis-Blm10 was purified from yeast (left panel, Coomassie blue stained gel). GST-Gsp1Q71L was loaded with GTP and GST-Gsp1 with GDP prior to immobilization on glutathione sepharose beads (load; Coomassie blue stained gel). Equal amounts of Blm10 were incubated with the immobilized proteins (load; Coomassie blue stained gel). Bound proteins were analyzed by SDS-PAGE and subsequent immunoblotting against the 12xHis-tag of Blm10. (B) To analyze if the binding site for Gsp1-GTP is located within the C-terminal 339 amino acids of Blm10, solution binding assays were performed. 12xHis-Blm10  $\Delta$ 1804-2143 was purified from yeast, 6xHis-Blm10 1804-2143 and GST-Gsp1-Q71L-GTP from *E. coli* (purified proteins, Coomassie blue stained gel; \* represents undegraded 12xHis-Blm10  $\Delta$ 1804-2143). Immobilized GST-Gsp1-Q71L-GTP was incubated with comparable amounts of 12xHis-Blm10  $\Delta$ 1804-2143 and 6xHis-Blm10 1804-2143

## Results

(load; immunoblot) and bound proteins were analyzed by immunoblotting against the His-tags of the proteins.

The analysis of the bound proteins showed that Blm10 bound to GST-Gsp1Q71L-GTP. In contrast to that, a weaker signal was detected for Blm10 incubated with GST-Gsp1-GDP, and Blm10 did not bind to GST at all. It was therefore verified that Blm10 is capable of binding to Gsp1-GTP *in vitro* and that it is further able to distinguish between the GTP and the GDP bound form of Gsp1, which is a typical feature of importins (Floer & Blobel, 1996).

It is currently unknown which regions or residues of Blm10 bind to Gsp1. However, the C-terminal 339 amino acids of Blm10 were of interest since its sequence identity and similarity with Blm10 homologues is higher than the average for the rest of the Blm10 sequence (Schmidt et al., 2005). Interestingly, deletion of this C-terminal region resulted in the mislocalization of the truncated Blm10. Instead of the nuclear localization typical for fulllength Blm10 (see Figure 10; Fehlker et al., 2003), C-terminally truncated Blm10 localized in dividing cells diffusely to the cytosol (Schmidt et al., 2005; Doherty et al., 2012). Bioinformatic analysis of the C-terminus revealed that this region contains no NLS which would have explained the mislocalization. To further examine whether the Gsp1 binding domain of Blm10 is located in its C-terminal region, two constructs were created for subsequent solution binding assays: One of the constructs encoded a 12xHis-Blm10 with a deletion of the amino acids 1804-2143 (referred to as 12xHis-Blm10  $\Delta$ 1804-2143). The second construct encoded only the amino acids 1804-2143 tagged with a 6xHis-tag (6xHis-Blm10 1804-2143). 12xHis-Blm10  $\Delta$ 1804-2143 was purified from yeast and 6xHis-Blm10 1804-2143 from *E. coli* (Figure 23B, purified proteins; Coomassie blue stained gel). Purifications revealed that 12xHis-Blm10  $\Delta$ 1804-2143 is a highly unstable protein. For the solution binding assay, GST-Gsp1Q71L-GTP was purified from *E. coli*, loaded with GTP and immobilized on glutathione sepharose beads (Figure 23B, load; Coomassie blue stained gel). Equal amounts of 6xHis-Blm10 1804-2143 and of undegraded 12xHis-Blm10  $\Delta$ 1804-2143 were incubated with the beads (Figure 23B, load; immunoblot). Unbound proteins were washed off and bound proteins analyzed by SDS-PAGE and immunoblotting against the His-tags of the proteins (Figure 23B, bound).

## Results

12xHis-Blm10  $\Delta$ 1804-2143 and all degradation products failed to bind to Gsp1-GTP completely, whereas 6xHis-Blm10 1804-2143 bound to it with high affinity. This analysis showed that the Gsp1 binding sites of Blm10 are located within its C-terminal 339 amino acids.

In general, Ran is bound by two protein families: RanBPs as well as transport factors like importins and exportins. To find further evidence that Blm10 acts as an importin and to gain more insights into the binding of Blm10 to Gsp1-GTP, the C-terminal region of Blm10 was analyzed for features that are typical for importins or RanBPs.

Typically, importins have strong similarities in their secondary and tertiary structure since all of them consist mainly of  $\alpha$  helical HEAT/Arm repeats arranged in a toroid fold (Wente & Rout, 2010). The secondary and tertiary structure of Blm10 was analyzed in detail when the crystal structure of it in complex with the CP was solved and like importins, Blm10 consists mainly of HEAT-like repeats arranged in the typical toroid fold (Kajava et al., 2004; Sadre-Bazzaz et al., 2010).

Until 2007, only ten different  $\beta$  importins were identified in yeast (Fries et al., 2007). The analysis of their primary structures revealed only a very low degree of similarity and the residues that mediate the contact between Ran/Gsp1 and the importin were highly variable, both of the importin and of Ran/Gsp1 (Macara, 2001). A sequence analysis of Ran binding domains in importins revealed only a 10% sequence similarity and, aside from an N-terminally located CRIME region and a loop consisting of 7-10 acidic amino acids, which interact directly with Gsp1, no specific binding motifs or invariant residues could be assigned for the interaction between Ran/Gsp1 and importins (Enenkel et al., 1996; Görlich et al., 1997; Macara, 2001). The primary structure of the C-terminal region of Blm10 was therefore searched for the presence of the CRIME region and a comparable acidic patch. No CRIME region could be identified; however five acidic amino acids were found in the C-terminal region of Blm10, located within residues 2127-2134. These residues were aligned with the acidic loop of Kap95, the importin  $\beta$  of yeast (Figure 24A). As a potential Gsp1 interaction site, the acidic patch has to be accessibly located on the surface of the protein. To test this, the crystal structure of Blm10-CP-Blm10 (file 1VSY; Sadre-Bazzaz et al., 2010) was downloaded from PDB and illustrated using the software PyMOL (Figure 24B and C; Blm10 in red, each subunit of the CP in a different color). Resi-

## Results

dues 2127-2134 of Blm10, containing the acidic amino acids (blue patch, arrow) were highlighted from the rest of Blm10.

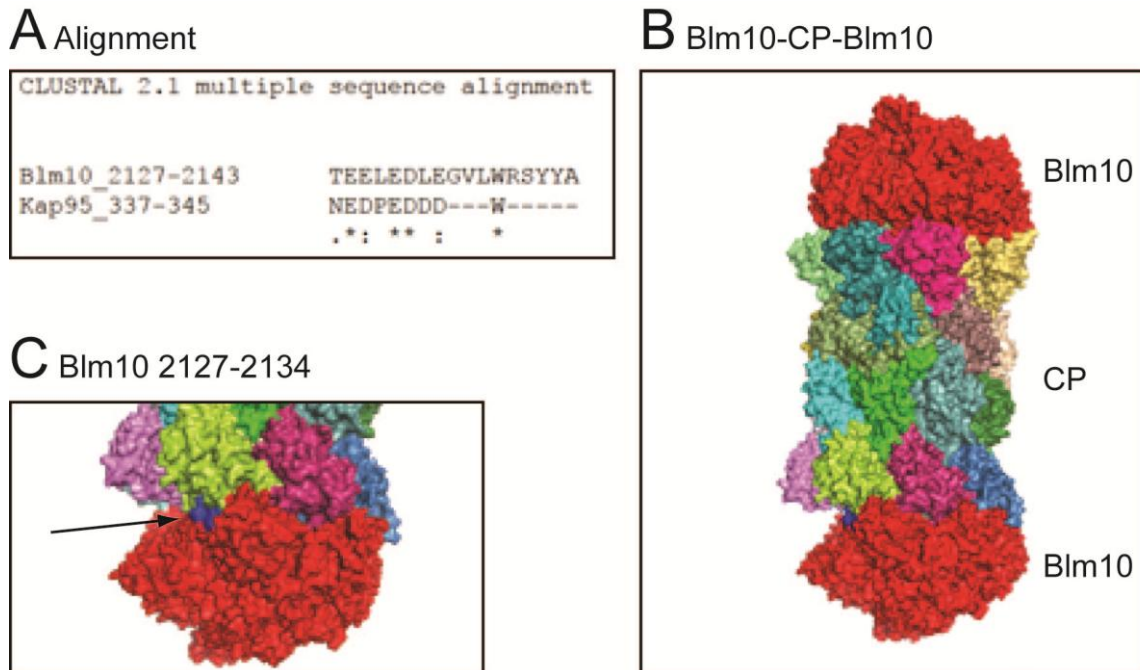


Figure 24: Blm10 contains an acidic patch. (A) Alignment of residues 2127-2143 of Blm10, which contain the acidic patch, to the acidic loop of yeast importin  $\beta$  using the software Clustal 2.1. (B), (C) The location of the acidic patch is illustrated in blue (arrow) in the Blm10-CP-Blm10 complex using the software PyMOL and the file 1VSY. One molecule of Blm10 is shown in red on top and on the bottom of the CP (colored).

The analysis of the structure of the Blm10-CP-Blm10 complex showed one noticeable rift located at the interface between Blm10 and the CP. The acidic patch is located on the surface of this rift, close to the edge of the Blm10 and CP interaction sites and could be suited for the binding of Gsp1 molecules. The bioinformatic analysis of Blm10 and its C-terminus showed that three important features typical of importins, namely the consistency of HEAT repeats, their overall structure, and the existence of an acidic patch, are also present in Blm10 and its C-terminal region (Figure 24; Sadre-Bazzaz et al., 2010).

RanBPs represent the second protein family that interacts with Ran. In contrast to importins, the binding of RanBPs is highly conserved and specific residues in RanBPs and in Ran were identified as conserved interaction sites (Vetter et al., 1999b). In order to test if these residues are present in the C-terminal 339 residues of Blm10, this amino acid sequence was aligned with the conserved interaction sites of RanBPs. As a representative of RanBPs, the yeast homologue of RanBP1, Yrb1, was chosen (Figure 25A). The alignment showed that the highly conserved motif

## Results

WKE is also present in Blm10 (residues 2021-2023). In Yrb1, this motif is in direct contact with Ran. In order to determine whether Blm10's W2021 mediates the binding to Gsp1-GTP, this residue was mutated to an alanine and the affinities of the C-terminus and the mutated C-terminus to Gsp1-GTP were compared. To achieve better yields in the protein purification, a slightly longer version of the C-terminal region was chosen (residues 1749-2143; also referred to 6xHis-Blm10 1749-2143 or 6xHis-Blm10 1749-2143 W2021A, respectively; the construct encoding for 6xHis-Blm10 1749-2143 and the mutagenesis of 6xHis-Blm10 1749-2143 W2021A were performed by T. Bissinger). All proteins were purified from *E. coli*. GST-Gsp1Q71L was loaded with GTP prior to the immobilization on glutathione sepharose beads (Figure 25B, load, bottom panel; Coomassie blue stained gel). Equal amounts of both C-terminal fragments were incubated with GST-Gsp1Q71L-GTP (Figure 25B, load, immunoblot) the beads were washed and binding was analyzed by immunoblotting (Figure 25B, bound). As a control for un-specific binding, GST was purified, immobilized on glutathione sepharose beads and incubated with 6xHisBlm10 1749-2143.

## Results

### A Alignment

Yrb1_84-131	-----
Blm10_1804-2143	DYVLPFLIGLVKHKDVCALASLDPVRLYAGLGYMPIRKNHVAAIVDYVCSSNVALSSNQT
Yrb1_84-131	-----EVLYKVRAKLFRFDADAKE-WKE-
Blm10_1804-2143	KLQLAFIQHFLSAELLQLTEEEKNKILEFVVSNLVNEQFVEVVRRAASILSDIVHNWKEE
	* : : * * . : : * . * * *
Yrb1_84-131	RGTGD--CKFLKNKKTNKVRILMRRDKT-----
Blm10_1804-2143	QPLLSLIERFAKGLDVNKYTSKERQKLSKTDIKIHGNVLGLGAIISAFPYVFPPLPWIPK
	: . : * * . . * * * * : . : :
Yrb1_84-131	-----
Blm10_1804-2143	QLSNLSSWARTSGMTGQAAKNTISEFKKVRADTWKFDRASFNTEELEDEGLVLRSSYYA

### B

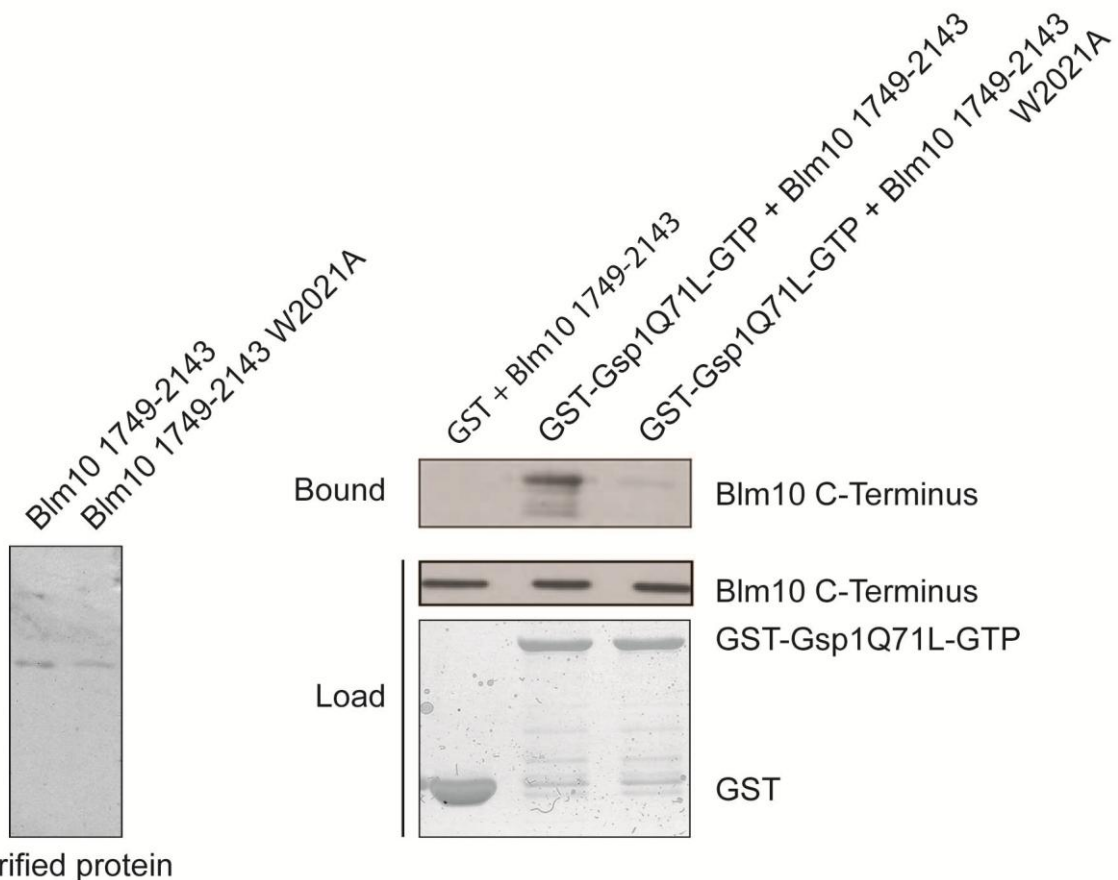


Figure 25: Mutation of Blm10's W2021 affects the binding of Blm10 1749-2143 to Gsp1-GTP. (A) Alignment of the C-terminal 339 amino acid of Blm10 with the conserved Ran binding region of Yrb1 using ClustalW. The marked residue is Blm10's W2021. (B) To examine whether mutation of W2021 affects the affinity of the C-terminus of Blm10 to Gsp1-GTP, solution binding assays were performed. GST-Gsp1Q71L-GTP, GST, Blm10 1749-2143 and Blm10 1749-2142 W2021A were purified from *E. coli*. GST-Gsp1Q71L was loaded with GTP prior to immobilization on glutathione sepharose beads (load; Coomassie blue stained gel). Equal amounts of the versions of the Blm10 C-terminus were incubated with the immobilized proteins (load; immunoblot against 6xHis-tag). Bound proteins were analyzed by SDS-PAGE and subsequent immunoblotting against the 6xHis-tag of the Blm10 C-terminus.

In comparison to the wt Blm10 C-terminal region, the W2021A mutation reduced the affinity of the C-terminal fragment of Blm10 to GST-Gsp1Q71L-GTP substantially,

## Results

indicating that this residue is either directly involved in the binding, or that its mutation indirectly affected the binding, for example by changing the structure of the protein.

### **3.4.6. Association of Gsp1-GTP dissociates a CP-Blm10 complex**

The nuclear import cycle comprises of first the association of the cargo and the importin, and then their translocation through the NPCs. Once the translocation is completed, Ran-GTP binds to the importin resulting in the release of the cargo. The newly formed dimeric Ran-GTP-importin complex is subsequently exported into the cytosol (Moore & Blobel, 1993; Rexach & Blobel, 1995; Floer & Blobel, 1996). The dissociation of the importin-cargo complex resulting from Ran-GTP association is an important feature of the nuclear import cycle and represents an important property for the identification of a potential importin. Thus, experiments were performed in this work to test whether the Blm10-CP complex can be dissociated by Gsp1-GTP binding. Two approaches were chosen, including dissociation experiments *in vivo* and *in vitro*.

To test for potential dissociation *in vivo*, a yeast strain in which the  $\alpha 4$  subunit of the proteasome was tagged with HA-TevProA was transformed with a plasmid expressing FLAG-Gsp1G21V behind a galactose-inducible promoter. Gsp1G21V is a mutant of Gsp1 which is stabilized in its GTP-bound state. Proteasomes from uninduced and induced cells were purified using IgG sepharose beads and the preparations were analyzed by SDS-PAGE followed by Coomassie blue staining or immunoblotting against Blm10. The induction of FLAG-Gsp1G21V was verified by immunoblotting against the FLAG-tag (Figure 26).

## Results

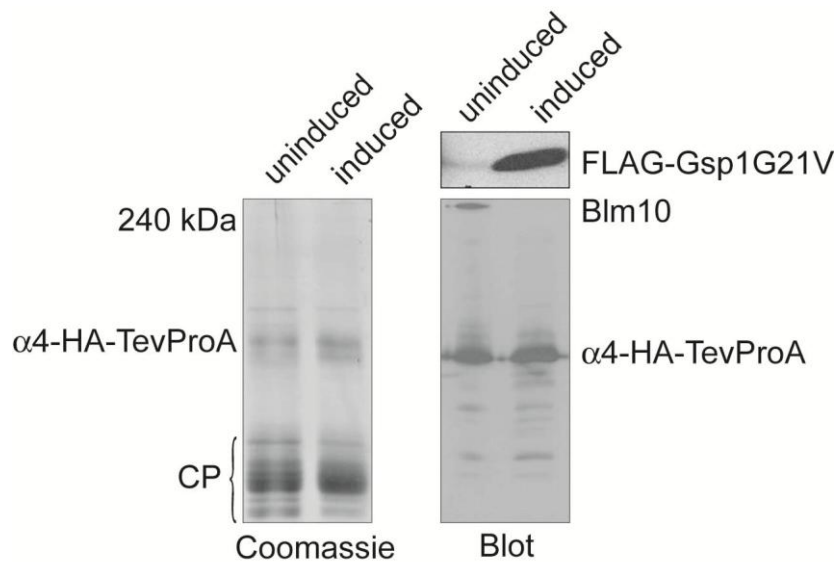


Figure 26: Expression of Gsp1G21V dissociates Blm10-CP complexes *in vivo*. A wt strain was transformed with a plasmid expressing FLAG-Gsp1G21V behind a galactose-inducible promoter. Proteasomes were purified with IgG sepharose beads from uninduced and induced cultures using an HA-TevProA-tag of the  $\alpha 4$  subunit. Preparations were analyzed by Coomassie blue staining and immunoblotting against Blm10 and FLAG-Gsp1G21V.

The analysis of the purified proteasomes from uninduced cells showed the typical pattern representing the CP subunits. In the Coomassie blue stained gel, no band for Blm10 was visible, however, when the same sample was analyzed by immunoblotting against Blm10, a strong band appeared showing that Blm10 was associated with proteasomes. The second band detected on this immunoblot resulted from binding of the antibody to the HA-TevProA-tag of  $\alpha 4$ .

Coomassie blue staining of the proteasome preparation purified from induced cells revealed no difference to the preparation from uninduced cells. However, the immunoblot against Blm10 showed that upon induction of the expression of FLAG-Gsp1G21V, Blm10 was no longer bound to the CP, and only the band representing  $\alpha 4$ -HA-TevProA was detected in the immunoblot. This result suggests that expression of FLAG-Gsp1G21V, which is predominantly present in its GTP-bound state, interfered with the binding of Blm10 to the CP.

To test for a potential dissociation of the CP-Blm10 complex caused by Gsp1-GTP *in vitro*, Blm10 was purified as 12xHis-Blm10 from yeast, and the CP was purified from a *blm10* $\Delta$  strain in which the  $\beta 5$  subunit was tagged with GFPS allowing the native preparation of the GFP-tagged complex. Finally, GST-Gsp1Q71L was purified from *E. coli*. To avoid any interference of the GST-tag of the fusion-protein with the function of Gsp1, the GST-tag was removed by thrombin cleavage (Figure 27A, purified



## Results

proteins; Coomassie blue stained gel). However, this cleavage resulted in low yields of the protein and most of the fusion protein remained bound on the glutathione sepharose beads. For the *in vitro* dissociation experiment, CP-GFPS was first incubated with Blm10, to allow the formation of Blm10-CP-Blm10 complexes. Subsequently, it was incubated with (Figure 27A, lane 2) or without Gsp1Q71L-GTP preloaded with GTP (Figure 27A, lane 3). CP configurations were analyzed by phosphofluoroimaging and compared to Blm10-free CPs (Figure 27A, lane 1).

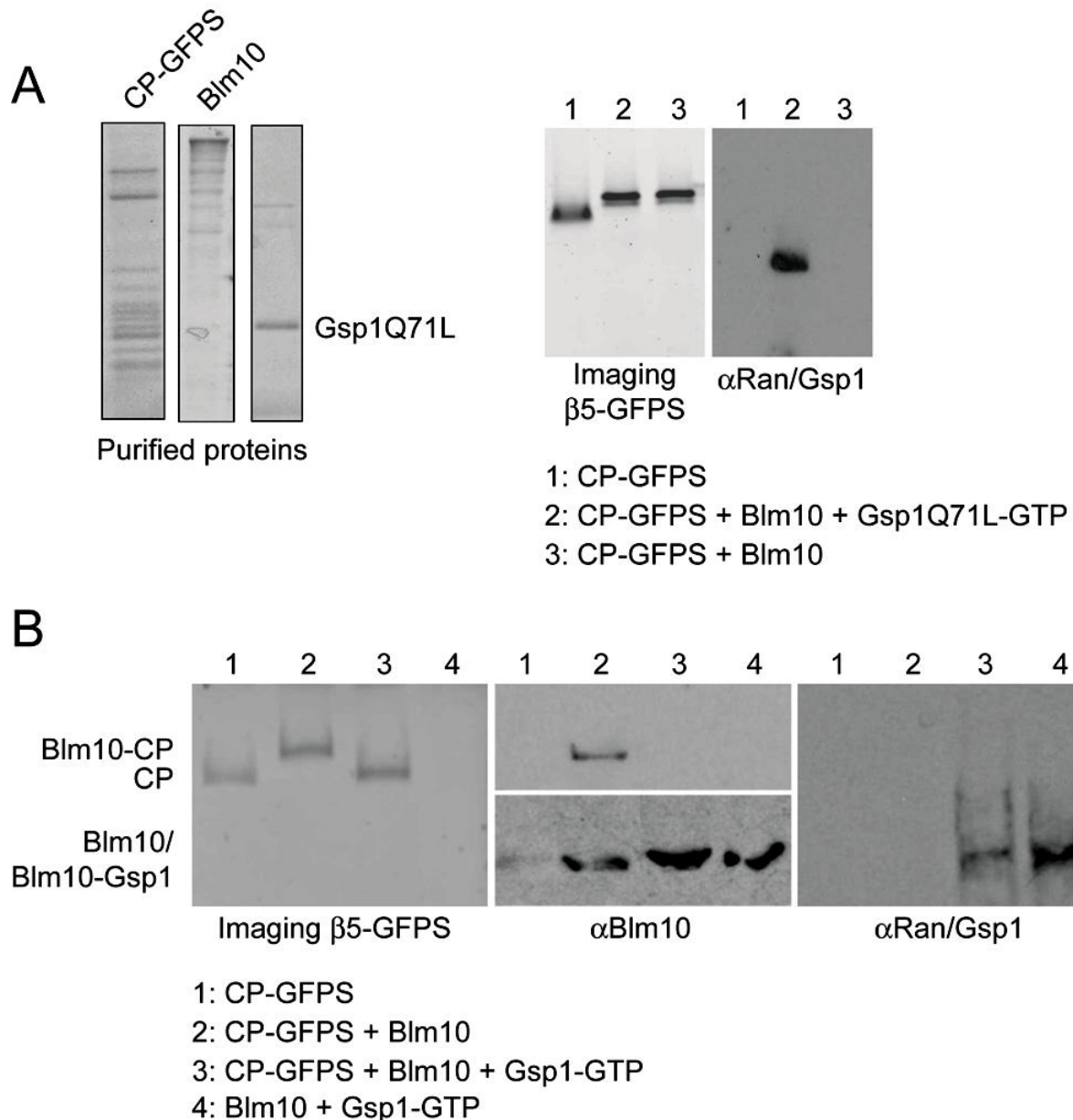


Figure 27: Gsp1-GTP dissociates Blm10-CP complexes *in vitro*. (A) Initial attempt: CP-GFPS and 12xHis-Blm10 were purified from yeast and GST-Gsp1Q71L from *E. coli* (purified proteins). GST-tag of the fusion protein was removed by thrombin cleavage. Gsp1Q71L was loaded with GTP prior to the dissociation experiment. All samples were analyzed by phosphofluoroimaging and immunoblotting against Ran. (B) CP-GFPS and 12xHis-Blm10 were purified from yeast and 6xHis-Gsp1-GTP from *E. coli*. The samples mentioned above were prepared and analyzed by phosphofluoroimaging and immunoblotting against Blm10 and Ran (experiment completed by C. Enenkel).

## Results

As expected, incubation of CPs with Blm10 resulted in the formation of slower migrating Blm10-CP-Blm10 complexes (Figure 27A, compare lanes 1 and 3). However, addition of Gsp1Q71L-GTP to Blm10-CP-Blm10 did not result in the dissociation of the Blm10-CP-Blm10 complex (Figure 27A, lane 2). Immunoblotting against Ran/Gsp1 revealed that the protein did not associate with Blm10-CP-Blm10, but was found to form a complex migrating between the CP and Gsp1 (Figure 27A, lane 2; immunoblot).

After the work in this study was finished, the experiment was repeated by C. Enenkel using 6xHis-Gsp1-GTP instead of GST-Gsp1Q71L-GTP. This was advantageous since thrombin cleavage of GST-Gsp1Q71L-GTP resulted in preparations of Gsp1Q71L-GTP that contained most likely non-functional proteins. In contrast, usage of 6xHis-Gsp1-GTP yielded in high concentrations of the functional protein.

As seen before, Blm10 associated with the CP to form a slower migrating complex (Figure 27B, compare lanes 1 and 2). Addition of Gsp1-GTP to Blm10-CP-Blm10 complexes resulted in the faster migrating complex, indicating that Gsp1-GTP dissociated Blm10-CP-Blm10 *in vitro* (Figure 27B, lane 3). Immunoblotting against Blm10 and Ran/Gsp1 showed that Blm10 and Gsp1-GTP form a complex (Figure 27B, lanes 3 and 4) confirming the previous result showing that Gsp1-GTP associates with Blm10 in solution.

## 4. Discussion

A functional proteolytic system is essential for the viability of each cell. In eukaryotic and some prokaryotic cells, the specific degradation of proteins is achieved by the proteasome. Research on proteasome function is of special interest since misregulated or insufficient proteasome activity has been brought in context with a variety of diseases in humans (Goldberg, 2003; Römisch, 2005). One example is the non-functional or insufficient protein degradation in neuronal cells, resulting in protein aggregation into plaques and the formation of neurodegenerative diseases (Rubinsztein, 2006). Since neuronal cells are non-dividing cells, recent research also focused in yeast on proteasomes and their activity in cells grown to quiescence. Interestingly, the localization of proteasomes in dividing and non-dividing yeast cells differs drastically (Laporte et al., 2008). In quiescent cells, proteasomes are focused in cytosolic spots named PSGs, whereas in dividing cells they are mainly localized to the nucleus (Laporte et al., 2008; Enenkel et al., 1998; Russell et al., 1999). Currently, the mechanism of PSG formation, the proteins which accumulate in these structures, and how PSGs dissolve when cells exit quiescence are unknown. The goal of this work was to study the function of PSGs and the possible involvement of the conserved proteasome activator Blm10 in the formation and dissolution of PSGs.

### 4.1. The sequestration of the CP into PSGs is dependent on Blm10

The intracellular localization of proteasomes and their potential activity is highly dynamic (Laporte et al., 2008). In the unicellular organism *S. cerevisiae*, proteasome localization is dependent on the metabolic state of the cell itself (Laporte et al., 2011). In dividing cells with high intracellular ATP levels and low AMP levels, 80% of all proteasomes localize to the nucleus or to the nuclear envelope (Enenkel et al., 1998; Russell et al., 1999; Laporte et al., 2011). The distribution of proteasomes changes when yeast cells enter quiescence, and most proteasomes are focused in cytosolic clusters named PSGs (Laporte et al., 2008). The trigger for PSG formation was initially identified as glucose deprivation (Laporte et al., 2008), but further studies revealed that the lack of glucose results in a decrease of intracellular ATP levels and an increase in AMP levels (Laporte et al., 2011). A third study identified the decreasing intracellular pH as the trigger for PSG formation (Peters et al., 2013).

## Discussion

When yeast cells enter quiescence, proteasomes first localize to the nuclear periphery and are subsequently exported into the cytosol, where they are sequestered into PSGs (Laporte et al., 2008). In this study, the conserved proteasome activator Blm10 was identified as an essential component for the sequestration of the CP into PSGs. Deletion of *BLM10* resulted in diffuse cytosolic localization of the CP, indicating that Blm10's function is specific for the sequestration of the CP into PSG and that it is not required for the export of the CP into the cytosol. Based on the data obtained in this study, it is possible that Blm10 itself sequesters the CP into PSGs; however, it cannot be excluded that the observed effects are indirect. For example, there may be additional proteins which associate with Blm10 and sequester the complex to the PSGs. Importantly, Blm10's function in PSG formation is specific for CPs and Blm10 does not seem to be pivotal for PSG formation or protein sequestration *per se*, since both the RP base and lid were sequestered into PSGs in *blm10Δ* cells. The fact that RP sequestration is independent of Blm10 is not surprising as Blm10 by itself does not bind to the RP. Additionally, CP and RP are not associated with each other in stationary phase, although they colocalize to PSGs (Laporte et al., 2008; Bajorek et al., 2003). This presumably excludes the possibility of sequestering the Blm10-CP-RP hybrid complex to PSGs and suggests the separate sequestration of proteasome CPs and RPs.

Based on the data obtained so far, the mechanism for how Blm10 potentially sequesters the CP into PSGs remains unknown and will be the goal of future research. It is conceivable that Blm10 and the CP associate prior to sequestration; however, it has not been investigated whether this association occurs in the nucleus or after the export of Blm10 and the CP into the cytosol. After export and association, the Blm10-CP complex is sequestered into PSGs. The question arises of whether Blm10 remains associated to the CP within the PSGs or whether the association is only temporary, such that Blm10 dissociates with the CP in PSGs and can subsequently shuttle additional CPs. The latter idea is supported by native PAGE performed in this study showing that in stationary phase, most CPs exist as free CP that are not associated with Blm10. After the sequestration of the CP is completed, Blm10 itself finally colocalizes with CPs to PSGs. Interestingly, transcription and protein levels of Blm10 are both increased in non-dividing cells (Lopez et al., 2011; Weberruss et al., 2013), which may suggest that Blm10 fulfills an important function that is specific for station-

## Discussion

ary phase. This function of Blm10 could potentially be the regulation of CP localization by promoting its sequestration into PSGs.

To identify additional proteins involved in PSG formation and further investigate its mechanism, an SGA (synthetic genetic array) screen was performed by J. Jando. In this screen, the ability of a collection of yeast strains with single deletions of non-essential genes to form PSGs was examined and Blm10 was amongst the target proteins, confirming the results of this work (see diploma thesis of J. Jando).

### **4.2. PSGs function as proteasome stocks**

Research on PSGs raised the question of why PSGs are formed in non-dividing yeast cells. To date, two hypotheses exist: the same study that discovered the existence of PSGs revealed that they were rapidly resolved after the quiescent cells resumed cell proliferation, resulting in a fast re-import of the CP and RP into the nucleus (Laporte et al., 2008). Since it was excluded in that study that the rapid increase in nuclear proteasomes originated from newly synthesized proteasomal precursor complexes, it was concluded that PSGs serve as storage compartments for mature proteasomes. Therefore, PSG formation guarantees the rapid import of proteasomes into the nucleus and avoids the highly time- and energy-consuming *de novo* proteasomal synthesis (Laporte et al., 2008). A later study suggested that the storage of proteasomes in PSGs additionally represents a protective mechanism for the proteasomes against autophagocytosis (Peters et al., 2013).

Simultaneous to the discovery of PSGs, a second study addressed the fate of misfolded proteins when proteasome function was inhibited (Kaganovich et al., 2008). In yeast and mammalian cells, misfolded proteins were shown to be sequestered into the cytosolic JUNQ and IPOD clusters. JUNQs contained misfolded but soluble proteins, whereas IPOD contained insoluble proteins. The fact that proteasomes were found to colocalize with JUNQs led to the hypothesis that JUNQs function as degradation sites for misfolded proteins and that sequestration of misfolded proteins was thought to be conducive to their degradation by increasing their local concentration (Kaganovich et al., 2008). JUNQs and PSGs were later found to be identical structures (Weberruss et al., 2013) that were termed PSGs in this work.

## Discussion

To further address whether PSGs serve as storage granules or whether the sequestration of proteasomes into PSGs is essential for the degradation of misfolded proteins, proteasome configurations were analyzed in cells grown to stationary phase and compared to configurations in logarithmic phase. For potential degradation of polyubiquitylated substrates in PSGs, it is pivotal that CPs are associated with RPs, which are essential for the recognition, unfolding and translocation of polyubiquitylated substrates (for an overview see Wolf & Hilt, 2004). Native PAGE performed in this study showed that RP-CP complexes were, despite the colocalization of the CP and RP, almost completely dissociated from each other, which is consistent with previous data (Bajorek et al., 2003). The fact that RP and CP dissociate in quiescence is additionally supported by the fact that intracellular ATP levels decrease and AMP levels increase in stationary phase (Laporte et al., 2011). Since RP and CP association is known to be ATP-dependent (Eytan et al., 1989; Liu et al., 2006), low intracellular ATP and high AMP levels found in quiescent cells presumably cause RP-CP dissociation.

Although a small fraction of the RP existed as RP-CP complexes in non-dividing cells, the majority of RPs existed mainly as  $RP_n$  complexes based on their migration pattern in native PAGE.  $RP_n$  were previously identified in RP preparations performed under conditions of ATP and ADP depletion (Kleijnen et al., 2007), an experimental condition that is similar to intracellular metabolic conditions in cells grown to quiescence (Laporte et al., 2011). The formation of RP complexes into  $RP_n$  complexes, which were previously shown to be incompetent for association with CPs due to conformational changes (Kleijnen et al., 2007), might, in addition to low intracellular ATP levels, prevent RP and CP reassociation.

The majority of proteasome CPs is sequestered to PSGs in stationary phase and CPs exist there as free particles, or to a lesser extent associated with one or two molecules of Blm10. This finding indicates that these CPs are not proteolytically active against polyubiquitylated substrates. Based on this data, PSG presumably represent storage granules instead of degradation sites.

A second experiment assayed the degradation of the cytosolic misfolded substrate  $\Delta$ ssCPY\* in non-dividing wt and *blm10 $\Delta$*  cells. In the latter cells, no CPs are sequestered to PSGs. In this assay, the degradation kinetic was identical in both strains, showing that the sequestration of the CP into the PSGs is not required for the degra-

## Discussion

dation of this substrate. Presumably,  $\Delta$ ssCPY\* is degraded by remaining RP-CP complexes.

In general, the dissociation of RP-CP complexes in stationary phase reduces the capacity of the proteasomal degradation machinery. However, since the cell metabolism is down-regulated in stationary phase, less newly synthesized misfolded and short-lived proteins, such as regulators of the cell cycle, arise. Therefore, the degradative capacity of the cell is likely not challenged (Bajorek et al., 2003).

The result of the degradation assay is consistent with the data obtained from native PAGE showing that the majority of sequestered CPs exists as free CPs in PSGs which are thought to be capable of degrading unfolded, oxidized protein (Liu et al., 2003; Goldberg, 2003; Jung et al., 2009; Glickman et al., 1998a) but not of polyubiquitylated substrates. Based on the data obtained in this study, it can be concluded that PSGs presumably do not represent degradation sites for polyubiquitylated proteins, but storage granules for mature proteasomes. However, it cannot currently be excluded that unfolded oxidized proteins could be degraded in PSGs.

### **4.3. The import of mature CPs is dependent on Blm10**

The trigger for PSG formation is the deprivation of glucose in the media, which was suggested to either cause a decrease of the intracellular pH or the intracellular ATP levels (Laporte et al., 2008; Laporte et al., 2011; Peters et al., 2013). Consequently, addition of glucose to quiescent yeast cells results in the rapid dissolution of PSGs and the re-import of RPs and CPs into the nucleus (Laporte et al., 2008). It is so far unknown what the molecular mechanisms are for PSG dissolution and re-import of mature proteasomes.

This study showed that Blm10 is required for the sequestration of the CP into PSGs. Since Blm10 is structurally related to importins (Raveh & Glickman, 2005; Huber & Groll, 2012), its involvement in proteasome re-import upon PSG dissolution was examined in this work. Fluorescence microscopy revealed that deletion of *BLM10* delayed the re-import of mature CPs, suggesting that Blm10 represents an essential component for the rapid re-import of mature CPs into the nucleus. The examination of Blm10's function in CP re-import is discussed in section 4.4 in detail. In *blm10* $\Delta$  cells, the intranuclear concentration of CPs increased two hours after the transfer of

## Discussion

the cell into fresh media. It remains unknown whether this increase results from proteasome *de novo* synthesis or whether the re-import of the mature CPs is delayed.

*BLM10* deletion had no effect on RP base or lid re-import. Since RP re-import is independent of Blm10 but CP re-import is dependent on Blm10, it is conceivable that RPs and CPs do not associate prior to the import, that they are not imported as the Blm10-CP-RP hybrid complex and that the mechanisms for RP and CP re-import differ from each other. The mechanism for RP import upon PSG dissolution is currently unknown and will be a goal of future research. It is conceivable that the re-import of base and lid occurs in one complex since the RP exists predominantly as RP<sub>n</sub> complexes in PSGs. Hypothetically, the base subunits Rpn2 and Rpt2, which both contain functional NLS required for RP base import in logarithmic growth phase (Wendler et al., 2004), could also participate in the re-import upon PSG dissolution. Alternatively, the lid is imported in dividing yeast cells with adaptor proteins to which importin  $\alpha$  binds (Yen et al., 2003a; Yen et al., 2003b; Chen et al., 2011).

Subsequent to their re-import into the nucleus, RPs and CPs have to reassociate to form RP-CP complexes that are competent for the degradation of polyubiquitylated proteins. Amongst those proteins are regulators of the cell cycle whose regulated degradation is essential to resume cell division. Examination of RP-CP reassociation in wt and *blm10* $\Delta$  strains by native PAGE showed that in the wt strain, RP-CP complexes were found to be increased 15 min after the transfer of the cells into fresh media. The reassociation kinetic is therefore slightly slower than the kinetic for the re-import as assessed by fluorescence microscopy, which showed that re-import is accomplished within 5 min. This time difference between re-import and reassociation of CP and RP could be caused by the use of different experimental procedures for the relocalization and native PAGE analyses whose time courses are difficult to synchronize. Additionally, RPs exist in stationary phase as RP<sub>n</sub> complexes that are not competent for CP binding (Kleijnen et al., 2007). Therefore, these RP<sub>n</sub> complexes may have to undergo conformational changes before they are able to associate with CPs.

As a consequence of the delayed CP re-import in *blm10* $\Delta$  cells, the reassembly of RP-CP complexes was found to be drastically delayed and *BLM10* deletion prevented the formation of nuclear RP-CP complexes for two hours. Consistent with this experiment, *blm10* $\Delta$  cells, in which PSG formation is inhibited and CP re-import and subsequent RP-CP reassembly are delayed, showed sensitivity against phleomycin



when grown to quiescence (this study; Doherty et al., 2012). Presumably, the rapid re-import of proteasomes into the nucleus, which is facilitated by PSG formation, and the subsequent rapid reassociation of nuclear RP-CP complexes allows higher stress tolerance in wt cells and represents their ability to respond quickly to changing environmental conditions. This hypothesis is supported by computational analysis showing that proteasome function provides the cells with the ability to react to changing environmental conditions through the degradation of potentially toxic transcription factors that are expressed when cells leave quiescence (Bonzanni et al., 2011).

#### **4.4. Bim10 represents the importin for mature CPs**

In dividing cells, the import of proteasome CPs into the nucleus is well studied and occurs at the stage of CP precursor complexes (see also the model of CP import in logarithmic growth phase in Figure 28; Lehmann et al., 2002). The nuclear transport of precursor complexes occurs via the import receptor complex importin  $\alpha\beta$ , which binds to classical NLS located in the  $\alpha$  subunits of the CP (Zwickl et al., 1992; Lehmann et al., 2002). Subsequent to the import, maturation is completed in the nucleus and matured CPs mask their NLS after conformational changes. Consequently, matured CPs are not recognized by importin  $\alpha\beta$ , which is consistent with the early hypothesis that proteasomes exist in transport competent and transport incompetent states (Tanaka et al., 1990; Lehmann et al., 2002).

logarithmic phase

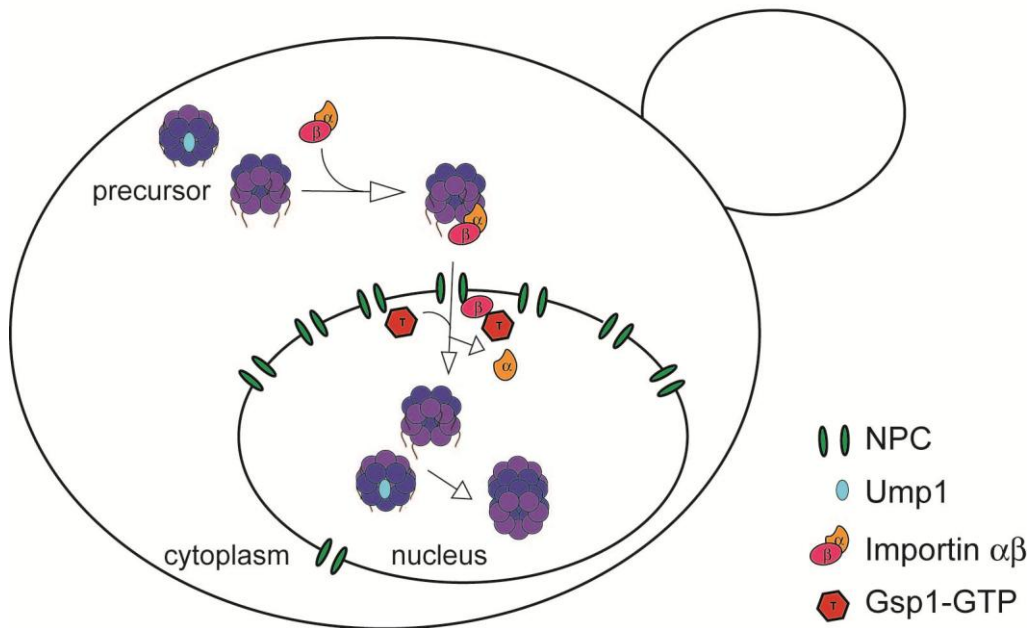


Figure 28: Model of CP import in logarithmic phase. Precursor complexes have accessible NLS in their  $\alpha$  subunits, which are recognized by the classical nuclear transport receptor importin  $\alpha\beta$ . In the nucleus, the importin-cargo complex is dissociated by Ran/Gsp1-GTP and the final steps of maturation occur. Due to conformational changes in the  $\alpha$  rings, NLS of  $\alpha$  subunits are masked in matured CPs.

The findings that proteasomes are sequestered into PSGs in quiescence, and that these proteasomes are rapidly re-imported into the nucleus upon resuming of cell proliferation (Laporte et al., 2008) raised the question of how these proteasomes are translocated back into the nucleus. This work showed that only mature CPs and no proteasomal precursor complexes are found in non-dividing cells, and consistent with previous data (Lehmann et al., 2002; Savulescu et al., 2011), matured CPs and Blm10-CP complexes were shown not to be re-imported via the classical transport receptor importin  $\alpha\beta$ . Therefore, an alternative import mechanism has to exist for the rapid re-import of mature CPs after dissolution of PSGs. Data obtained by fluorescence microscopy showed that *BLM10* deletion caused a delay in CP re-import suggesting that Blm10 is essential for re-import and that it could therefore either function as importin for the mature CP or, alternatively, as an adaptor protein to which the importin binds.

To confirm the CP re-import study performed in living yeast cells, the nuclear import of matured CPs in the presence and absence of Blm10 was examined in reconstituted *Xenopus* egg nuclei. This assay showed that Blm10 increased the recruitment of

## Discussion

yeast CP to the NPCs by a factor of 1.8 and the import of the CP into the nuclei by a factor of 1.9. This data is consistent with previous studies using this assay, in which the *Xenopus* CP was found not to be imported into the reconstituted nuclei. Instead, the *Xenopus* specific 20S+ complex consisting of the CP, Rpn1, Rpn2, Hsp90 and importin  $\beta$  was actively imported (Savulescu et al., 2011). The fact that the CP without Blm10 showed a weak rim-like and intranuclear signal in the assay may be explained by the fact that during reconstitution of the nuclei small amounts of PA200, the homologue of Blm10, remained in the assay. PA200 may associate with the yeast CP and recruit it to the NPCs as well as initiate its import. Control experiments showed that the rim-like signal in the absence of Blm10 is caused by the specific association of the CP to NPCs and could additionally result from CP interacting with and degrading the hydrophobic unfolded regions of some Nups.

The data obtained by reconstitution experiments and the *in vivo* data from yeast showed clearly that Blm10 facilitates the nuclear import of CPs, which represents the first criterion for its identification as an importin. Importantly, no further import factors were added to the reconstitution assay, suggesting that Blm10 functions as CP importin and not as adaptor to which an additional importin binds. However, as cytosolic fractions were used for the reconstitution of the *Xenopus* egg nuclei, it cannot be excluded that minute presence of an additional factor originating from the cytosolic fractions participated in CP import in this experiment.

Additional evidence that Blm10 itself could function as importin for the mature CP was found by analysis of the secondary and tertiary structure of Blm10 (Glickman & Raveh, 2005; Huber & Groll, 2012). Blm10 consists of 32  $\alpha$ -helical HEAT-like repeats (Sadre-Bazzaz et al., 2010), a structural feature that is typically found in importins, but does not *per se* represent a criterion for the identification of importins (Macara, 2001). However, analysis of the tertiary structure of Blm10 and importins showed that, in addition to similarities in the secondary structure, Blm10's toroid  $\alpha$ -helical fold is related to the tertiary structure of importin  $\beta$  (Huber & Groll, 2012).

In the nuclear import cycle, the importin-cargo complex is translocated through the NPCs subsequent to the association of cargo and importin. This translocation through NPCs is mediated by interactions of the importin with Nups. The *in vitro* interaction of Blm10 with Nup53, a representative NPC protein, was verified in this study by solution binding assays. Nup53 was chosen as a representative for

## Discussion

FG-Nups since it was previously shown to interact with the importins Pse1/Kap121 and Kap95 (importin  $\beta$  in yeast), therefore representing an important interaction partner for importins. In contrast, Nup53 does not participate in protein export (Marelli et al., 1998; Fahrenkrog et al., 2000; Tetenbaum-Novatt et al., 2012). In a second experiment, the affinity of Nup53 to the CP or the Blm10-CP complex was tested. The CP alone showed only weak binding to Nup53 which increased when the CP was capped with Blm10, suggesting that association of the CP with Blm10 increased the CP's affinity for Nups. The weak signal of the CP incubated with Nup53 in the absence of Blm10 could be due to the fact that Nup53 is an FG-Nup, containing unstructured repetitive motifs enriched in phenylalanine and glycine, which can be recognized as substrate by the CP (Liu et al., 2003; Jung et al., 2009). To rule out this possibility, the proteolytic activity of the CP was inhibited with MG-132. However, a residual activity of the CP remained, potentially resulting in the unspecific binding of the CP to Nup53.

In summary, both *in vitro* experiments show that Blm10 is the mediator for the interaction of the Blm10-CP complex with the NPC, representing a second important property of an importin.

In yeast, the nuclear import of RNA and proteins is dependent on the GTP-binding protein Gsp1, the homologue of mammalian Ran, as well as an established Gsp1-GTP-Gsp1-GDP gradient which ensures the directionality of the nuclear transport (Moore & Blobel, 1993; Melchior et al., 1993; Wong et al., 1997; Richards et al., 1997). Fluorescence microscopy performed in this study using the *gsp1-1* mutant showed that the import of Blm10 released from the cytosolic PSGs is also dependent on a functional Gsp1-GTP-Gsp1-GDP gradient. A genome-wide genetic interaction map showed further correlation between Blm10 and the Gsp1 gradient. Blm10 has positive genetic interactions with the RanGEF Prp20 and negative genetic interaction with the RanGAP Rna1 (Costanzo et al., 2010), both essential enzymes for the maintenance of the Gsp1 gradient (Amberg et al., 1993; Klebe et al., 1995b; Becker et al., 1995).

In the nucleus, Ran-GTP/Gsp1-GTP binds to the importin in the importin-cargo-complex, resulting in the release of the cargo (Rexach & Blobel, 1995). This important property of an importin was proven in this work for the CP, Gsp1-GTP and Blm10 both in an *in vitro* and *in vivo* assay.

## Discussion

After the dissociation, the newly formed importin-Ran-GTP complex is subsequently exported into the cytosol where GTP hydrolysis and dissociation of this complex occurs (Becker et al., 1995). In contrast to adaptors, importins bind directly to Ran-GTP/Gsp1-GTP, and therefore Blm10's interaction with Gsp1-GTP was tested in this study by an *in vitro* assay. The results of this assay showed that Blm10 indeed bound to Gsp1-GTP and furthermore, that Blm10 was capable of distinguishing between the GTP-bound and the GDP-bound forms of Gsp1, which is typical for importins (Rexach & Blobel, 1995). The affinity of different importins for Ran/Gsp1-GTP ranges from low nanomolar to micromolar, presumably representing one of the regulation mechanisms of the nuclear transport (Macara, 2001; Hahn & Schlenstedt, 2011). Although not quantified in this work, solution binding assays performed in this study showed that the affinity of Blm10 for Gsp1-GTP to be relatively low, as association of Blm10 with Gsp1-GTP was difficult to detect in Coomassie blue stained gels and required additional analysis by immunoblotting.

The results of the dissociation experiments and the *in vitro* binding assays of Blm10 and Gsp1-GTP strongly support the hypothesis that Blm10 acts as the importin for mature CPs.

Additional solution binding assays narrowed the binding region of Blm10 to Gsp1-GTP to Blm10's C-terminal region. This result is consistent with previous data showing that C-terminally truncated Blm10 was not imported into the nucleus in dividing cells, but mislocalized to the cytosol (Schmidt et al., 2005; Doherty et al., 2012). Interestingly, this C-terminal region is the most conserved between Blm10 and its homologues, and is required for its correct localization. For Blm10, this region contains the Gsp1 binding site, while for Blm10 homologues, it contains their NLS (Schmidt et al., 2005). In addition to the Gsp1 binding site, the C-terminus of Blm10 also contains the binding site for the CP, with the last three amino acids of Blm10 especially important for binding (Sadre-Bazzaz et al., 2010; Dange et al., 2011). The finding that the C-terminus of Blm10 is involved in both the binding of the CP and Gsp1-GTP is consistent with the competitive binding of importin  $\beta$  to importin  $\alpha$  and Ran-GTP. Previous data showed that the region of importin  $\beta$ /Kap95 which binds to importin  $\alpha$  overlaps with the region of importin  $\beta$ /Kap95 which binds to Ran-GTP, a property that suggests a competitive replacement of importin  $\alpha$  by Ran-GTP (Enenkel et al., 1996). This could also be true for Blm10, the CP and Gsp1-GTP as both bind

## Discussion

to the C-terminal region of Blm10. In the crystal structure of the Blm10-CP-Blm10 complex, Blm10 was found to form a closed dome on top of the CP; however, one indentation located in the C-terminal region of Blm10 could potentially allow Gsp1 binding to Blm10, causing the displacement of the CP. Based on the data obtained so far, this possibility remains speculative and the binding of Blm10 to Gsp1-GTP has to be characterized in greater detail to test this hypothesis.

To further characterize the binding of Blm10 to Gsp1-GTP, the primary structure of the C-terminal region of Blm10 was bioinformatically examined in this study for similarities to importins and RanBPs. This search showed that Blm10 contains a patch of acidic residues similar to the one identified in importin  $\beta$  (Macara, 2001). Interestingly, this acidic patch is located accessibly in the indentation of the Blm10-CP-Blm10 complex that was previously speculated to allow the docking of Gsp1-GTP. However, the alignment of Blm10's C-terminus and the conserved Ran-binding site of the yeast RanBP Yrb1 (Vetter et al., 1999b) showed that Blm10 also contains motifs related to the binding sites of RanBPs and the mutation of one of these residues, W2021, resulted in a lower affinity of the C-terminus of Blm10 for Gsp1-GTP. It remains speculative whether W2021 is directly involved in Gsp1-GTP binding or whether the mutation results in conformational changes indirectly affecting binding.

In addition to the analysis of the binding site, Blm10's structure and function were compared to RanBPs and transportins/importins. Blm10 functions as importin for the mature CP and does not stimulate the GTPase activity of Gsp1, which is typical for RanBPs (Bischoff et al., 1995; Bischoff & Görlich, 1997). Additionally, it consists of  $\alpha$ -helical HEAT-like repeats arranged in a toroid fold, which is a typical feature of importins (Macara, 2001; Sadre-Bazzaz et al., 2010). In summary, it is likely that the binding of Blm10 to Gsp1-GTP occurs similarly to the binding of importins to Ran/Gsp1-GTP. However, with the data obtained so far, it is only speculative which residues in Blm10 and Gsp1 mediate the contact for the formation of the Blm10-Gsp1-GTP complex.

stationary phase

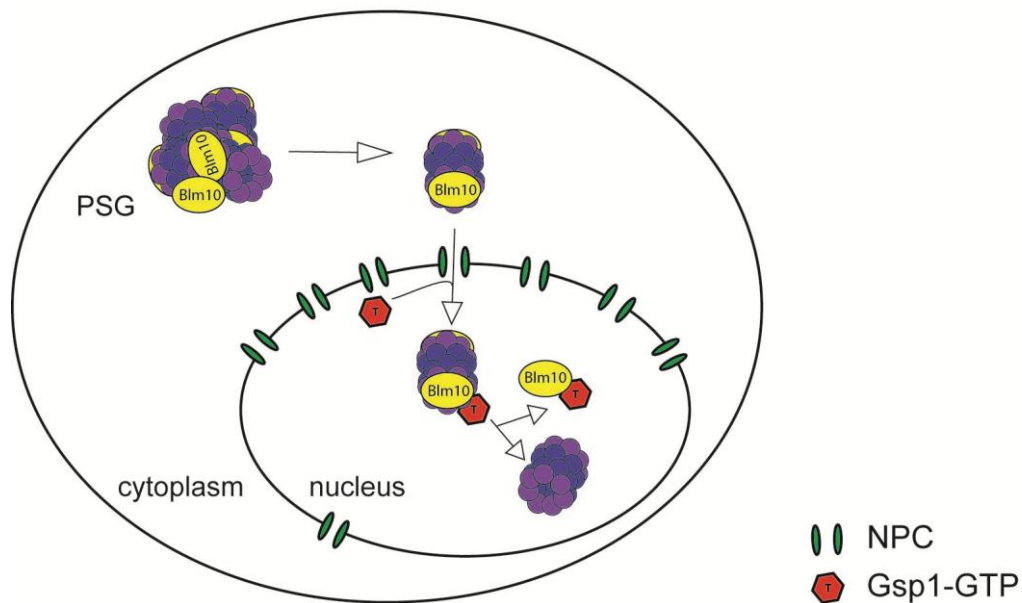


Figure 29: Model of the CP import in stationary phase. Blm10 associates with the CP prior to import and mediates the contact to proteins of the NPC (green) resulting in the translocation of the complex through the NPC. In the nucleus Gsp1-GTP binds to Blm10, resulting in the dissociation of the CP.

Based on the data obtained in this study, Blm10 was identified as the first known importin for mature CPs (Figure 29). Upon PSG dissolution, Blm10 caps the CP entrance gates during re-import into the nucleus and facilitates the translocation through NPC. In the nucleus, Gsp1-GTP binding to Blm10 releases the mature CP so that it can reassociate with RPs. The association of Blm10 with the CP during the transport might prevent the CP from degrading the unstructured regions of the Nups. Similarly, CPs are imported as inactive precursor complexes in dividing cells (Lehmann et al., 2002). The last part of the nuclear import cycle includes the export of the importin-Ran-GTP complex to the cytosol. Consistently, C-terminally truncated Blm10 that is due to the deletion of the Gsp1 binding domain unable to bind to Gsp1-GTP was previously shown not to be recycled to the cytosol but to remain localized to the nucleus in non-dividing cells (Doherty et al., 2012).

Indeed, mechanisms analogous to mature proteasome CP import have been shown for other highly complex transport cargo such as ribosomal precursor complexes, which depend on the HEAT-repeat containing protein Rrp12 interacting with Gsp1 and Nups for export (Oeffinger et al., 2004).

## 4.5. Future directions

### 4.5.1. The sequestration of the CP into PSGs

This study revealed that in non-dividing cells, the sequestration of the CP into PSGs is dependent on Blm10. Based on the data obtained by fluorescence microscopy it is known that the export of the CP out of the nucleus occurs independently of Blm10 and that Blm10 is only required for sequestration. Presumably, the CP associates with Blm10 for sequestration either prior to or subsequent to the export. However, the mechanism and regulation of the sequestration is currently unknown. Since sequestration of the CP into PSGs has not been observed in dividing cells, a regulation mechanism has to exist to initiate the cytosolic re-localization of the CP-Blm10 complex. Post-translational modifications are known to be important for the localization of the proteasome as it was reported previously that deletion of an N-myristoylation site in the RP subunit Rpt2 resulted in mislocalization of the 26S proteasome (Kimura et al., 2012). Both, Blm10 and the proteasome were previously found to be co- and post-translationally modified. In the case of Blm10, 12 phosphorylation sites were identified, some of which are regulated by the cell cycle (phosphoGRID). The proteasome contains in total 110 different modifications, such as N-acetylations, phosphorylations and N-myristoylations (Kikuchi et al., 2010). Therefore, it is imaginable that the proteasome or Blm10 are modified in quiescence to promote sequestration. To test this, it could be examined by mass spectrometry whether the proteasome or Blm10 show a different pattern in post-translational modifications when isolated from cells grown to logarithmic or stationary phase. A difference in the pattern of post-translational modifications would suggest a regulative function for these modifications. This could be further tested by mutagenesis of the modification sites, which should result in inhibited CP sequestration. Alternatively, no difference in the pattern of post-translational modifications between cells in logarithmic and stationary phase could suggest a different mechanism of regulation or that additional proteins are required for sequestration, indicating that Blm10 represents an adaptor for sequestration to which these proteins can bind.

The transcription and protein levels of Blm10 are increased in stationary phase (Dange et al., 2011; Weberruss et al., 2013), however, only approximately one third of CPs sequestered to PSGs are capped with one or two molecules of Blm10. Since



## Discussion

Blm10 is essential for the sequestration of each CP, CPs and Blm10 consequently have to dissociate subsequent to sequestration. Therefore, the question arose of whether Blm10 shuttles constantly between the cytoplasm and PSGs to sequester additional CPs to PSGs, which themselves remain localized to the granules. To test this possibility, FRAP (fluorescence recovery after photobleaching) experiments could be performed with quiescent yeast cells with GFP-labeled CP or Blm10 (Lippincott-Schwartz & Patterson, 2003; Kaganovich et al., 2008). The fluorescence of the GFP-tag of Blm10 or of the CP could be photobleached either in the cytosol, or alternatively in the PSGs by a laser pulse, and subsequently, the exchange rate of Blm10 or the CP could be assessed by changes of the fluorescence signal in PSGs or the cytosol after the initial bleaching. If unbleached proteins move into bleached areas, a non-steady localization of the protein is indicated. High exchange rates for both proteins would suggest that both the CP and Blm10 leave and re-enter the PSGs constantly. Low exchange rates would indicate that until dissolution, PSGs represent steady structures. A high exchange rate for Blm10 and a low exchange rate for the CP would suggest that the CP remains steadily localized to the PSGs but dissociated from Blm10, and that Blm10 constantly sequesters additional CPs to PSGs.

### 4.5.2. The function of PSGs

This study showed that PSGs most likely serve as storage sites for proteasomes in quiescent yeast cells. This conclusion was based on analysis of proteasome configurations in quiescence and on analysis of the degradation kinetics of the reporter substrate  $\Delta$ ssCPY\*, which were found to be identical in wt and *blm10* $\Delta$  strains. Presumably,  $\Delta$ ssCPY\* was degraded efficiently in both strains by remaining RP-CP complexes. To exclude the possibility that a potential function of PSGs in protein degradation was masked by residual RP-CP complexes, the degradation of an overexpressed substrate like VHL-GFP could be additionally assayed in wt and *blm10* $\Delta$  strains. An overexpression substrate would further challenge the degradative capacity of RP-CP complexes. Prior to degradation, it should be confirmed that the substrate is sequestered to PSGs and colocalizes with the CP in wt cells. If the degradation kinetics are identical in both strains, it can be concluded that PSGs are not formed in order to degrade polyubiquitylated substrates.

## Discussion

To further investigate the possibility that free CPs sequestered to PSGs degrade oxidized proteins, the degradation of oxidized reporter substrates could be assayed by CHX chase analysis in quiescent wt and *blm10* $\Delta$  strains. If the formation of PSGs is conducive for the degradation of these substrates, the degradation should be more efficiently achieved in wt cells than in *blm10* $\Delta$  cells. If PSGs function as proteasome storage granules and CPs are proteolytically inactive in these structures, no difference in the degradation should be observable between the two strains.

### 4.5.3. The function of Blm10 as importin for mature CPs

Blm10 was identified in this study to function as a CP-specific importin. Part of the import cycle is the association of Blm10 with Gsp1-GTP. Based on solution binding assays, the affinity of both proteins for each other, although not quantified, appeared to be rather low in this work. Quantification could be achieved by analysis of the interaction by surface plasmon resonance-based methods, such as Biacore® (GE Healthcare).

Based on the data obtained through solution binding assays in this work, it is currently unknown which residues in the C-terminal region of Blm10 and Gsp1 represent the binding sites for their interaction. In this study, an acidic patch, commonly found in importins, was identified in the C-terminal region of Blm10. To test whether this acidic patch interacts directly with Gsp1-GTP, the acidic patch could be mutated in the C-terminal fragment of Blm10 that was previously also used to determine a potential participation of Blm10's residue W2021 in the binding to Gsp1-GTP. If the acidic patch of Blm10 participates in Gsp1 binding, the affinity of the C-terminus with the mutated acidic patch for Gsp1-GTP should be decreased significantly *in vitro*.

Additionally, the acidic patch could be mutated in the full length version of Blm10, and the binding of wt and mutant Blm10 to Gsp1-GTP could be examined *in vitro* as described for the C-terminal region above. If the acidic patch is part of the binding site of Blm10 to Gsp1-GTP, its mutation should decrease the affinity of Blm10 to Gsp1-GTP. If this is the case, the mutated full length Blm10 encoded on a plasmid could be transformed into *blm10* $\Delta$  cells and subsequently be used for *in vivo* studies. For example, whether the mutation affects the rapid nuclear re-import of CPs out of the PSGs could be tested. If the mutation of the acidic patch blocks the interaction between Blm10 and Gsp1-GTP, the import cycle should be blocked resulting in a de-

## Discussion

delayed re-import of mature CPs. This result in combination with a significantly decreased affinity of Blm10 to Gsp1-GTP would suggest that the acidic patch is essential for the interaction of Blm10 and Gsp1-GTP and also for the re-import of mature CPs. To exclude the possibility that the mutation of the acidic patch affects re-import through disrupting the interaction of Blm10 and Nups, or Blm10 and the CP, it should be confirmed that the mutated Blm10 and wt Blm10 have comparable affinities to Nups or the CP, respectively. If the re-import of mature CPs occurs with mutated Blm10 as observed for wt Blm10, the acidic patch would not be essential for the re-import and additional residues have to be tested.

Importin  $\beta$  was shown to make contact with Ran-GTP over several HEAT repeats (Vetter et al., 1999a) and therefore, it may not be possible to map all residues involved in binding through single residue mutagenesis. A technically more demanding experiment would be the crystallization of the Blm10-Gsp1-GTP complex. If this is successful, the interaction could be analyzed in detail.

Blm10 functions in dividing cells in proteasome maturation, quality control or is required for the degradation of specific proteins (Fehlker et al., 2003; Lopez et al., 2011; Lehmann et al., 2008). In contrast, Blm10 sequesters CPs into PSGs in stationary phase and the transfer of quiescent cells into fresh media results in a rapid nuclear re-import of cytosolic CPs facilitated by Blm10's function as importin. Due to the variety of different functions proposed for Blm10, the question arose of whether Blm10's function as importin is specific to dividing cells or cells leaving quiescence. To test this possibility, it would be interesting to assess whether the affinity of Blm10 for Gsp1-GTP or Nups changes with the growth phase. Instead of purifying Blm10 expressed from an overexpression plasmid, endogenous Blm10 could be purified from a culture grown to logarithmic phase, a culture grown to stationary phase, and from a culture grown to stationary phase whose cells were transferred into fresh media. After purification, the affinity of Blm10 for Gsp1-GTP or Nup53 could be tested by solution binding assays or surface plasmon resonance-based methods. Differences in the affinities would consequently mean that the function of Blm10 as importin might be dependent on the growth phase or metabolic state of the cell, which might represent a regulatory mechanism for Blm10's function as importin. If no difference is detectable, Blm10 may function as importin during all growth phases, but since CPs are imported as immature precursor complexes in dividing cells via the import receptor importin  $\alpha\beta$ , the function of Blm10 as importin could be irrelevant for CP import in

## Discussion

dividing cells. However, the import function of Blm10 would have to be inhibited in non-dividing cells, to allow the sequestration of CPs.

A potential regulation of Blm10's function as importin could be achieved by post-translational modifications which could be examined as described in 4.5.1 by mass spectrometry. However, to show that Blm10's function as importin could be enhanced in cells leaving quiescence, Blm10 could be additionally purified from non-dividing cells that were transferred into fresh media. If a change in the pattern of modifications was detected, its functionality could be verified by mutagenesis of the site(s) and subsequent tests whether this affects the function of Blm10 as importin.

### **4.5.4. Nuclear import of Blm10**

Like proteasomes, Blm10 localizes in logarithmic phase to the nucleus of yeast cells and is sequestered into PSGs in stationary phase. This study identified Blm10 as importin for mature CPs that facilitates their nuclear re-import out of PSGs. Currently, the mechanism of nuclear import of Blm10 is undetermined in logarithmic phase. Results of previous studies showed that truncation of the C-terminal region of Blm10 resulted in a diffuse cytosolic localization instead of the nuclear localization observed for fulllength Blm10 (Schmidt et al., 2005; Doherty et al., 2012). However, in contrast to Blm10's homologues, no NLS could be identified in the C-terminal region (Schmidt et al., 2005). Instead, it is known that this region of Blm10 interacts with the proteasome CPs (Sadre-Bazzaz et al., 2010; Dange et al., 2011). As Blm10 associates in logarithmic phase with proteasomal precursor complexes that are themselves imported via the classical nuclear import receptor complex importin  $\alpha\beta$  (Fehlker et al., 2003; Lehmann et al., 2002), it is possible that Blm10 is imported into the nucleus as it is associated with proteasome precursors. To test this possibility, a mutant version of Blm10 could be created that is not capable of binding to CPs. Therefore, the last three C-terminal residues of Blm10 that were previously shown to be essential for Blm10-CP interaction could be deleted (Sadre-Bazzaz et al., 2010; Dange et al., 2011). If the import of Blm10 in logarithmic phase is dependent on an interaction with the CP, this mutant version of Blm10 should mislocalize to the cytosol as previously observed for the C-terminally truncated Blm10. If this mutant of Blm10 localizes to the nucleus, a different mechanism for Blm10 import has to exist mediated by a different interaction located within the C-terminus. Aside from the CP binding site, the C-terminus encodes for Blm10's Gsp1-GTP binding site. However, deletion of this

## Discussion

site should not result in a mislocalization in logarithmic phase, as the association of Blm10 to Gsp1-GTP occurs after Blm10's import into the nucleus resulting in the export of Blm10-Gsp1-GTP. Therefore, a prevented interaction of Blm10 and Gsp1-GTP should not affect Blm10's import but only block its export.

In stationary phase, Blm10 co-localizes with proteasomes to PSGs and promotes nuclear import of mature CPs after dissolution of PSGs by interacting with proteins of the NPC and Gsp1-GTP. Contrary to logarithmic phase, however, C-terminally truncated Blm10 was recently found to be localized to the nucleus in cells grown to G<sub>0</sub> phase (Doherty et al., 2012). This finding suggests that an import mechanism or importin function for Blm10 exists that is specific for stationary phase, as the import of C-terminally truncated Blm10 is prevented in dividing cells. In addition, its C-terminal truncation prevents Blm10's interaction with Gsp1-GTP in stationary phase and causes in consequence that Blm10 remains localized to the nucleus and is not recycled to the cytosol. Hypothetically, fulllength Blm10 could shuttle constantly between the nucleus and PSGs, whereby the import is mediated by Blm10 itself and the export by its interaction with Gsp1-GTP. After the export, Blm10 could shuttle exported CPs to PSGs.



## 5. References

- Achstetter, T., and Wolf, D.H.** (1985). Proteinases, proteolysis and biological control in the yeast *Saccharomyces cerevisiae*. *Yeast* **1**, 139-157.
- Adam, S.A., Marr, R.S., and Gerace, L.** (1990). Nuclear protein import in permeabilized mammalian cells requires soluble cytoplasmic factors. *J Cell Biol* **111**, 807-816.
- Ahn, J.Y., Tanahashi, N., Akiyama, K., Hisamatsu, H., Noda, C., Tanaka, K., Chung, C.H., Shibmara, N., Willy, P.J., Mott, J.D., et al.** (1995). Primary structures of two homologous subunits of PA28, a gamma-interferon-inducible protein activator of the 20S proteasome. *FEBS Lett* **366**, 37-42.
- Aitchison, J.D., Rout, M.P., Marelli, M., Blobel, G., and Wozniak, R.W.** (1995). Two novel related yeast nucleoporins Nup170p and Nup157p: complementation with the vertebrate homologue Nup155p and functional interactions with the yeast nuclear pore-membrane protein Pom152p. *J Cell Biol* **131**, 1133-1148.
- Alber, F., Dokudovskaya, S., Veenhoff, L.M., Zhang, W., Kipper, J., Devos, D., Suprpto, A., Karni-Schmidt, O., Williams, R., Chait, B.T., et al.** (2007). The molecular architecture of the nuclear pore complex. *Nature* **450**, 695-701.
- Amberg, D.C., Fleischmann, M., Stagljar, I., Cole, C.N., and Aebi, M.** (1993). Nuclear PRP20 protein is required for mRNA export. *EMBO J* **12**, 233-241.
- Amerik, A., Swaminathan, S., Krantz, B.A., Wilkinson, K.D., and Hochstrasser, M.** (1997). In vivo disassembly of free polyubiquitin chains by yeast Ubp14 modulates rates of protein degradation by the proteasome. *EMBO J* **16**, 4826-4838.
- Amerik, A.Y., Li, S.J., and Hochstrasser, M.** (2000). Analysis of the deubiquitinating enzymes of the yeast *Saccharomyces cerevisiae*. *Biol Chem* **381**, 981-992.
- Aravind, L., and Koonin, E.V.** (2000). The U box is a modified RING finger - a common domain in ubiquitination. *Curr Biol* **10**, R132-134.
- Arrigo, A.P., Simon, M., Darlix, J.L., and Spahr, P.F.** (1987). A 20S particle ubiquitous from yeast to human. *J Mol Evol* **25**, 141-150.
- Arrigo, A.P., Tanaka, K., Goldberg, A.L., and Welch, W.J.** (1988). Identity of the 19S 'prosome' particle with the large multifunctional protease complex of mammalian cells (the proteasome). *Nature* **331**, 192-194.
- Askjaer, P., Jensen, T.H., Nilsson, J., Englmeier, L., and Kjems, J.** (1998). The specificity of the CRM1-Rev nuclear export signal interaction is mediated by RanGTP. *J Biol Chem* **273**, 33414-33422.
- Bajorek, M., Finley, D., and Glickman, M.H.** (2003). Proteasome disassembly and downregulation is correlated with viability during stationary phase. *Curr Biol* **13**, 1140-

## References

1144.

**Baumeister, W., Dahlmann, B., Hegerl, R., Kopp, F., Kuehn, L., and Pfeifer, G.** (1988). Electron microscopy and image analysis of the multicatalytic proteinase. *FEBS Lett* **241**, 239-245.

**Baumeister, W., Walz, J., Zuhl, F., and Seemuller, E.** (1998). The proteasome: paradigm of a self-compartmentalizing protease. *Cell* **92**, 367-380.

**Bech-Otschir, D., Helfrich, A., Enenkel, C., Consiglieri, G., Seeger, M., Holzhueter, H.G., Dahlmann, B., and Kloetzel, P.M.** (2009). Polyubiquitin substrates allosterically activate their own degradation by the 26S proteasome. *Nat Struct Mol Biol* **16**, 219-225.

**Becker, J., Melchior, F., Gerke, V., Bischoff, F.R., Ponstingl, H., and Wittinghofer, A.** (1995). RNA1 encodes a GTPase-activating protein specific for Gsp1p, the Ran/TC4 homologue of *Saccharomyces cerevisiae*. *J Biol Chem* **270**, 11860-11865.

**Belhumeur, P., Lee, A., Tam, R., DiPaolo, T., Fortin, N., and Clark, M.W.** (1993). GSP1 and GSP2, genetic suppressors of the prp20-1 mutant in *Saccharomyces cerevisiae*: GTP-binding proteins involved in the maintenance of nuclear organization. *Mol Cell Biol* **13**, 2152-2161.

**Bingol, B., and Schuman, E.M.** (2006). Activity-dependent dynamics and sequestration of proteasomes in dendritic spines. *Nature* **441**, 1144-1148.

**Bischoff, F.R., and Gorlich, D.** (1997). RanBP1 is crucial for the release of RanGTP from importin beta-related nuclear transport factors. *FEBS Lett* **419**, 249-254.

**Bischoff, F.R., Krebber, H., Smirnova, E., Dong, W., and Ponstingl, H.** (1995). Co-activation of RanGTPase and inhibition of GTP dissociation by Ran-GTP binding protein RanBP1. *EMBO J* **14**, 705-715.

**Bonzanni, N., Zhang, N., Oliver, S.G., and Fisher, J.** (2011). The role of proteasome-mediated proteolysis in modulating potentially harmful transcription factor activity in *Saccharomyces cerevisiae*. *Bioinformatics* **27**, i283-287.

**Botstein, D., Chervitz, S.A., and Cherry, J.M.** (1997). Yeast as a model organism. *Science* **277**, 1259-1260.

**Butler, G., and Wolfe, K.H.** (1994). Yeast homologue of mammalian Ran binding protein 1. *Biochim Biophys Acta* **1219**, 711-712.

**Chau, V., Tobias, J.W., Bachmair, A., Marriott, D., Ecker, D.J., Gonda, D.K., and Varshavsky, A.** (1989). A multiubiquitin chain is confined to specific lysine in a targeted short-lived protein. *Science* **243**, 1576-1583.

**Chen, L., Romero, L., Chuang, S.M., Tournier, V., Joshi, K.K., Lee, J.A., Kovvali, G., and Madura, K.** (2011). Sts1 plays a key role in targeting proteasomes to the nucleus. *J Biol Chem* **286**, 3104-3118.



## References

- Chen, P., and Hochstrasser, M.** (1996). Autocatalytic subunit processing couples active site formation in the 20S proteasome to completion of assembly. *Cell* **86**, 961-972.
- Chu-Ping, M., Vu, J.H., Proske, R.J., Slaughter, C.A., and DeMartino, G.N.** (1994). Identification, purification, and characterization of a high molecular weight, ATP-dependent activator (PA700) of the 20 S proteasome. *J Biol Chem* **269**, 3539-3547.
- Ciehanover, A., Hod, Y., and Hershko, A.** (1978). A heat-stable polypeptide component of an ATP-dependent proteolytic system from reticulocytes. *Biochem Biophys Res Commun* **81**, 1100-1105.
- Costanzo, M., Baryshnikova, A., Bellay, J., Kim, Y., Spear, E.D., Sevier, C.S., Ding, H., Koh, J.L., Toufighi, K., Mostafavi, S., et al.** (2010). The genetic landscape of a cell. *Science* **327**, 425-431.
- da Fonseca, P.C., He, J., and Morris, E.P.** (2012). Molecular model of the human 26S proteasome. *Mol Cell* **46**, 54-66.
- Dahlmann, B., Kopp, F., Kuehn, L., Niedel, B., Pfeifer, G., Hegerl, R., and Baumeister, W.** (1989). The multicatalytic proteinase (prosome) is ubiquitous from eukaryotes to archaeobacteria. *FEBS Lett* **251**, 125-131.
- Dange, T., Smith, D., Noy, T., Rommel, P.C., Jurzitza, L., Cordero, R.J., Legendre, A., Finley, D., Goldberg, A.L., and Schmidt, M.** (2011). Blm10 protein promotes proteasomal substrate turnover by an active gating mechanism. *J Biol Chem* **286**, 42830-42839.
- DeMarini, D.J., Papa, F.R., Swaminathan, S., Ursic, D., Rasmussen, T.P., Culbertson, M.R., and Hochstrasser, M.** (1995). The yeast SEN3 gene encodes a regulatory subunit of the 26S proteasome complex required for ubiquitin-dependent protein degradation in vivo. *Mol Cell Biol* **15**, 6311-6321.
- DeMartino, G.N., Moomaw, C.R., Zagnitko, O.P., Proske, R.J., Chu-Ping, M., Afendis, S.J., Swaffield, J.C., and Slaughter, C.A.** (1994). PA700, an ATP-dependent activator of the 20 S proteasome, is an ATPase containing multiple members of a nucleotide-binding protein family. *J Biol Chem* **269**, 20878-20884.
- Denning, D.P., Patel, S.S., Uversky, V., Fink, A.L., and Rexach, M.** (2003). Disorder in the nuclear pore complex: the FG repeat regions of nucleoporins are natively unfolded. *Proc Natl Acad Sci U S A* **100**, 2450-2455.
- Deveraux, Q., Ustrell, V., Pickart, C., and Rechsteiner, M.** (1994). A 26 S protease subunit that binds ubiquitin conjugates. *J Biol Chem* **269**, 7059-7061.
- Devos, D., Dokudovskaya, S., Williams, R., Alber, F., Eswar, N., Chait, B.T., Rout, M.P., and Sali, A.** (2006). Simple fold composition and modular architecture of the nuclear pore complex. *Proc Natl Acad Sci U S A* **103**, 2172-2177.
- Dingwall, C., Robbins, J., Dilworth, S.M., Roberts, B., and Richardson, W.D.**

## References

(1988). The nucleoplasmin nuclear location sequence is larger and more complex than that of SV-40 large T antigen. *J Cell Biol* **107**, 841-849.

**Doherty, K.M., Pride, L.D., Lukose, J., Snydsman, B.E., Charles, R., Pramanik, A., Muller, E.G., Botstein, D., and Moore, C.W.** (2012). Loss of a 20S proteasome activator in *Saccharomyces cerevisiae* downregulates genes important for genomic integrity, increases DNA damage, and selectively sensitizes cells to agents with diverse mechanisms of action. *G3 (Bethesda)* **2**, 943-959.

**Eleuteri, A.M., Kohanski, R.A., Cardozo, C., and Orlowski, M.** (1997). Bovine spleen multicatalytic proteinase complex (proteasome). Replacement of X, Y, and Z subunits by LMP7, LMP2, and MECL1 and changes in properties and specificity. *J Biol Chem* **272**, 11824-11831.

**Elsasser, S., Chandler-Militello, D., Muller, B., Hanna, J., and Finley, D.** (2004). Rad23 and Rpn10 serve as alternative ubiquitin receptors for the proteasome. *J Biol Chem* **279**, 26817-26822.

**Elsasser, S., Gali, R.R., Schwickart, M., Larsen, C.N., Leggett, D.S., Muller, B., Feng, M.T., Tubing, F., Dittmar, G.A., and Finley, D.** (2002). Proteasome subunit Rpn1 binds ubiquitin-like protein domains. *Nat Cell Biol* **4**, 725-730.

**Enenkel, C., Blobel, G., and Rexach, M.** (1995). Identification of a yeast karyopherin heterodimer that targets import substrate to mammalian nuclear pore complexes. *J Biol Chem* **270**, 16499-16502.

**Enenkel, C., Lehmann, A., and Kloetzel, P.M.** (1998). Subcellular distribution of proteasomes implicates a major location of protein degradation in the nuclear envelope-ER network in yeast. *EMBO J* **17**, 6144-6154.

**Enenkel, C., Lehmann, A., and Kloetzel, P.M.** (1999). GFP-labelling of 26S proteasomes in living yeast: insight into proteasomal functions at the nuclear envelope/rough ER. *Mol Biol Rep* **26**, 131-135.

**Enenkel, C., Schulke, N., and Blobel, G.** (1996). Expression in yeast of binding regions of karyopherins alpha and beta inhibits nuclear import and cell growth. *Proc Natl Acad Sci U S A* **93**, 12986-12991.

**Eytan, E., Ganoth, D., Armon, T., and Hershko, A.** (1989). ATP-dependent incorporation of 20S protease into the 26S complex that degrades proteins conjugated to ubiquitin. *Proc Natl Acad Sci U S A* **86**, 7751-7755.

**Fahrenkrog, B., Hubner, W., Mandinova, A., Pante, N., Keller, W., and Aebi, U.** (2000). The yeast nucleoporin Nup53p specifically interacts with Nic96p and is directly involved in nuclear protein import. *Mol Biol Cell* **11**, 3885-3896.

**Febres, D.E., Pramanik, A., Caton, M., Doherty, K., McKoy, J., Garcia, E., Alejo, W., and Moore, C.W.** (2001). The novel BLM3 gene encodes a protein that protects against lethal effects of oxidative damage. *Cell Mol Biol (Noisy-le-grand)* **47**, 1149-1162.

## References

- Fehlker, M., Wendler, P., Lehmann, A., and Enenkel, C.** (2003). Blm3 is part of nascent proteasomes and is involved in a late stage of nuclear proteasome assembly. *EMBO Rep* **4**, 959-963.
- Floer, M., and Blobel, G.** (1996). The nuclear transport factor karyopherin beta binds stoichiometrically to Ran-GTP and inhibits the Ran GTPase activating protein. *J Biol Chem* **271**, 5313-5316.
- Forster, A., Masters, E.I., Whitby, F.G., Robinson, H., and Hill, C.P.** (2005). The 1.9 Å structure of a proteasome-11S activator complex and implications for proteasome-PAN/PA700 interactions. *Mol Cell* **18**, 589-599.
- Forster, A., Whitby, F.G., and Hill, C.P.** (2003). The pore of activated 20S proteasomes has an ordered 7-fold symmetric conformation. *EMBO J* **22**, 4356-4364.
- Frey, S., Richter, R.P., and Gorlich, D.** (2006). FG-rich repeats of nuclear pore proteins form a three-dimensional meshwork with hydrogel-like properties. *Science* **314**, 815-817.
- Fries, T., Betz, C., Sohn, K., Caesar, S., Schlenstedt, G., and Bailer, S.M.** (2007). A novel conserved nuclear localization signal is recognized by a group of yeast importins. *J Biol Chem* **282**, 19292-19301.
- Gerards, W.L., de Jong, W.W., Bloemendal, H., and Boelens, W.** (1998). The human proteasomal subunit HsC8 induces ring formation of other alpha-type subunits. *J Mol Biol* **275**, 113-121.
- Gerards, W.L., Enzlin, J., Haner, M., Hendriks, I.L., Aebi, U., Bloemendal, H., and Boelens, W.** (1997). The human alpha-type proteasomal subunit HsC8 forms a double ringlike structure, but does not assemble into proteasome-like particles with the beta-type subunits HsDelta or HsBPROS26. *J Biol Chem* **272**, 10080-10086.
- Gille, C., Goede, A., Schloetelburg, C., Preissner, R., Kloetzel, P.M., Gobel, U.B., and Frommel, C.** (2003). A comprehensive view on proteasomal sequences: implications for the evolution of the proteasome. *J Mol Biol* **326**, 1437-1448.
- Gillette, T.G., Kumar, B., Thompson, D., Slaughter, C.A., and DeMartino, G.N.** (2008). Differential roles of the COOH termini of AAA subunits of PA700 (19 S regulator) in asymmetric assembly and activation of the 26 S proteasome. *J Biol Chem* **283**, 31813-31822.
- Glickman, M.H., and Raveh, D.** (2005). Proteasome plasticity. *FEBS Lett* **579**, 3214-3223.
- Glickman, M.H., Rubin, D.M., Coux, O., Wefes, I., Pfeifer, G., Cjeka, Z., Baumeister, W., Fried, V.A., and Finley, D.** (1998a). A subcomplex of the proteasome regulatory particle required for ubiquitin-conjugate degradation and related to the COP9-signalosome and eIF3. *Cell* **94**, 615-623.
- Glickman, M.H., Rubin, D.M., Fried, V.A., and Finley, D.** (1998b). The regulatory particle of the *Saccharomyces cerevisiae* proteasome. *Mol Cell Biol* **18**, 3149-3162.

## References

- Goffeau, A., Barrell, B.G., Bussey, H., Davis, R.W., Dujon, B., Feldmann, H., Galibert, F., Hoheisel, J.D., Jacq, C., Johnston, M., et al.** (1996). Life with 6000 genes. *Science* **274**, 546, 563-547.
- Goldberg, A.L.** (2003). Protein degradation and protection against misfolded or damaged proteins. *Nature* **426**, 895-899.
- Goldfarb, D.S., Gariepy, J., Schoolnik, G., and Kornberg, R.D.** (1986). Synthetic peptides as nuclear localization signals. *Nature* **322**, 641-644.
- Gorlich, D., Dabrowski, M., Bischoff, F.R., Kutay, U., Bork, P., Hartmann, E., Prehn, S., and Izaurralde, E.** (1997). A novel class of RanGTP binding proteins. *J Cell Biol* **138**, 65-80.
- Gorlich, D., Vogel, F., Mills, A.D., Hartmann, E., and Laskey, R.A.** (1995). Distinct functions for the two importin subunits in nuclear protein import. *Nature* **377**, 246-248.
- Groll, M., Ditzel, L., Lowe, J., Stock, D., Bochtler, M., Bartunik, H.D., and Huber, R.** (1997). Structure of 20S proteasome from yeast at 2.4 Å resolution. *Nature* **386**, 463-471.
- Groll, M., Heinemeyer, W., Jager, S., Ullrich, T., Bochtler, M., Wolf, D.H., and Huber, R.** (1999). The catalytic sites of 20S proteasomes and their role in subunit maturation: a mutational and crystallographic study. *Proc Natl Acad Sci U S A* **96**, 10976-10983.
- Guterman, A., and Glickman, M.H.** (2004). Complementary roles for Rpn11 and Ubp6 in deubiquitination and proteolysis by the proteasome. *J Biol Chem* **279**, 1729-1738.
- Guthrie, C., and Fink, G.R.** (1991). Guide to yeast genetics and molecular biology. *Methods Enzymol* **194**, 1-863.
- Haass, C., Pesold-Hurt, B., Multhaup, G., Beyreuther, K., and Kloetzel, P.M.** (1989). The PROS-35 gene encodes the 35 kD protein subunit of Drosophila melanogaster proteasome. *EMBO J* **8**, 2373-2379.
- Hahn, S., and Schlenstedt, G.** (2011). Importin beta-type nuclear transport receptors have distinct binding affinities for Ran-GTP. *Biochem Biophys Res Commun* **406**, 383-388.
- Hampton, R.Y., Gardner, R.G., and Rine, J.** (1996). Role of 26S proteasome and HRD genes in the degradation of 3-hydroxy-3-methylglutaryl-CoA reductase, an integral endoplasmic reticulum membrane protein. *Mol Biol Cell* **7**, 2029-2044.
- Hatakeyama, S., and Nakayama, K.I.** (2003). U-box proteins as a new family of ubiquitin ligases. *Biochem Biophys Res Commun* **302**, 635-645.
- He, J., Kulkarni, K., da Fonseca, P.C., Krutauz, D., Glickman, M.H., Barford, D., and Morris, E.P.** (2012). The structure of the 26S proteasome subunit Rpn2 reveals its PC repeat domain as a closed toroid of two concentric alpha-helical rings. *Structu-*

## References

re **20**, 513-521.

**Heinemeyer, W., Fischer, M., Krimmer, T., Stachon, U., and Wolf, D.H.** (1997). The active sites of the eukaryotic 20 S proteasome and their involvement in subunit precursor processing. *J Biol Chem* **272**, 25200-25209.

**Heinemeyer, W., Gruhler, A., Mohrle, V., Mahe, Y., and Wolf, D.H.** (1993). PRE2, highly homologous to the human major histocompatibility complex-linked RING10 gene, codes for a yeast proteasome subunit necessary for chymotryptic activity and degradation of ubiquitinated proteins. *J Biol Chem* **268**, 5115-5120.

**Hellmuth, K., Lau, D.M., Bischoff, F.R., Kunzler, M., Hurt, E., and Simos, G.** (1998). Yeast Los1p has properties of an exportin-like nucleocytoplasmic transport factor for tRNA. *Mol Cell Biol* **18**, 6374-6386.

**Hershko, A., Ciechanover, A., and Rose, I.A.** (1979). Resolution of the ATP-dependent proteolytic system from reticulocytes: a component that interacts with ATP. *Proc Natl Acad Sci U S A* **76**, 3107-3110.

**Hershko, A., Heller, H., Elias, S., and Ciechanover, A.** (1983). Components of ubiquitin-protein ligase system. Resolution, affinity purification, and role in protein breakdown. *J Biol Chem* **258**, 8206-8214.

**Hershko, A., and Tomkins, G.M.** (1971). Studies on the degradation of tyrosine aminotransferase in hepatoma cells in culture. Influence of the composition of the medium and adenosine triphosphate dependence. *J Biol Chem* **246**, 710-714.

**Hieter, P., Bassett, D.E., Jr., and Valle, D.** (1996). The yeast genome--a common currency. *Nat Genet* **13**, 253-255.

**Hiller, M.M., Finger, A., Schweiger, M., and Wolf, D.H.** (1996). ER degradation of a misfolded luminal protein by the cytosolic ubiquitin-proteasome pathway. *Science* **273**, 1725-1728.

**Hirano, Y., Hayashi, H., Iemura, S., Hendil, K.B., Niwa, S., Kishimoto, T., Kasahara, M., Natsume, T., Tanaka, K., and Murata, S.** (2006). Cooperation of multiple chaperones required for the assembly of mammalian 20S proteasomes. *Mol Cell* **24**, 977-984.

**Hirano, Y., Hendil, K.B., Yashiroda, H., Iemura, S., Nagane, R., Hioki, Y., Natsume, T., Tanaka, K., and Murata, S.** (2005). A heterodimeric complex that promotes the assembly of mammalian 20S proteasomes. *Nature* **437**, 1381-1385.

**Hisamatsu, H., Shimbara, N., Saito, Y., Kristensen, P., Hendil, K.B., Fujiwara, T., Takahashi, E., Tanahashi, N., Tamura, T., Ichihara, A., et al.** (1996). Newly identified pair of proteasomal subunits regulated reciprocally by interferon gamma. *J Exp Med* **183**, 1807-1816.

**Hoffman, L., Pratt, G., and Rechsteiner, M.** (1992). Multiple forms of the 20 S multicatalytic and the 26 S ubiquitin/ATP-dependent proteases from rabbit reticulocyte lysate. *J Biol Chem* **267**, 22362-22368.

## References

- Hoffman, L., and Rechsteiner, M.** (1994). Activation of the multicatalytic protease. The 11 S regulator and 20 S ATPase complexes contain distinct 30-kilodalton subunits. *J Biol Chem* **269**, 16890-16895.
- Hofmann, K., and Bucher, P.** (1998). The PCI domain: a common theme in three multiprotein complexes. *Trends Biochem Sci* **23**, 204-205.
- Hoyt, M.A., and Coffino, P.** (2004). Ubiquitin-free routes into the proteasome. *Cell Mol Life Sci* **61**, 1596-1600.
- Huber, E.M., and Groll, M.** (2012). The 19S cap puzzle: a new jigsaw piece. *Structure* **20**, 387-388.
- Husnjak, K., Elsasser, S., Zhang, N., Chen, X., Randles, L., Shi, Y., Hofmann, K., Walters, K.J., Finley, D., and Dikic, I.** (2008). Proteasome subunit Rpn13 is a novel ubiquitin receptor. *Nature* **453**, 481-488.
- Imamoto, N., Tachibana, T., Matsubae, M., and Yoneda, Y.** (1995). A karyophilic protein forms a stable complex with cytoplasmic components prior to nuclear pore binding. *J Biol Chem* **270**, 8559-8565.
- Isasa, M., Katz, E.J., Kim, W., Yugo, V., Gonzalez, S., Kirkpatrick, D.S., Thomson, T.M., Finley, D., Gygi, S.P., and Crosas, B.** (2010). Monoubiquitination of RPN10 regulates substrate recruitment to the proteasome. *Mol Cell* **38**, 733-745.
- Iwanczyk, J., Sadre-Bazzaz, K., Ferrell, K., Kondrashkina, E., Formosa, T., Hill, C.P., and Ortega, J.** (2006). Structure of the Bim10-20 S proteasome complex by cryo-electron microscopy. Insights into the mechanism of activation of mature yeast proteasomes. *J Mol Biol* **363**, 648-659.
- Jager, S., Groll, M., Huber, R., Wolf, D.H., and Heinemeyer, W.** (1999). Proteasome beta-type subunits: unequal roles of propeptides in core particle maturation and a hierarchy of active site function. *J Mol Biol* **291**, 997-1013.
- Jung, T., Catalgol, B., and Grune, T.** (2009). The proteasomal system. *Mol Aspects Med* **30**, 191-296.
- Kaganovich, D., Kopito, R., and Frydman, J.** (2008). Misfolded proteins partition between two distinct quality control compartments. *Nature* **454**, 1088-1095.
- Kajava, A.V., Gorbea, C., Ortega, J., Rechsteiner, M., and Steven, A.C.** (2004). New HEAT-like repeat motifs in proteins regulating proteasome structure and function. *J Struct Biol* **146**, 425-430.
- Kelly, A., Powis, S.H., Glynn, R., Radley, E., Beck, S., and Trowsdale, J.** (1991). Second proteasome-related gene in the human MHC class II region. *Nature* **353**, 667-668.
- Khan, S., van den Broek, M., Schwarz, K., de Giuli, R., Diener, P.A., and Groettrup, M.** (2001). Immunoproteasomes largely replace constitutive proteasomes during an antiviral and antibacterial immune response in the liver. *J Immunol* **167**,

## References

6859-6868.

**Kikuchi, J., Iwafune, Y., Akiyama, T., Okayama, A., Nakamura, H., Arakawa, N., Kimura, Y., and Hirano, H.** (2010). Co- and post-translational modifications of the 26S proteasome in yeast. *Proteomics* **10**, 2769-2779.

**Kimura, A., Kato, Y., and Hirano, H.** (2012). N-myristoylation of the Rpt2 subunit regulates intracellular localization of the yeast 26S proteasome. *Biochemistry* **51**, 8856-8866.

**Kisselev, A.F., Akopian, T.N., Castillo, V., and Goldberg, A.L.** (1999). Proteasome active sites allosterically regulate each other, suggesting a cyclical bite-chew mechanism for protein breakdown. *Mol Cell* **4**, 395-402.

**Kisselev, A.F., Akopian, T.N., and Goldberg, A.L.** (1998). Range of sizes of peptide products generated during degradation of different proteins by archaeal proteasomes. *J Biol Chem* **273**, 1982-1989.

**Klebe, C., Bischoff, F.R., Ponstingl, H., and Wittinghofer, A.** (1995a). Interaction of the nuclear GTP-binding protein Ran with its regulatory proteins RCC1 and RanGAP1. *Biochemistry* **34**, 639-647.

**Klebe, C., Prinz, H., Wittinghofer, A., and Goody, R.S.** (1995b). The kinetic mechanism of Ran--nucleotide exchange catalyzed by RCC1. *Biochemistry* **34**, 12543-12552.

**Kleijnen, M.F., Roelofs, J., Park, S., Hathaway, N.A., Glickman, M., King, R.W., and Finley, D.** (2007). Stability of the proteasome can be regulated allosterically through engagement of its proteolytic active sites. *Nat Struct Mol Biol* **14**, 1180-1188.

**Kleinschmidt, J.A., Escher, C., and Wolf, D.H.** (1988). Proteinase yscE of yeast shows homology with the 20 S cylinder particles of *Xenopus laevis*. *FEBS Lett* **239**, 35-40.

**Kloetzel, P.M.** (2001). Antigen processing by the proteasome. *Nat Rev Mol Cell Biol* **2**, 179-187.

**Koepp, D.M., Harper, J.W., and Elledge, S.J.** (1999). How the cyclin became a cyclin: regulated proteolysis in the cell cycle. *Cell* **97**, 431-434.

**Kostova, Z., and Wolf, D.H.** (2003). For whom the bell tolls: protein quality control of the endoplasmic reticulum and the ubiquitin-proteasome connection. *EMBO J* **22**, 2309-2317.

**Kusmierczyk, A.R., Kunjappu, M.J., Funakoshi, M., and Hochstrasser, M.** (2008). A multimeric assembly factor controls the formation of alternative 20S proteasomes. *Nat Struct Mol Biol* **15**, 237-244.

**Kutay, U., Bischoff, F.R., Kostka, S., Kraft, R., and Gorlich, D.** (1997). Export of importin alpha from the nucleus is mediated by a specific nuclear transport factor. *Cell* **90**, 1061-1071.

## References

- Lander, G.C., Martin, A., and Nogales, E.** (2013). The proteasome under the microscope: the regulatory particle in focus. *Curr Opin Struct Biol* **23**, 243-251.
- Laporte, D., Lebaudy, A., Sahin, A., Pinson, B., Ceschin, J., Daignan-Fornier, B., and Sagot, I.** (2011). Metabolic status rather than cell cycle signals control quiescence entry and exit. *J Cell Biol* **192**, 949-957.
- Laporte, D., Salin, B., Daignan-Fornier, B., and Sagot, I.** (2008). Reversible cytoplasmic localization of the proteasome in quiescent yeast cells. *J Cell Biol* **181**, 737-745.
- Le Tallec, B., Barrault, M.B., Courbeyrette, R., Guerois, R., Marsolier-Kergoat, M.C., and Peyroche, A.** (2007). 20S proteasome assembly is orchestrated by two distinct pairs of chaperones in yeast and in mammals. *Mol Cell* **27**, 660-674.
- Lehmann, A., Janek, K., Braun, B., Kloetzel, P.M., and Enenkel, C.** (2002). 20 S proteasomes are imported as precursor complexes into the nucleus of yeast. *J Mol Biol* **317**, 401-413.
- Lehmann, A., Jechow, K., and Enenkel, C.** (2008). Blm10 binds to pre-activated proteasome core particles with open gate conformation. *EMBO Rep* **9**, 1237-1243.
- Lehmann, A., Niewianda, A., Jechow, K., Janek, K., and Enenkel, C.** (2010). Ecm29 fulfils quality control functions in proteasome assembly. *Mol Cell* **38**, 879-888.
- Li, X., Kusmierczyk, A.R., Wong, P., Emili, A., and Hochstrasser, M.** (2007). beta-Subunit appendages promote 20S proteasome assembly by overcoming an Ump1-dependent checkpoint. *EMBO J* **26**, 2339-2349.
- Lim, R.Y., Fahrenkrog, B., Koser, J., Schwarz-Herion, K., Deng, J., and Aebi, U.** (2007). Nanomechanical basis of selective gating by the nuclear pore complex. *Science* **318**, 640-643.
- Lippincott-Schwartz, J., and Patterson, G.H.** (2003). Development and use of fluorescent protein markers in living cells. *Science* **300**, 87-91.
- Liu, C.W., Corboy, M.J., DeMartino, G.N., and Thomas, P.J.** (2003). Endoproteolytic activity of the proteasome. *Science* **299**, 408-411.
- Liu, C.W., Li, X., Thompson, D., Wooding, K., Chang, T.L., Tang, Z., Yu, H., Thomas, P.J., and DeMartino, G.N.** (2006). ATP binding and ATP hydrolysis play distinct roles in the function of 26S proteasome. *Mol Cell* **24**, 39-50.
- Lopez, A.D., Tar, K., Krugel, U., Dange, T., Ros, I.G., and Schmidt, M.** (2011). Proteasomal degradation of Sfp1 contributes to the repression of ribosome biogenesis during starvation and is mediated by the proteasome activator Blm10. *Mol Biol Cell* **22**, 528-540.
- Lowe, J., Stock, D., Jap, B., Zwickl, P., Baumeister, W., and Huber, R.** (1995). Crystal structure of the 20S proteasome from the archaeon *T. acidophilum* at 3.4 Å resolution. *Science* **268**, 533-539.



## References

- Macara, I.G.** (2001). Transport into and out of the nucleus. *Microbiol Mol Biol Rev* **65**, 570-594, table of contents.
- Mannhaupt, G., Schnall, R., Karpov, V., Vetter, I., and Feldmann, H.** (1999). Rpn4p acts as a transcription factor by binding to PACE, a nonamer box found upstream of 26S proteasomal and other genes in yeast. *FEBS Lett* **450**, 27-34.
- Marelli, M., Aitchison, J.D., and Wozniak, R.W.** (1998). Specific binding of the karyopherin Kap121p to a subunit of the nuclear pore complex containing Nup53p, Nup59p, and Nup170p. *J Cell Biol* **143**, 1813-1830.
- Marques, A.J., Glanemann, C., Ramos, P.C., and Dohmen, R.J.** (2007). The C-terminal extension of the beta7 subunit and activator complexes stabilize nascent 20 S proteasomes and promote their maturation. *J Biol Chem* **282**, 34869-34876.
- Martinez, C.K., and Monaco, J.J.** (1991). Homology of proteasome subunits to a major histocompatibility complex-linked LMP gene. *Nature* **353**, 664-667.
- Masson, P., Andersson, O., Petersen, U.M., and Young, P.** (2001). Identification and characterization of a Drosophila nuclear proteasome regulator. A homolog of human 11 S REGgamma (PA28gamma). *J Biol Chem* **276**, 1383-1390.
- Masson, P., Lundgren, J., and Young, P.** (2003). Drosophila proteasome regulator REGgamma: transcriptional activation by DNA replication-related factor DREF and evidence for a role in cell cycle progression. *J Mol Biol* **327**, 1001-1012.
- Maurer, P., Redd, M., Solsbacher, J., Bischoff, F.R., Greiner, M., Podtelejnikov, A.V., Mann, M., Stade, K., Weis, K., and Schlenstedt, G.** (2001). The nuclear export receptor Xpo1p forms distinct complexes with NES transport substrates and the yeast Ran binding protein 1 (Yrb1p). *Mol Biol Cell* **12**, 539-549.
- Medicherla, B., Kostova, Z., Schaefer, A., and Wolf, D.H.** (2004). A genomic screen identifies Dsk2p and Rad23p as essential components of ER-associated degradation. *EMBO Rep* **5**, 692-697.
- Melchior, F., Paschal, B., Evans, J., and Gerace, L.** (1993). Inhibition of nuclear protein import by nonhydrolyzable analogues of GTP and identification of the small GTPase Ran/TC4 as an essential transport factor. *J Cell Biol* **123**, 1649-1659.
- Moore, M.S., and Blobel, G.** (1993). The GTP-binding protein Ran/TC4 is required for protein import into the nucleus. *Nature* **365**, 661-663.
- Moroianu, J., Blobel, G., and Radu, A.** (1995). Previously identified protein of uncertain function is karyopherin alpha and together with karyopherin beta docks import substrate at nuclear pore complexes. *Proc Natl Acad Sci U S A* **92**, 2008-2011.
- Murata, S., Kawahara, H., Tohma, S., Yamamoto, K., Kasahara, M., Nabeshima, Y., Tanaka, K., and Chiba, T.** (1999). Growth retardation in mice lacking the proteasome activator PA28gamma. *J Biol Chem* **274**, 38211-38215.
- Murata, S., Sasaki, K., Kishimoto, T., Niwa, S., Hayashi, H., Takahama, Y., and**

## References

- Tanaka, K.** (2007). Regulation of CD8+ T cell development by thymus-specific proteasomes. *Science* **316**, 1349-1353.
- Murata, S., Udono, H., Tanahashi, N., Hamada, N., Watanabe, K., Adachi, K., Yamano, T., Yui, K., Kobayashi, N., Kasahara, M., et al.** (2001). Immunoproteasome assembly and antigen presentation in mice lacking both PA28alpha and PA28beta. *EMBO J* **20**, 5898-5907.
- Nandi, D., Woodward, E., Ginsburg, D.B., and Monaco, J.J.** (1997). Intermediates in the formation of mouse 20S proteasomes: implications for the assembly of precursor beta subunits. *EMBO J* **16**, 5363-5375.
- Nehrbass, U., Rout, M.P., Maguire, S., Blobel, G., and Wozniak, R.W.** (1996). The yeast nucleoporin Nup188p interacts genetically and physically with the core structures of the nuclear pore complex. *J Cell Biol* **133**, 1153-1162.
- Oeffinger, M., Dlakic, M., and Tollervey, D.** (2004). A pre-ribosome-associated HEAT-repeat protein is required for export of both ribosomal subunits. *Genes Dev* **18**, 196-209.
- Orr-Weaver, T.L., Szostak, J.W., and Rothstein, R.J.** (1981). Yeast transformation: a model system for the study of recombination. *Proc Natl Acad Sci U S A* **78**, 6354-6358.
- Ortega, J., Heymann, J.B., Kajava, A.V., Ustrell, V., Rechsteiner, M., and Steven, A.C.** (2005). The axial channel of the 20S proteasome opens upon binding of the PA200 activator. *J Mol Biol* **346**, 1221-1227.
- Papa, F.R., and Hochstrasser, M.** (1993). The yeast DOA4 gene encodes a deubiquitinating enzyme related to a product of the human tre-2 oncogene. *Nature* **366**, 313-319.
- Park, K.C., Woo, S.K., Yoo, Y.J., Wyndham, A.M., Baker, R.T., and Chung, C.H.** (1997). Purification and characterization of UBP6, a new ubiquitin-specific protease in *Saccharomyces cerevisiae*. *Arch Biochem Biophys* **347**, 78-84.
- Park, S.H., Bolender, N., Eisele, F., Kostova, Z., Takeuchi, J., Coffino, P., and Wolf, D.H.** (2007). The cytoplasmic Hsp70 chaperone machinery subjects misfolded and endoplasmic reticulum import-incompetent proteins to degradation via the ubiquitin-proteasome system. *Mol Biol Cell* **18**, 153-165.
- Peters, L.Z., Hazan, R., Breker, M., Schuldiner, M., and Ben-Aroya, S.** (2013). Formation and dissociation of proteasome storage granules are regulated by cytosolic pH. *J Cell Biol* **201**, 663-671.
- Peth, A., Besche, H.C., and Goldberg, A.L.** (2009). Ubiquitinated proteins activate the proteasome by binding to Usp14/Ubp6, which causes 20S gate opening. *Mol Cell* **36**, 794-804.
- Pickart, C.M., and Eddins, M.J.** (2004). Ubiquitin: structures, functions, mechanisms. *Biochim Biophys Acta* **1695**, 55-72.

## References

- Preckel, T., Fung-Leung, W.P., Cai, Z., Vitiello, A., Salter-Cid, L., Winqvist, O., Wolfe, T.G., Von Herrath, M., Angulo, A., Ghazal, P., et al.** (1999). Impaired immunoproteasome assembly and immune responses in PA28<sup>-/-</sup> mice. *Science* **286**, 2162-2165.
- Rabl, J., Smith, D.M., Yu, Y., Chang, S.C., Goldberg, A.L., and Cheng, Y.** (2008). Mechanism of gate opening in the 20S proteasome by the proteasomal ATPases. *Mol Cell* **30**, 360-368.
- Radu, A., Blobel, G., and Moore, M.S.** (1995a). Identification of a protein complex that is required for nuclear protein import and mediates docking of import substrate to distinct nucleoporins. *Proc Natl Acad Sci U S A* **92**, 1769-1773.
- Radu, A., Moore, M.S., and Blobel, G.** (1995b). The peptide repeat domain of nucleoporin Nup98 functions as a docking site in transport across the nuclear pore complex. *Cell* **81**, 215-222.
- Ramos, P.C., Hockendorff, J., Johnson, E.S., Varshavsky, A., and Dohmen, R.J.** (1998). Ump1p is required for proper maturation of the 20S proteasome and becomes its substrate upon completion of the assembly. *Cell* **92**, 489-499.
- Rao, H., and Sastry, A.** (2002). Recognition of specific ubiquitin conjugates is important for the proteolytic functions of the ubiquitin-associated domain proteins Dsk2 and Rad23. *J Biol Chem* **277**, 11691-11695.
- Rastogi, N., and Mishra, D.P.** (2012). Therapeutic targeting of cancer cell cycle using proteasome inhibitors. *Cell Div* **7**, 26.
- Rechsteiner, M., and Hill, C.P.** (2005). Mobilizing the proteolytic machine: cell biological roles of proteasome activators and inhibitors. *Trends Cell Biol* **15**, 27-33.
- Rendueles, P.S., and Wolf, D.H.** (1988). Proteinase function in yeast: biochemical and genetic approaches to a central mechanism of post-translational control in the eukaryote cell. *FEMS Microbiol Rev* **4**, 17-45.
- Rexach, M., and Blobel, G.** (1995). Protein import into nuclei: association and dissociation reactions involving transport substrate, transport factors, and nucleoporins. *Cell* **83**, 683-692.
- Ribbeck, K., and Gorlich, D.** (2002). The permeability barrier of nuclear pore complexes appears to operate via hydrophobic exclusion. *EMBO J* **21**, 2664-2671.
- Richards, S.A., Carey, K.L., and Macara, I.G.** (1997). Requirement of guanosine triphosphate-bound ran for signal-mediated nuclear protein export. *Science* **276**, 1842-1844.
- Rock, K.L., Gramm, C., Rothstein, L., Clark, K., Stein, R., Dick, L., Hwang, D., and Goldberg, A.L.** (1994). Inhibitors of the proteasome block the degradation of most cell proteins and the generation of peptides presented on MHC class I molecules. *Cell* **78**, 761-771.

## References

- Romisch, K.** (2005). Endoplasmic reticulum-associated degradation. *Annu Rev Cell Dev Biol* **21**, 435-456.
- Rosenzweig, R., Bronner, V., Zhang, D., Fushman, D., and Glickman, M.H.** (2012). Rpn1 and Rpn2 coordinate ubiquitin processing factors at proteasome. *J Biol Chem* **287**, 14659-14671.
- Rout, M.P., Aitchison, J.D., Suprpto, A., Hjertaas, K., Zhao, Y., and Chait, B.T.** (2000). The yeast nuclear pore complex: composition, architecture, and transport mechanism. *J Cell Biol* **148**, 635-651.
- Rubinsztein, D.C.** (2006). The roles of intracellular protein-degradation pathways in neurodegeneration. *Nature* **443**, 780-786.
- Russell, S.J., Steger, K.A., and Johnston, S.A.** (1999). Subcellular localization, stoichiometry, and protein levels of 26 S proteasome subunits in yeast. *J Biol Chem* **274**, 21943-21952.
- Sadre-Bazzaz, K., Whitby, F.G., Robinson, H., Formosa, T., and Hill, C.P.** (2010). Structure of a Blm10 complex reveals common mechanisms for proteasome binding and gate opening. *Mol Cell* **37**, 728-735.
- Savulescu, A.F., Shorer, H., Kleifeld, O., Cohen, I., Gruber, R., Glickman, M.H., and Harel, A.** (2011). Nuclear import of an intact preassembled proteasome particle. *Mol Biol Cell* **22**, 880-891.
- Schauber, C., Chen, L., Tongaonkar, P., Vega, I., Lambertson, D., Potts, W., and Madura, K.** (1998). Rad23 links DNA repair to the ubiquitin/proteasome pathway. *Nature* **391**, 715-718.
- Scheffner, M., Nuber, U., and Huibregtse, J.M.** (1995). Protein ubiquitination involving an E1-E2-E3 enzyme ubiquitin thioester cascade. *Nature* **373**, 81-83.
- Schlenstedt, G., Saavedra, C., Loeb, J.D., Cole, C.N., and Silver, P.A.** (1995). The GTP-bound form of the yeast Ran/TC4 homologue blocks nuclear protein import and appearance of poly(A)<sup>+</sup> RNA in the cytoplasm. *Proc Natl Acad Sci U S A* **92**, 225-229.
- Schmidt, M., Haas, W., Crosas, B., Santamaria, P.G., Gygi, S.P., Walz, T., and Finley, D.** (2005). The HEAT repeat protein Blm10 regulates the yeast proteasome by capping the core particle. *Nat Struct Mol Biol* **12**, 294-303.
- Schreiner, P., Chen, X., Husnjak, K., Randles, L., Zhang, N., Elsassner, S., Finley, D., Dikic, I., Walters, K.J., and Groll, M.** (2008). Ubiquitin docking at the proteasome through a novel pleckstrin-homology domain interaction. *Nature* **453**, 548-552.
- Seemuller, E., Lupas, A., and Baumeister, W.** (1996). Autocatalytic processing of the 20S proteasome. *Nature* **382**, 468-471.
- Seong, K.M., Baek, J.H., Yu, M.H., and Kim, J.** (2007). Rpn13p and Rpn14p are involved in the recognition of ubiquitinated Gcn4p by the 26S proteasome. *FEBS Lett*

## References

581, 2567-2573.

**Sikorski, R.S., and Hieter, P.** (1989). A system of shuttle vectors and yeast host strains designed for efficient manipulation of DNA in *Saccharomyces cerevisiae*. *Genetics* **122**, 19-27.

**Siniooglou, S., Wimmer, C., Rieger, M., Doye, V., Tekotte, H., Weise, C., Emig, S., Segref, A., and Hurt, E.C.** (1996). A novel complex of nucleoporins, which includes Sec13p and a Sec13p homolog, is essential for normal nuclear pores. *Cell* **84**, 265-275.

**Smith, D.M., Chang, S.C., Park, S., Finley, D., Cheng, Y., and Goldberg, A.L.** (2007). Docking of the proteasomal ATPases' carboxyl termini in the 20S proteasome's alpha ring opens the gate for substrate entry. *Mol Cell* **27**, 731-744.

**Song, X., Mott, J.D., von Kampen, J., Pramanik, B., Tanaka, K., Slaughter, C.A., and DeMartino, G.N.** (1996). A model for the quaternary structure of the proteasome activator PA28. *J Biol Chem* **271**, 26410-26417.

**Stoffler, D., Feja, B., Fahrenkrog, B., Walz, J., Typke, D., and Aepli, U.** (2003). Cryo-electron tomography provides novel insights into nuclear pore architecture: implications for nucleocytoplasmic transport. *J Mol Biol* **328**, 119-130.

**Tanaka, K., Yoshimura, T., Tamura, T., Fujiwara, T., Kumatori, A., and Ichihara, A.** (1990). Possible mechanism of nuclear translocation of proteasomes. *FEBS Lett* **271**, 41-46.

**Tetenbaum-Novatt, J., Hough, L.E., Mironska, R., McKenney, A.S., and Rout, M.P.** (2012). Nucleocytoplasmic transport: a role for nonspecific competition in karyopherin-nucleoporin interactions. *Mol Cell Proteomics* **11**, 31-46.

**Thrower, J.S., Hoffman, L., Rechsteiner, M., and Pickart, C.M.** (2000). Recognition of the polyubiquitin proteolytic signal. *EMBO J* **19**, 94-102.

**Udvardy, A.** (1993). Purification and characterization of a multiprotein component of the *Drosophila* 26 S (1500 kDa) proteolytic complex. *J Biol Chem* **268**, 9055-9062.

**Unno, M., Mizushima, T., Morimoto, Y., Tomisugi, Y., Tanaka, K., Yasuoka, N., and Tsukihara, T.** (2002). The structure of the mammalian 20S proteasome at 2.75 Å resolution. *Structure* **10**, 609-618.

**Ustrell, V., Hoffman, L., Pratt, G., and Rechsteiner, M.** (2002). PA200, a nuclear proteasome activator involved in DNA repair. *EMBO J* **21**, 3516-3525.

**Verma, R., Aravind, L., Oania, R., McDonald, W.H., Yates, J.R., 3rd, Koonin, E.V., and Deshaies, R.J.** (2002). Role of Rpn11 metalloprotease in deubiquitination and degradation by the 26S proteasome. *Science* **298**, 611-615.

**Vetter, I.R., Arndt, A., Kutay, U., Gorlich, D., and Wittinghofer, A.** (1999a). Structural view of the Ran-Importin beta interaction at 2.3 Å resolution. *Cell* **97**, 635-646.

## References

- Vetter, I.R., Nowak, C., Nishimoto, T., Kuhlmann, J., and Wittinghofer, A.** (1999b). Structure of a Ran-binding domain complexed with Ran bound to a GTP analogue: implications for nuclear transport. *Nature* **398**, 39-46.
- Wang, X., Xu, H., Ju, D., and Xie, Y.** (2008). Disruption of Rpn4-induced proteasome expression in *Saccharomyces cerevisiae* reduces cell viability under stressed conditions. *Genetics* **180**, 1945-1953.
- Waxman, L., Fagan, J.M., and Goldberg, A.L.** (1987). Demonstration of two distinct high molecular weight proteases in rabbit reticulocytes, one of which degrades ubiquitin conjugates. *J Biol Chem* **262**, 2451-2457.
- Weberruss, M.H., Savulescu, A.F., Jando, J., Bissinger, T., Harel, A., Glickman, M.H., and Enenkel, C.** (2013). Blm10 facilitates nuclear import of proteasome core particles. *EMBO J* **32**, 2697-2707.
- Wendler, P., Lehmann, A., Janek, K., Baumgart, S., and Enenkel, C.** (2004). The bipartite nuclear localization sequence of Rpn2 is required for nuclear import of proteasomal base complexes via karyopherin alpha and proteasome functions. *J Biol Chem* **279**, 37751-37762.
- Wente, S.R., and Rout, M.P.** (2010). The nuclear pore complex and nuclear transport. *Cold Spring Harb Perspect Biol* **2**, a000562.
- Wilkinson, C.R., Seeger, M., Hartmann-Petersen, R., Stone, M., Wallace, M., Semple, C., and Gordon, C.** (2001). Proteins containing the UBA domain are able to bind to multi-ubiquitin chains. *Nat Cell Biol* **3**, 939-943.
- Wilkinson, K.D., Urban, M.K., and Haas, A.L.** (1980). Ubiquitin is the ATP-dependent proteolysis factor I of rabbit reticulocytes. *J Biol Chem* **255**, 7529-7532.
- Wolf, D.H., and Hilt, W.** (2004). The proteasome: a proteolytic nanomachine of cell regulation and waste disposal. *Biochim Biophys Acta* **1695**, 19-31.
- Wong, D.H., Corbett, A.H., Kent, H.M., Stewart, M., and Silver, P.A.** (1997). Interaction between the small GTPase Ran/Gsp1p and Ntf2p is required for nuclear transport. *Mol Cell Biol* **17**, 3755-3767.
- Wozniak, R.W., Rout, M.P., and Aitchison, J.D.** (1998). Karyopherins and kissing cousins. *Trends Cell Biol* **8**, 184-188.
- Xie, Y., and Varshavsky, A.** (2001). RPN4 is a ligand, substrate, and transcriptional regulator of the 26S proteasome: a negative feedback circuit. *Proc Natl Acad Sci U S A* **98**, 3056-3061.
- Yano, R., Oakes, M., Yamagishi, M., Dodd, J.A., and Nomura, M.** (1992). Cloning and characterization of SRP1, a suppressor of temperature-sensitive RNA polymerase I mutations, in *Saccharomyces cerevisiae*. *Mol Cell Biol* **12**, 5640-5651.
- Yao, T., and Cohen, R.E.** (2002). A cryptic protease couples deubiquitination and degradation by the proteasome. *Nature* **419**, 403-407.

## References

- Yashiroda, H., Mizushima, T., Okamoto, K., Kameyama, T., Hayashi, H., Kishimoto, T., Niwa, S., Kasahara, M., Kurimoto, E., Sakata, E., et al.** (2008). Crystal structure of a chaperone complex that contributes to the assembly of yeast 20S proteasomes. *Nat Struct Mol Biol* **15**, 228-236.
- Yen, H.C., Espiritu, C., and Chang, E.C.** (2003a). Rpn5 is a conserved proteasome subunit and required for proper proteasome localization and assembly. *J Biol Chem* **278**, 30669-30676.
- Yen, H.C., Gordon, C., and Chang, E.C.** (2003b). Schizosaccharomyces pombe Int6 and Ras homologs regulate cell division and mitotic fidelity via the proteasome. *Cell* **112**, 207-217.
- Zhang, M., Pickart, C.M., and Coffino, P.** (2003). Determinants of proteasome recognition of ornithine decarboxylase, a ubiquitin-independent substrate. *EMBO J* **22**, 1488-1496.
- Zwickl, P., Grziwa, A., Puhler, G., Dahlmann, B., Lottspeich, F., and Baumeister, W.** (1992). Primary structure of the Thermoplasma proteasome and its implications for the structure, function, and evolution of the multicatalytic proteinase. *Biochemistry* **31**, 964-972.
- Zwickl, P., Kleinz, J., and Baumeister, W.** (1994). Critical elements in proteasome assembly. *Nat Struct Biol* **1**, 765-770.
- Zwickl, P., Ng, D., Woo, K.M., Klenk, H.P., and Goldberg, A.L.** (1999). An archaeobacterial ATPase, homologous to ATPases in the eukaryotic 26 S proteasome, activates protein breakdown by 20 S proteasomes. *J Biol Chem* **274**, 26008-26014.





## 6. Acknowledgements

First, I want to thank Prof. Dr. Cordula Enenkel and Prof. Dr. Dieter H. Wolf for the opportunity to work on this interesting project. I am thankful to Prof. Enenkel for her scientific supervision, discussions on the project and all her support throughout the work on this thesis.

I would also like to acknowledge Anca Savulescu for the collaboration and for performing all experiments in the *Xenopus* system.

I want to thank all members of the Enenkel, Ernst and Wolf lab for their discussions and the good working atmosphere. Special thanks to Paula Balisi, Thomas Bissinger and Julia Jando for their contributions to this project.

Moreover, I would like to thank Prof. Dr. Angus McQuibban and all members of his lab for discussions and for the use of his microscope. Additionally, I would like to thank Prof. Dr. Jacqueline Segall for providing material and working space.

Special thanks go to my parents for their life-long love, support and encouragement. Thanks go also to my brother, his family and my friends for their support. I would like to express my gratitude to my boyfriend Matt for his love and support. I also want to thank him for proofreading of this thesis.



## 7. Lebenslauf

### Persönliche Angaben

Name Marion Heiderose Weberruß  
Geburtsdatum 15.01.1985  
Geburtsort Mühlacker

### Ausbildung

Seit März 2010	Dissertation „The proteasome activator Blm10 facilitates nuclear import of mature proteasome core particles in yeast“ bei Prof. Dr. C. Enenkel, Department of Biochemistry, University of Toronto und Prof. Dr. D. H. Wolf, Institut für Biochemie, Universität Stuttgart Die Arbeit wurde an der University of Toronto, Kanada, der Universität Stuttgart und der Charité Universitätsmedizin Berlin durchgeführt.
Mai 2009 – Februar 2010	Diplomarbeit mit dem Titel „Studien zur Funktion von Sec61 im ERAD-System“ bei Prof. Dr. D. H. Wolf Institut für Biochemie, Universität Stuttgart
Oktober 2004 – Februar 2010	Studium der Technischen Biologie Universität Stuttgart Vertiefungsfächer: industrielle Genetik, Technische Biochemie, Mikrobielle Biotechnologie und Biochemie <i>Diplom</i>
September 1995 – Juni 2004	Friedrich-Abel-Gymnasium, Vaihingen an der Enz <i>Abitur</i>

### Berufliche Erfahrung

Januar 2011 – März 2013	Akademische Mitarbeiterin am Institut für Biochemie an der Universität Stuttgart bei Prof. Dr. D. H. Wolf
März 2010 – Dezember 2010	Wissenschaftliche Mitarbeiterin am Institut für Biochemie an der Charité Universitätsmedizin Berlin bei Prof. Dr. P. M. Kloetzel, AG Dr. C. Enenkel

### Wissenschaftliche Publikation

**Weberruss, M.H., Savulescu, A.F., Jando, J., Bissinger, T., Harel, A., Glickman, M.H., and Enenkel, C.** (2013). Blm10 facilitates nuclear import of proteasome core particles. *EMBO J* **32**, 2697-2707